Chromatin dynamics in Arabidopsis development

A live cell imaging approach

Stefanie Nunes Rosa

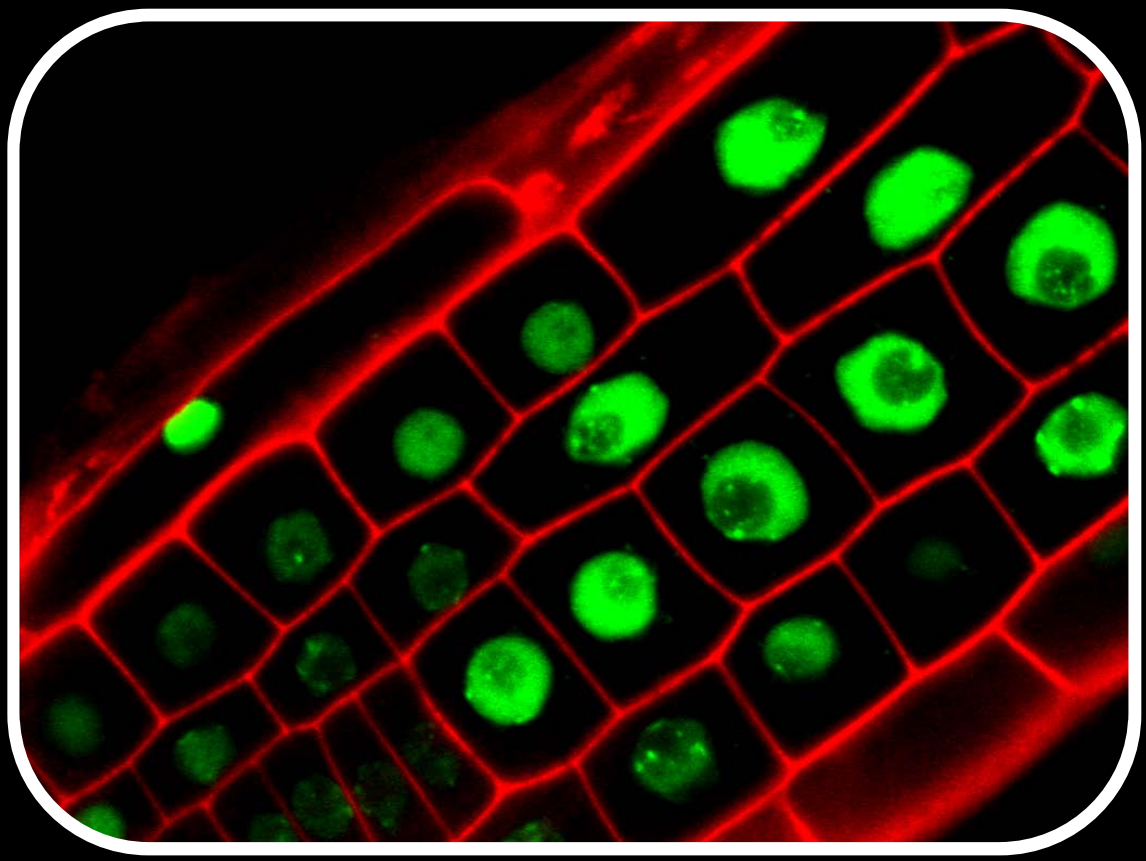

Dissertation presented to obtain the Ph.D degree in Biology

Instituto de Tecnologia Química e Biológica | Universidade Nova de Lisboa

Oeiras,
October, 2011

INSTITUTO
DE TECNOLOGIA
QUÍMICA E BIOLÓGICA
/UNL

Knowledge Creation

Chromatin dynamics in Arbidopsis development

A live cell imaging approach

Stefanie Nunes Rosa

Dissertation presented to obtain the Ph.D degree in Biology

Instituto de Tecnologia Química e Biológica | Universidade Nova de Lisboa

Oeiras, October, 2011

INSTITUTO
DE TECNOLOGIA
QUÍMICA E BIOLÓGICA
/UNL

Knowledge Creation

Acknowledgments

First of all, I would like to thank my supervisor Peter Shaw for giving me the opportunity to be part of his group and to do my PhD in his laboratory. Thank you for your help and endless support during the course of this research. I am also deeply grateful to my supervisor Rita Abranches for the help, encouragement and for guidance on my first steps in scientific research.

Secondly, I would like give a special "thank you" to the members of the Nuclear Structure Group: Rouyu and Emma, my partners in suffering during our PhDs, thank you so much for being always so nice with me, for helping with everything I needed, for the precious advices, and, of course, for keeping the most brilliant atmosphere in our office and in the lab (Ruoyu, I will miss our nonsense chatting "after normal working hours..."); Ali, for your kindness, help, support, for always organizing everything we needed in the lab and outside the lab, and for being my "hug" when I needed; Azahara and (Professor) Nobuko, thank you both for being so wonderfully nice and crazy. Thanks for the funny times we had together, for your help, for tolerating my bad moods, for your friendship (Meerkat, the ballet shoes will be waiting for you in Berlin); Vardis and Isabelle, the veteran bench-mates, thank you so much for all the help, tricks, tips, friendship and for the constant sense of humour.

I also would like to thank the enthusiasm and support I received from Liam and his group, Caroline Dean, Silvia Costa, Menita DeLucia and Josh Mylne during my stay in the John Innes Centre. To Georgina, for her kindness, competence and unbelievable efficiency in organizing all the paper work for us. To Grant, for the help with the microscopes and for the discussions over cups of tea. I am also grateful to José Feijó and Nuno Moreno, for all the help and assistance during my stay in the Gulbenkian Institute. To Sofia Pires, for the help during the stressful period of thesis submission.

Above all, I would like to express my endless gratitude to my parents, my brother and my sister for literally everything - for being there when I need, for all your support, love and for tolerating my continued existence as a student.

And at last, because the most beautiful of all scientific discoveries took place in the corridors of the lab and on the way home by bike, I can't finish without thanking the one who made it all worthwhile. My dear Adrien, thank you so much for your support, love and endless patience.

Summary

The proper development of multicellular organisms demands the distinct specification of a variety of specialized cell types. While this is one of the oldest statements of developmental genetics, how different patterns of gene expression are established in genetically identical cells and maintained during somatic cell divisions is still an active topic of research.

Chromatin structure is now recognized to regulate gene activity playing a crucial role in cell differentiation and development. Chromatin is not simply a packaging tool but a dynamic entity that reflects the regulatory cues necessary to program appropriate cellular pathways. There are several ways by which chromatin structure can be remodelled. These mechanisms include DNA-methylation, post-translational modifications of histone proteins, histone variants and, nuclear localization. While the dynamic nature of chromatin structure has been previously described its biological function and repercussions on development are only now beginning to be revealed. In this work we used *in vivo* microscopy techniques to assess how different aspects of chromatin organization play a role on various aspects of development.

We used *Arabidopsis thaliana* as a model system. Arabidopsis has a small genome and a simple organization of euchromatin and heterochromatin. It is a multicellular organism and it faces successive developmental phase changes during its life cycle. These features make Arabidopsis a well suited organism to study chromatin dynamics and development. Additionally, the root of Arabidopsis, with only 150 µm in thickness, is an ideal organ for microscopic studies on nuclei in an intact organ.

In recent years it has been shown that chromatin is quite dynamic, and even histones can be rapidly exchanged within the chromatin. In chapters 2 and 3, we examined how histone exchanging dynamics vary during plant cell differentiation. For that we used the well established developmental gradient of the Arabidopsis root to evaluate the mobility of different histone-GFP fusion proteins during cell differentiation. We showed that the Quiescent Center cells (QCs) and the surrounding stem cells have reduced histone mobilities. Further, the mobility of histones increase in the division zone of the root and decreases again when cells differentiate. Moreover, we revealed that one mechanism accounting for the differential mobilities is histone acetylation and that auxin, a plant hormone long known to regulate plant development, acts at least in part by regulating core histone acetylation.

An additional mechanism for chromatin regulation is brought by the possibility of replacing the major histones by histone variants. H2A.Z, a highly conserved variant of histone H2A, is of particular interest because it is essential for viability in multicellular organisms and it has been implicated in many distinct functions. However a role for H2A.Z in controlling cell fate decisions has not yet been investigated. In chapter 4, we examined how the incorporation of the histone variant H2A.Z affect cell-fate switches in root hair development. We showed that a higher incorporation of H2A.Z in atrichoblasts cells is crucial for the development of a non-hair cell, and that plants where this process is impaired reveal the formation of ectopic hair cells.

Finally, the physical position of a gene relative to nuclear domains can also contribute to transcriptional control. In chapter 5, we used the *lac* operator system to analyze the repositioning of alleles of a Polycomb target gene, FLC, during an environmentally-triggered silencing process involved in the control of flowering time - vernalization. We observed that alleles of FLC locus physically associate and reposition in the nucleus during in the silencing process. The biological significance of clustering was revealed by its dependence on trans factors previously shown to be required for the Polycomb silencing mechanism.

In summary, the results obtained in this work provide new insights into the relationship between chromatin dynamics and development of multicellular organisms.

Resumo

O correcto desenvolvimento de organismos multicelulares requer a diferenciação de um conjunto de células especializadas. Embora este seja um dos conceitos mais antigos da genética do desenvolvimento, a forma como diferentes padrões de expressão genética são estabelecidos e mantidos durante divisões somáticas em células geneticamente idênticas são ainda temas de investigação intensiva.

A estrutura da cromatina é actualmente reconhecida como reguladora da actividade genética desempenhando um papel fundamental na diferenciação e desenvolvimento celular. A cromatina não se resume a uma estrutura de empacotamento, mas representa uma entidade dinâmica que revela sinais reguladores necessários à correcta programação das vias de desenvolvimento celular. Existem diversas formas pelas quais a estrutura da cromatina pode ser alterada. Estes mecanismos incluem a metilação de DNA, modificações pós-traducionais de histonas, variantes de histonas e a localização de genes dentro do núcleo. Embora a natureza dinâmica da estrutura da cromatina tenha sido já amplamente descrita, a sua função biológica e respectivas repercussões no desenvolvimento dos organismos só agora está a ser revelada.

Neste trabalho foram utilizadas técnicas de microscopia *in vivo* para avaliar de que modo os diferentes padrões de organização da cromatina influenciam vários aspectos do desenvolvimento celular. A espécie *Arabidopsis thaliana* foi utilizada como modelo biológico. Esta espécie caracteriza-se por apresentar um genoma pequeno e uma organização simples da eucromatina e da heterocromatina. É um organismo multicelular e sofre sucessivas mudanças de fase de desenvolvimento durante o seu ciclo de vida. Estas características tornam a Arabidopsis um organismo adequado ao estudo da dinâmica da cromatina no contexto do desenvolvimento. Além disso, a raiz de Arabidopsis, com uma espessura de apenas 150 µm, é um órgão ideal para estudos de microscopia *in vivo*.

Nos últimos anos tem sido demonstrado que a cromatina é bastante dinâmica, e que até mesmo as histonas podem ser mobilizadas dentro da cromatina. Nos capítulos 2 e 3, foi avaliada a forma como a dinâmica das histonas varia durante a diferenciação das células vegetais. Para tal, recorreu-se a um sistema bem estabelecido de gradiente de diferenciação do desenvolvimento da raiz em Arabidopsis para avaliar a mobilidade de diferentes construções histona-GFP durante a diferenciação celular. Foi demonstrado que as histonas das células do centro quiescente (CQs) e as células estaminais que o rodeiam possuem uma

mobilidade reduzida. A mobilidade das histonas aumenta na zona de divisão da raiz e diminui novamente quando as células se diferenciam. Adicionalmente, foi determinado que um mecanismo responsável pelas mobilidades diferenciais observadas é a acetilação das histonas e que a hormona vegetal auxina actua pelo menos em parte, regulando a acetilação das histonas no núcleo.

Um mecanismo alternativo também responsável pela regulação da cromatina é a possibilidade de substituição das histonas convencionais pela variantes de histonas. H2A.Z é uma variante altamente conservada da histona H2A, e é de particular interesse, pois é essencial para a viabilidade de organismos multicelulares e tem sido implicada em funções distintas. No entanto o papel desta variante no controlo do destino celular ainda não foi investigado. No capítulo 4, foi estudada a forma como a incorporação da variante H2A.Z afecta mudanças no destino celular do desenvolvimento de pêlos radiculares. Foi demonstrado que a incorporação de H2A.Z em atricoblastos é crucial para o desenvolvimento de células não formadoras de pelos radiculares, e que as plantas onde esse processo é afectado desenvolvem pelos radiculares ectópicos.

Por fim, a localização física de um gene relativamente a domínios nucleares também pode contribuir para o controlo da transcrição. No capítulo 5, foi utilizado o sistema do operador *lac* para analisar o reposicionamento de alelos de um gene (FLC) regulado por Polycombs, durante o processo de silenciamento envolvido no controle do tempo de floração - vernalização. Observou-se que alelos do locus FLC associam-se fisicamente no núcleo durante o processo de silenciamento. O significado biológico deste fenómeno foi revelado pela sua dependência a factores *trans* já demonstrados necessários para o mecanismo de silenciamento através de Polycombs.

Em resumo, os resultados obtidos neste trabalho permitem clarificar a relação entre a dinâmica da cromatina e o desenvolvimento de organismos multicelulares.

List of abbreviations

3D – Three-dimensional

3C – Chromosome conformation capture

°C – degrees Celsius

% – Percent

ATP – Adenosine triphosphate

BLAST – Basic Local Alignment Search Tool

bp – base pair

BSA – Bovine serum albumin

CCD – Charge-coupled device

CDK – Cyclin dependent kinase

ChIP – Chromatin immunoprecipitation

CHO – Chinese hamster ovary

Col-0 – Colombia-0

Da - Dalton

DAPI – 4'-6-diamidino-2-phenylindole

DMSO – Dimethyl sulphoxide

DNA – Deoxyribonucleic acid

DTT – Dithiolthreitol

DZ – Differentiation zone

EDTA – Ethylenediaminetetraacetic acid

EZ – Elongation zone

FISH – fluorescence in situ hybridization

FLC – Flowering locus C

FRAP – Fluorescence recovery after photobleaching

GFP – Green fluorescent protein

h – Hour

HAT – Histone acetyltransferase

HCL - Hydrochloric acid

HDAC – Histone deacetylase

HMG – High Mobility Group domain

HP1 – Heterochromatin protein 1

IAA – Indole acetic acid

IF – Immunofluorescence

kDa – kiloDalton

Km^R – Kanamicin resistance

Ler – Landsberg erecta

M – Molar

MES – 2-N-morpholino-ethane-sulfonic acid

ml - millilitre

mm – millimetre

mM – millimolar

μM – micromolar

mRFP – modified red fluorescent protein

mRNA – messenger RNA

MS – Murashige Skoog

MW – Molecular weight

NAA – naphthaleneacetic acid

NLS – Nuclear localization signal

nm – Nanometre

NV – Non-vernalized

NOR – Nucleolar organiser region

PAGFP – Photoactivatable GFP

PcG – Polycomb group

PCR – Polymerase chain reaction

PFA – Paraformaldehyde

PHD – Plant homeo domain

PI – Propidium iodide

PIPES - Potassium piperazine-1,4-bis(2-ethane)sulfonic acid

PPT – Phosphinothricin

PTM – Post-translational modification

QC – Quiecent centre

r.p.m. – Revolutions per minute

rDNA – ribosomal DNA

RI – Replication-independent

RNA – Ribonucleic acid

ROI – Region of interest

rRNA – ribosomal RNA

SDS-PAGE – Sodium dodecyl sulfate polyacrylamide gel electrophoresis

TAIR – The Arabidopsis Information Resource

TSA – Trichostatin A

UTR – Untranslated region

V – Vernalized

w/v – Weight / volume

WB – Western blot

WT – Wild type

YFP – Yellow fluorescent protein

TABLE OF CONTENTS

LIST OF FIGURES

LIST OF TABLES

Chapter 1

General Introduction

Chapter 1:

General Introduction

1.1. Abstract

The packaging of chromatin into the nucleus of a eukaryotic cell requires an extraordinary degree of compaction and physical organization. In recent years, it has been shown that this organization is dynamically orchestrated to regulate responses to exogenous stimuli as well as to guide complex cell-type-specific developmental programmes. Gene expression is regulated by the compartmentalization of functional domains within the nucleus, by differential nucleosome composition, via differential modifications on the histone tails and through the replacement by histone variants. In this chapter, we will focus on these three main aspects of chromatin organization and discuss novel approaches such as live cell imaging and photobleaching as important tools likely to give significant insights into our understanding of the very dynamic nature of chromatin and chromatin regulatory processes.

1.2. Chromatin and Nuclear Architecture

In eukaryotic cells the nuclear DNA does not appear naked but is associated with many proteins to form the complex called chromatin. The most prominent proteins in chromatin are the histone proteins. Histones are basic proteins responsible for the vast degree of packaging of the DNA within the confines of the eukaryotic nucleus. Approximately 146 base pairs of DNA are wrapped around an octamer of histones containing two copies of each of the four core histones (H2A, H2B, H3 and H4) forming the most fundamental unit of chromatin – the nucleosome (Kornberg, 1974).

Core histones are proteins that have been structurally conserved through evolution and that have evolved to accomplish two conflicting and yet vital tasks: on one hand the long DNA has to be packaged within the limits of the eukaryotic nucleus, preventing knots and tangles and protecting the genome from physical damage; on the other hand the information that is encoded on the DNA needs to be accessed at appropriate times. These functions are at least in part regulated by local changes in nucleosome and chromatin structure by complex mechanisms that are only now emerging.

The nucleosomes are positioned every ~200bp on a DNA strand, and can be linked together by the linker histone H1. Electron microscopy of isolated polynucleosomes clearly reveals an open beads-on-a-string structure of the DNA fibre (Locklear et al., 1990). It was proposed more than 30 years ago that an early stage in compaction is the formation of a fibre with approximately 30 nm in diameter, in what can be designated a secondary structure of chromatin (Finch and Klug, 1976). However, the arrangement of nucleosomes and linker DNA within isolated 30 nm fibres has been difficult to study and remains controversial (Maeshima et al., 2010).

The histone H1 and other proteins are believed to stabilize nucleosome structures involved in the higher order organization of the nucleus (Schwarz and Hansen, 1994). According to one model, the nucleosome fibre containing H1 is folded into a solenoid of 30 nm diameter forming a superhelix with 6 nucleosomes per turn (Finch and Klug, 1976; Robinson et al., 2006). Recently an alternative "zigzag" model is emerging with stronger support (Schalch et al., 2005; Woodcock et al., 1993). According to this model the 30 nm fibre is formed by zigzag nucleosome arrays and the spacer DNA frequently passes through the central axes of the fibre. Although there is no definitive information concerning the secondary structure of chromatin there is no doubt that some higher levels of organization are present.

Chromatin has historically been divided in two distinct classes: euchromatin and heterochromatin. These terms refer to states of compaction and transcriptional potential; the higher-order structural differences are still debated. Heterochromatin is very condensed and consists mainly of repetitive sequences whereas euchromatin is less compacted and gene rich, with irregularly spaced nucleosome arrays (Fransz et al., 2003; Heitz, 1928; Sun et al., 2001). In nuclei of mammals and some other eukaryotes these domains are relatively well organized in the nucleus with heterochromatin mainly localized towards the nuclear periphery and euchromatin at the interior of the nucleus (de Nooijer et al., 2009; Solovei et al., 2004; Ye et al., 1997).

The ability of a gene to be transcribed depends on its accessibility to the transcription machinery. In fact nucleosomal DNA represents a barrier to many protein complexes that need to contact with the DNA and regulate gene expression (Kireeva et al., 2002). There are two main mechanisms by which the accessibility of genes can be regulated for transcription at the chromatin level: by the disruption of chromatin itself or by recruiting proteins that are able to specifically recognize the histone motifs in place. The first mechanism implies the disruption of interactions between nucleosomes or between the nucleosome and the DNA,

leaving the chromatin in a poised state favourable for transcription. The second mechanism is better characterized and relies on the recruitment of non-histone chromatin binding proteins. In many cases these proteins have two or more domains, one of which recognizes the modified histone motif using a conserved protein domain, while the other domain exerts one of a variety of regulatory functions. Generally, these functions involve post-translational modifications of histone tails, incorporation of histone variants, or nucleosome sliding or remodelling by the activity of ATP-dependent remodelling complexes.

Here we are going to consider two main aspects of chromatin regulation at the nucleosome level (histone modifications and histone variants) as well as the spatial distribution of genes within the three-dimensional space of the nucleus as means to regulate of transcriptional activity (Fig. 1.1).

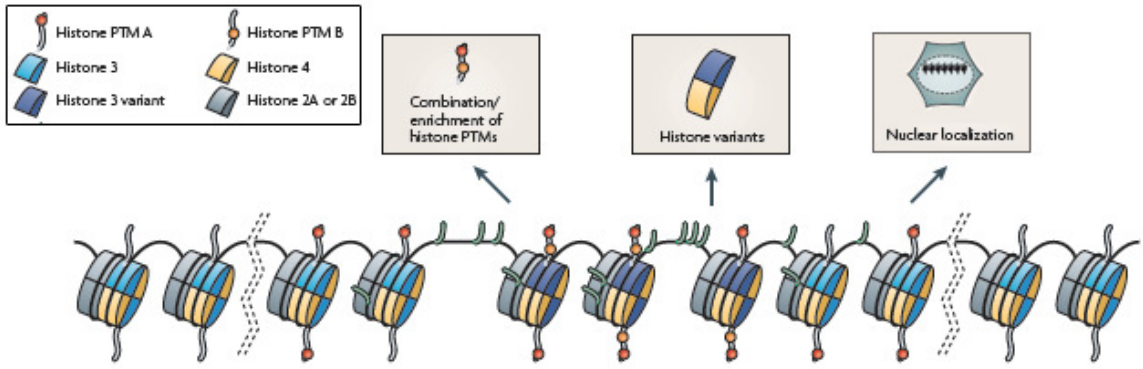

Figure 1.1. Scheme depicting different levels of chromatin regulation. (adapted from (Margueron and Reinberg, 2010)).

1.3. Regulation of gene expression at the level of the nucleosome

1.3.1. Histone modifications

Histone proteins contain flexible N-terminal tails that extend outward from the nucleosome core and that are subject to diverse post-translational modifications (PTMs). Although histone tails are the main targets for post-translational modifications, the histone core domains can also be modified (reviewed in (Cosgrove and Wolberger, 2005)). For the purpose of transcription, histone modifications can be divided into two groups: activation-related and repressive marks. In general acetylation and phosphorylation have been correlated

with activation while sumoylation, deimination, and proline isomerization have been associated with repressive states. Alternatively others like ubiquitination and methylation are known to be correlated both with activation and repression. (Berger, 2002; Jenuwein and Allis, 2001; Turner, 2002). These correlations led to the establishment of the histone code theory, which proposes that histone modifications act sequentially or in combination to recruit binding proteins to specific tasks (Strahl and Allis, 2000).

In recent years the number of modifications that have been identified on histones has increased quite dramatically. Over 8 different classes have been characterized to date and many sites have been described within each class. An additional degree of complexity is that multiple modifications can be added simultaneously in the same nucleosome or even on the same histone tail (Lee et al., 2010) creating an enormous number of regulatory possibilities. This suggests that the regulation is highly complex, rather than being a simple and predictable code in which each modification has a unique effect.

Histone modifications are caused by the direct action of histone-modifying enzymes. During the last few years enzymes have been identified for almost all types of modification (reviewed in (Kouzarides, 2007)). A number of proteins have been identified that are recruited to specific histone modifications. For instance, while methylation is recognized by PHD (Plant Homeo Domain) fingers, acetylation is recognized by bromodomains (Kouzarides, 2007). On the other hand some PTMs of histones have the potential to affect directly histone-DNA interactions playing a role in the accessibility the underlying DNA sequence and therefore in the regulation of gene expression.

1.3.1.1. Histone Acetylation

The best characterized post-translational modification regulating chromatin structure is the acetylation of one or more of the lysine residues in the histone N-terminal tails. Its regulatory role was proposed more than 40 years ago (Allfrey et al., 1964). Histone acetylation is thought to facilitate transcriptional activation either by forming a binding site for bromodomain-containing proteins or by neutralizing the charges of the basic tails that interact with the acidic DNA (Roth et al., 2001). A correlation between histone acetylation and transcriptional activity was shown for instance by immunostaining studies where antibodies specific to acetylated histones were used, revealing differential labelling at different chromosomal regions. In animals, immunolabelling of metaphase chromosomes

with antibodies against acetylated H4 (Hebbes et al., 1994; Jeppesen and Turner, 1993) and H3 (Boggs et al., 1996) revealed that regions enriched in coding DNA were more strongly labelled, in comparison with unlabelled heterochromatin.

Of all modifications acetylation has the highest potential to induce chromatin unfolding. The neutralization of the positive charge of lysine at the histone tails has a strong effect in destabilizing inter-nucleosome contacts and therefore the chromatin structure itself. Experiments in which tail residues were chemically modified on recombinant histone core preparations showed that acetylation of histone H4 on lysine 16 (H4-K16Ac) has a negative effect on the formation a higher order chromatin structures *in vitro* (Shogren-Knaak et al., 2006).

The enzymes that acetylate histones, the histone acetyltransferases, are classified into three main families, GNAT, MYST and CBP/p300 (Sterner and Berger, 2000). In general these enzymes can modify many different lysine residues but some are specifically limited to certain residues (reviewed in (Kouzarides, 2007)). Histone acetylation can be reversed by histone deacetylase enzymes that remove acetyl groups from the acetylated histone tails. Their activity is correlated with chromatin condensation and gene repression (Khochbin et al., 2001). The acetylation status of a given gene is therefore controlled by the balance between the activity of histone acetyltransferases (HAC) and histone deacetylases (HDACs).

1.3.1.2. Histone Methylation

The modification of histones by methylation has been known for many years but its function has only recently begun to be understood. Histone methylation marks can be correlated both with repression and with transcriptional activation. In contrast to histone acetyltransferases, histone methyltransferases are highly specific and may be restricted to modification of one single lysine in a single histone (Bannister and Kouzarides, 2005). For example, the lysine residues H3K4, H3K36 and H3K79 are methylation sites implicated in transcription while H3K9, H3K27 and H4K20 are methylation sites correlated with transcriptional repression. Additionally, lysine residues can be mono-, di- or trimethylated and each of these forms can have unique biological functions. For instance, in the budding yeast, dimethylated H3K4 occurs at both active and inactive genes whereas trimethylated H3K4 is present exclusively in active genes (Santos-Rosa et al., 2002). Many proteins have been identified that are able to recognize specific histone modifications. Recently, the

isolation of several proteins capable of recognizing H3K4me highlighted their role in tethering enzymatic activity onto chromatin. For instance the chromo-containing HP1 protein is recruited to H3K9me sites and brings with it deacetylase activity which in turn prevent the accessibility of the underlying DNA sequence to the transcription machinery (Fischle et al., 2005).

Rapid progress lasting recent years has brought plenty of data about the diverse roles and mechanisms of histone modifications in regulating gene expression. However not much is known about the interplay between the mechanisms responsible for the addition and removal of these marks and how they are involved in orchestrating development. Further studies to reveal the molecular role of these factors will be necessary to understand the mechanisms underlying cell differentiation and development.

1.3.2. Histone Variants

Histone modifications and their implications for chromatin structure and regulatory processes that act on DNA, such as replication, repair and regulation of gene expression, have long been recognized. Similarly to histone modifications, the incorporation of histone variants into chromatin contributes to its regulatory repertoire.

The expression of most of histones is tightly coupled to S phase of the cell cycle, when the newly synthesized DNA requires additional histone molecules (Henikoff and Ahmad, 2005). These histones are generally designated “canonical” histones and in most metazoans are found clustered in repeat arrays (Talbert and Henikoff, 2010). In contrast, histone variant genes are found dispersed in the genome and are expressed through all phases of the cell cycle (Malik and Henikoff, 2003). These variants possess particular characteristics that can dictate the switching on and off of the genes they are associated with, as well as other roles including DNA repair, meiotic recombination and chromosome segregation.

With the exception of histone H4, all of the core histones have a number of variants which probably arose through gene duplication (Malik and Henikoff, 2003). Here, we will focus on the histone variants with widespread occurrence and that have been so far better characterized - CenH3, H3.3 and H2AZ. The evolutionary origin of these histones dates back to the earliest known diversifications of eukaryotes (Talbert and Henikoff, 2010) and they can alter fundamental properties of the chromatin. However the molecular mechanisms and the specific integration pathways are not yet fully understood.

1.3.2.1. cenH3

The cenH3 is an H3 variant that is specialized for packaging chromatin at eukaryotic centromeres and is essential for the assembly of kinetochores (Buchwitz et al., 1999; Henikoff et al., 2000; Meluh et al., 1998; Palmer et al., 1991). Centromeres are specialized chromatin structures within eukaryotic chromosomes that ensure their correct segregation at mitosis. Thus the presence of cenH3 is essential for cell division, acting as an epigenetic mark to specify the positions of centromeres and their perpetuation from one generation to the next.

CenH3 variants have unusual features. Relative to the canonical H3, which is one of the most conserved proteins, cenH3 sequences are surprisingly divergent. Sequence analysis has revealed 50-60% similarity with the canonical form at the C-terminal histone-fold domain (HFD) and little or no conservation at the N-terminal region (Henikoff et al., 2001). In spite of these differences the function of cenH3 in organizing the kinetochores seems to be universal. Recent studies revealed that yeast cenH3 (Cse4) can substitute human centromeric H3 (CENPA) (Wieland et al., 2004). In this study, CENPA depleted cells induced by RNA interference were functionally complemented by expression of yeast Cse4. These results showed that there are conserved features in the structure of cenH3 nucleosomes that account for their universal role in forming the centromeres among different organisms.

The dynamic behaviour of cenH3 was studied in Arabidopsis by developing transgenic lines in which this variant was tagged with GFP (Fang and Spector, 2005). Using four-dimensional (4-D) live cell imaging, it was shown that the centromeres are constrained at the nuclear periphery during interphase but that global centromere position is not precisely transmitted from the mother cell to daughter cells.

CenH3-containing nucleosomes have been traditionally considered as octamers; however recent studies suggest that they might be organized as tetramers. Evidence for that comes from MNase (Micrococcal nuclease) assays in Drosophila (Dalal et al., 2007). Unlike canonical nucleosomes that are wrapped around ~150bp of DNA, cenH3 is wrapped around smaller sequences. Additionally, measurements by atomic force microscopy showed that CID (*Drosophila melanogaster* cenH3) nucleosomes have only half of the height of canonical nucleosomes. Together these observations support a model in which cenH3-containing nucleosomes consist of stable heterotypic tetramers (cenH3, H4, H2A and H2B) - the "hemisome" model (Dalal et al., 2007). However this composition is still a matter of debate. For instance, for the budding yeast CenH3 (Cse4), there are at the moment three models for

the composition of CenH3-containing-nucleosome: the octasome, the hemisome and the hexasome models (Camahort et al., 2009).

Another potentially important feature of cenH3 variants is that in common with archeal histones, they induce positive supercoils in DNA (Furuyama and Henikoff, 2009). This positive coiling is proposed to resist the mitotic negative coiling of chromosomes during mitosis. This feature might be important in that it allows the centromeres to be accessible to kinetochores and kinetochore proteins during chromosome segregation (Talbert and Henikoff, 2010).

1.3.2.2. H3.3

Besides cenH3, other H3 variants have been reported. H3.3 differs from the canonical H3 only at four amino acid residues and is known to be incorporated into chromatin in a replication independent fashion (Ahmad and Henikoff, 2002). Three of these amino acid substitutions have been shown to be important for replication independent incorporation into chromatin. Mutation in any of these three residues was shown to be sufficient to confer partial replication independent activity to the canonical H3 (Ahmad and Henikoff, 2002).

Additionally, while the canonical H3 is incorporated in chromatin by the chromatin-assembly factor 1 (CAF1) during DNA replication and repair, H3.3 is assembled into chromatin by another complex – histone regulator A (HIRA) – independently of DNA synthesis (Tagami et al., 2004).

In spite of the close similarity in amino acid sequence with the canonical form, H3.3s exhibit distinct posttranslational “signatures” that in turn, influence epigenetic states during cellular differentiation and development. This variant is enriched for the presence of marks, such as di- and tri-methylation of K4, acetylation at K9, K18 and K23, and methylation of K79, that reflect transcriptional competence (Hake and Allis, 2006). H3.3 is therefore present at active loci as previously suggested by the observation that H3.3 was incorporated into active rDNA (Ahmad and Henikoff, 2002). To examine H3.3, many groups have made use of tagged versions of the protein to perform Chromatin Immunoprecipitation (ChIP) and have shown that it is generally present at actively transcribed regions (Chow et al., 2005; Mito et al., 2005; Wirbelauer et al., 2005). In addition, fluorescently labelled H3.3 has been shown to be incorporated *in vivo* into a transgene array as the array undergoes activation (Janicki et al., 2004).

Studies in *D. melanogaster* revealed that H3.3 is turned over more rapidly than H3 (Schwartz and Ahmad, 2005), which might contribute to keeping chromatin accessible in transcribed genes. It was also shown recently that nucleosomes containing tagged H3.3 in chicken cells are more sensitive to salt based disruption than those containing the canonical H3 (Jin and Felsenfeld, 2007). A possible explanation for the reduced stability of H3.3 containing nucleosomes comes from the fact that three amino acid residues that differ from the canonical H3 do not make contact with H2A or H2B, leaving those nucleosomes containing them more susceptible to disruption by cellular processes such as transcription, chromatin remodelling and modification (Talbert and Henikoff, 2010). On that basis, H3.3-containing nucleosomes seem to be intrinsically less stable and this may reduce the energy needed to move or displace nucleosomes from promoter, enhancers and gene-coding regions.

1.3.2.3. H2A.Z

H2A.Z is a highly conserved variant of the canonical histone H2A. Phylogenetic analysis indicates that H2A.Z diverged from the canonical form early on during the evolution of eukaryotes but since then it has been fairly well conserved. In fact, the H2A.Z variants of different organisms show a higher degree of sequence similarity (approximately 90%) than the H2A.Z and H2A within the same organism (Thatcher and Gorovsky, 1994; van Daal et al., 1990).

The H2A.Z variant has been widely studied and has been shown to be essential in both mammals and in Drosophila (Clarkson et al., 1999; Faast et al., 2001). In *Saccharomyces cerevisiae* it is not essential for viability but has a function that can not be substituted by the canonical H2A (Jackson and Gorovsky, 2000). Unlike the single, non-essential H2A.Z gene from yeast, higher organisms have several H2A.Z genes. Vertebrates have two H2A.Z genes (H2A.Z1 and H2AZ.2) which encode proteins that differ by three residues (Eirin-Lopez et al., 2009). In *Arabidopsis thaliana* there are three different H2A.Z genes (HTA11, HTA8 and HTA9) which are redundant to some extent and differ in cell-cycle regulation (March-Diaz et al., 2008).

The H2A.Z variant is incorporated into nucleosomes by the action of a specific multi-subunit complex termed SWR1 in yeast and SRCAP in humans. SWR1 is an ATP-dependent remodelling complex that exchanges H2A-H2B dimers for H2A.Z-H2B in the nucleosomes (Cai et al., 2005; Choi et al., 2009; Krogan et al., 2003; Mizuguchi et al., 2004). Little is

known about how H2A.Z is incorporated into specific chromatin regions, but it has been suggested that the bromodomain factor 1 (BDF1) binds to acetylated histone tails, targeting the SWR-H2A.Z complex to chromatin containing acetylated H3 and H4 (Ladurner et al., 2003). PIE1 is the homologue of SWR1 in Arabidopsis (Noh and Amasino, 2003), and ARP6 and SEF are homologues of Arp6 and Swc6, two conserved subunits of the Swr1 complex in yeast, that, while not being essential, are required for the optimal function of the complex (Choi et al., 2005; Deal et al., 2005; March-Diaz et al., 2007; Martin-Trillo et al., 2006).

In *Tetrahymena thermophila* H2A.Z was found to be associated with the transcriptionally active macronucleus but absent in the transcriptionally inert micronucleus (Allis et al., 1980). These observations suggested for the first time that this variant had a function related with transcription. The crystal structure of H2A.Z-containing nucleosomes suggested that its incorporation subtly destabilises the interface between H2A.Z-H2B and the H3-H4 dimers (Suto et al., 2000). Accordingly chicken nucleosomes reconstituted with H2A.Z were also less stable when assessed by sedimentation at different ionic concentrations (Abbott et al., 2001). However, a separate series of studies has concluded, in contrast, that the incorporation of H2A.Z into chromatin leads to more stable nucleosomes; on the other hand it impedes oligomerization of chromatin fibres suggesting that H2A.Z may create a transcriptionally poised higher order chromatin domain (Fan et al., 2002; Park et al., 2004).

Studies of the properties of H2A.Z-containing nucleosomes have led to conflicting conclusions over the past few years. It appears that in spite of great sequence conservation, its function might have diverged considerably, with different functions described for different organisms (Dryhurst et al., 2004; Guillemette and Gaudreau, 2006). In *Saccharomyces cerevisiae* H2A.Z has been implicated in many diverse biological processes including the control of gene expression (Adam et al., 2001; Brickner et al., 2007; Li et al., 2005; Raisner et al., 2005; Santisteban et al., 2000), cell cycle progression (Dhillon et al., 2006), chromosome segregation (Carr et al., 1994), DNA repair (Downs et al., 2004) and prevention of heterochromatin spreading to euchromatic regions (Meneghini et al., 2003). In higher eukaryotes H2A.Z has roles in suppression of antisense RNAs (Zofall et al., 2009), embryonic stem cell differentiation (Creyghton et al., 2008) and antagonizing DNA methylation in plants (Zilberman et al., 2008). Its function, however, is not well understood given the fact that it has been associated with both euchromatin and heterochromatin.

H2A.Z, surprisingly, can show contradictory functions even within the same organism. In differentiated mouse fibroblasts H2A.Z is distributed across the entire interphase nucleus and is excluded from transcriptionally silent and HP1 enriched

pericentromeric regions (Sarcinella et al., 2007). However in trophoblast cells of the developing mouse embryo, H2A.Z appears to be concentrated at the heterochromatic pericentric regions and colocalizes with HP1 (Rangasamy et al., 2003), suggesting that H2A.Z role switches at different stages of development and differentiation.

Recent studies have suggested one reason why H2A.Z function shows such contrasting effects. Genome-wide ChIP sequencing or ChIP-microarray experiments showed that H2A.Z preferentially localizes in the 5' regions of genes within euchromatic regions (Barski et al., 2007; Guillemette et al., 2005; Li et al., 2005; Raisner and Madhani, 2006; Zhang et al., 2005). It was suggested that the deposition of H2A.Z at the 5' end of genes may act to set up an architecture that is compatible with gene regulation at promoters (Draker and Cheung, 2009). In mammalian cells, mapping of DNA hypersensitive sites, based on the activity of micrococcal nuclease digestion, has been used to define open chromatin regions of the genome, which often correspond to enhancers and promoters (Gross and Garrard, 1988). Overlaying these sites with ChIP-chip data from T cells revealed an enrichment of H2A.Z at DNAse hypersensitive sites (Barski et al., 2007). Therefore the presence of H2A.Z at promoter regions might act so as to maintain an open chromatin structure that in turn allows the binding and action of either transcriptional activators or repressors. This feature of H2A.Z together with differential effects of PTMs or the association with other variants like H3.3 (Jin and Felsenfeld, 2007) may be a possible explanation for the dual behaviour observed of this variant.

Finally, a research in Arabidopsis presented a new concept where H2A.Z-containing nucleosomes provide a thermosensory information for coordinating temperature responses in plants (Kumar and Wigge, 2010). H2A.Z nucleosome occupancy decreases with increasing temperature, independently of local transcription levels. The authors thus propose a model where the tight H2A.Z-nucleosomes are loosen up by higher temperatures. This study suggests that temperature perception may take place at the chromatin level, with H2A.Z-containing nucleosomes monitoring the shifts in ambient temperature and executing the corresponding alterations in global gene expression.

1.3.3. ATP-Dependent remodelling complexes

As described in the previous sections, nucleosomes can be modified either covalently by histone post-translational modifications or by incorporation of histone variants. In addition

to these properties, nucleosomes can also be mobilized to different positions along the DNA, or evicted by ATP-dependent remodelling enzymes. ATP-dependent remodelling factors play an essential role in gene expression by regulating the access of the transcription machinery to DNA sequences (Saha et al., 2006). Generally they are composed of several subunits (up to 15 subunits) one of them being an ATPase belonging to the SNF2 superfamily of DNA helicase/ATPase. The ATPase-containing subunit is embedded in a multiprotein complex which mediates different nucleosome remodelling activities (Langst and Becker, 2004). A number of ATP-dependent chromatin remodelling enzymes have been identified. All eukaryotes contain at least 5 types of ATP-dependent remodellers: SWI/SNF, ISWI, NURD/Mi-2/CHD, INO80 and SWR1 (Saha et al., 2006).

Current data from studies in animals suggest that the biochemical mechanism by which each type of remodeller acts is distinct and may account for their unique biological functions. For example SWI/SNF complexes are able to induce ATP-dependent disruption of nucleosome structure, facilitating the binding of transcription factors to their target sites on nucleosomal templates (Kingston and Narlikar, 1999). In contrast, the ISWI members relocate nucleosomes by sliding the histone octamers along the DNA template (Langst and Becker, 2004). The SWI/SNF subfamily functions mainly in transcriptional activation or repression, while the ISWI subfamily has additional roles in maintaining stable higher-order chromatin structure and chromatin assembly. Despite the different outcomes, common mechanisms seem to underlie their action. These mechanisms include both the unwrapping of DNA segments from the nucleosome core and the translocation of DNA loops through the nucleosomes (Strohner et al., 2005; Zofall et al., 2006).

An obvious question is how these ATP remodelers are targeted to the appropriate genomic regions. Different mechanisms have been proposed; the most well studied is based on targeting via DNA-sequence-specific factors (Fazzio et al., 2005). For instance the ISW2 is targeted to the promoters of early meiotic genes by the transcriptional repressor UME6 (Goldmark et al., 2000). The consequence is the formation of an inaccessible chromatin structure that is not compatible with gene expression. The interaction between transcription factors and ATP-dependent remodelling enzymes can also be a mechanism for targeting to specific sites, as described for the interaction between SWI/SNF proteins and the basic-Helix-Loop-Helix (bHLH) proneural transcription factors in neurogenesis (Seo et al., 2005). Other modes targeting ATP-dependent nucleosome remodelling factors that have been proposed include the interaction with methylated DNA and intergenic RNA transcription (Feng and Zhang, 2001; Mayer et al., 2006).

Another way by which ATP remodelers regulate chromatin structure and gene regulation is via incorporation of histone variants. One example, mentioned previously, is the ATP-dependent remodelling enzyme responsible exchanging the canonical histone H2A with the variant H2A.Z. The SWR1 complex is named after its ATPase sub-unit Swr1 (for *Swi*2/Snf2 *r*elated). This complex seems to be targeted to specific sites by a mechanism that involves the recognition of histone acetylation. This conclusion came from the identification of Bdf1 (*Bromodomain factor 1*) as a member of the SWR1 complex (Kobor et al., 2004; Krogan et al., 2003). An interesting study revealed that the absence of a functional Bdf1 protein has a similar phenotype as absence of SWR1 or H2A.Z (Ladurner et al., 2003). However it is not yet clear whether Bdf1 is able to recognize specific acetylation motifs, or what sets the signal in the first place.

1.4. Regulation of gene expression by higher-order chromatin organization

Although the nucleosomes represent the basic unit of chromatin compaction, they constitute only the first level of chromatin condensation. The amount of condensation needed for a typical genome to be fitted into an interphase nucleus or set of metaphase chromosomes, indicates that there are additional "higher order" levels of chromatin organization.

In the context of chromatin, higher-order structure may be defined as any reproducible conformation of nucleosomes in 3D space. The most evident form of higher-order chromatin structure is the mitotic/meiotic chromosomes in which the DNA is highly compacted.

Studies on 3D spatial locations and transcriptional competence of genes in respect to their chromosome territories have provided some important insights on the importance of this level of chromatin organization on regulation of gene expression.

1.4.1. Chromosome territories

The idea that chromosomes occupy distinct regions in the interphase nucleus when they are decondensed during interphase was first proposed by Carl Rabl in 1885 (Rabl, 1885) and later developed by Theodor Boveri, who applied the term chromosome territory for the

first time (Bovery, 1909). Years later advances in *in situ* hybridization techniques finally allowed the direct observation of distinct non-overlapping chromosome territories (Manuelidis, 1985; Schardin et al., 1985). The discovery of chromosome territories leads to intriguing questions: Is the position within the nucleus, and the position relative to each other, an inherent property of chromosomes, cell types and tissues? Is such chromosome positioning a cause or consequence of their gene expression state?

The emerging view is that the location of a gene within a chromosome territory seems to influence its access to the machinery responsible for specific nuclear functions, such as transcription. One typical example of relocation within a chromosome territory is the ANT2 (Adenine Nucleotide Translocase-2) gene located on the X chromosome. When present on its inactive homolog this gene is found in the interior of the chromosome territory, however its position changes on the active homolog where it can be found at the periphery of the territory (Dietzel et al., 1999). This observation of an inactive gene being located in the middle of a chromosome territory and its relocation towards the periphery by a "looping out" mechanism has been shown several times (Chambeyron et al., 2005; Volpi et al., 2000) Nevertheless counter observations have also been reported. For instance, in the case of wheat roots transcription sites revealed by BrUTP incorporation were not preferentially localized with respect to the chromosome territorial boundaries but uniformly distributed throughout the nucleoplasm (Abranches et al., 1998). Movements at larger scale have also been reported. Loci undergoing changes in transcriptional status as part of a developmental program can relocate to specific regions of the nucleus. An example of this scenario was provided by the nuclear reorganization that accompanied the differentiation of mouse lymphocytes (Brown et al., 1999; Brown et al., 1997), where lymphoid genes targeted for silencing are relocated to pericentromeric heterochromatin clusters. However it appears that, at least in this example, transcriptional repression precedes the relocation, suggesting that relocation is not vital for transcriptional repression of the gene. In contrast, genes marked for active transcription were shown to move away from centromeric chromatin (Schubeler et al., 2000) or the nuclear periphery (Kosak et al., 2002). Although there is strong evidence regarding the correlation between intra-nuclear or intra-territory location with transcription, the chromatin conformational changes that follow the switch in transcriptional status are still far from being understood.

Although it seems in principle unlikely that the large transcription machinery complexes could access DNA and operate in compact chromatin, making the concept of the chromatin looping to facilitate transcription attractive, the fact is that highly compact

chromatin can still be accessible in some extent. A recent study designed to examine the compaction state of active and inactive chromatin in interphase nuclei has indicated quite small transcription-related changes in higher-order structure, implying that transcription can proceed in quite compact chromatin (Hu et al., 2009).

These observations bring the question of how transcription can proceed in a compact structure that is over 10-times more compact than a 30-nm fiber. In terms of accessibility, several studies have shown that rather large molecules can penetrate compact chromatin structures (Bancaud et al., 2009; Chen et al., 2005; Verschure et al., 2003). This suggests a new view of chromatin behavior in which it is regarded as a highly dynamic structure where binding sites are continuously being scanned by chromatin proteins in a random way. Novel approaches to study these and other dynamics aspects of chromatin such as live cell imaging and photobleaching are discussed below.

Another possibility is the occurrence of discrete sites for transcription in the nucleus, which have been termed transcription factories (Cook, 1999). According to this model DNA and RNA polymerases are immobilised by attachment to an underlying nuclear substructure or matrix (Cook, 1999). These polymerases are suggested to be concentrated in discrete factories, where they work together on many different templates (reviewed in Cook, 2010). This view arose from visualization of nascent transcripts by BrU incorporation and has some support from recent data produced by technical advances in fluorescence in situ hybridization (FISH) and immunofluorescence-FISH (immuno-FISH), and in molecular approaches such as chromosome conformation capture (3C) and related methods (Dekker, 2006; Simonis et al., 2007) that have the power to scan the genome for sequences or regions that are closely apposed in nuclei. Even though it is an attractive model it still lacks direct evidence and the existence of factories remains a matter of debate (reviewed in(Sutherland and Bickmore, 2009).

1.5. A live-cell imaging approach to study chromatin dynamics

For many years the majority of studies that examined the mechanisms by which chromatin regulates transcriptional activity focused on measuring steady-state levels. A typical biochemical approach is chromatin immunoprecipitation, in which chromatin fragments still associated with histones or other chromatin proteins (after formaldehyde cross-linking) are precipitated using a specific antibody, and the DNA or proteins associated

with the target are then analysed. The trouble with this type of approaches is that often they do not take into account cell type specificity and the dynamic properties of chromatin, leading to rigid assumptions about stable interactions between chromatin and chromatin proteins *in vivo*. Recently, a combination of molecular biology and live cell microscopy techniques has allowed observation of the dynamic behaviour of chromatin *in vivo* within the natural environment of the nucleus.

1.5.1. Measuring histone mobility - FRAP

The first experimental evidence to indicate that the protein composition of chromatin was not static came from radio-labelling studies in the early 1980s (Caron and Thomas, 1981; Louters and Chalkley, 1985; Thomas and Rees, 1983). Using radio-labelled histones, these experiments clearly showed histones being exchanged with pre-existing histones in the chromatin. However, this method did not allow a precise measure of the exchange rates and could not demonstrate exchange in vivo.

New techniques such as fluorescence recovery after photobleaching (FRAP) confirmed that most of the functionally important characteristics of chromatin show a dynamic behaviour. With the development of confocal microscopes and their laser illumination systems, FRAP became a very accessible technique for analyzing the kinetics of molecules in living cells (FRAP is reviewed in (Phair and Misteli, 2001; White and Stelzer, 1999)). FRAP experiments require that the protein of interest is tagged with a fluorescent label (usually the green fluorescent protein, GFP, or a related tag) and expressed in a living cell. A typical FRAP experiment consists of three phases. First, the initial fluorescence intensity is measured, after which a high power laser pulse is used to photobleach the fluorophore in a small region of interest (ROI), and finally the recovery of the fluorescence intensity in that region is monitored in a time-course series. The exchange of non-bleached proteins for the bleached molecules in the bleached region produces a recovery of fluorescence intensity. In a situation in which all the molecules are immobile, the bleached area remains bleached and unbleached area unaltered, and no recovery is observed. On the other hand, if all the molecules are mobile and free to diffuse, the fluorescence in the bleached area recovers quickly to close to the original intensity levels. In a third situation, when both immobile and mobile fractions are present, the recovery curve reaches a plateau below the level before bleaching, depending on the relative abundance of the two fractions.

The rate at which fluorescence is regained in the photobleached region is determined by the rate at which fluorescent molecules can move from the surrounding unbleached region into the bleached region. By analysing that rate a diffusion constant can be determined.

The first results of FRAP experiments on histone H1-GFP fusion appeared in 2000 (Lever et al., 2000; Misteli et al., 2000). Both studies showed that instead of being permanently fixed in chromatin, the majority of H1 proteins were being exchanged, with a residence time of only a few minutes. In another study a number of nuclear proteins fused to GFP confirmed the earlier results on H1 and additionally demonstrated that a wide class of other nuclear proteins have also a high turnover rate (Phair et al., 2004). These results indicated that chromatin-binding proteins find their binding sites by 3D scanning of the nuclear space and that this property might be crucial for generating high plasticity in genome expression.

Apart from histone H1 the mobility of many other histones has also been assessed by FRAP (reviewed in (Kimura, 2005)). Compared to the linker histone H1, core histones have much slower exchange rates. Generally, core histones have a small pool of free proteins and another pool that is tightly bound to the DNA, with residence times of several minutes. H3 and H4 assemble to DNA during replication and only a minor population is exchanged independently of transcription and replication (Kimura and Cook, 2001). H2B and H2A, however, exhibit considerably higher exchange rates. In HeLa cell lines H2B seems to have different populations of molecules that exchange at different rates. There is a small population that exchanges rapidly, another population (~40%) that exchanges slowly ($t_{1/2}$ ~130 min) independent of ongoing DNA replication and transcription, and another (>50%) that remains bound stably ($t_{1/2} > 8.5$ h) (Kimura and Cook, 2001).

The mechanism that accounts for the differences in kinetics between different histones and between the different pools within the same type of histone is related to differences in biochemical modifications. For instance it is known that acetylation of histone tails alters the stability of nucleosomes and also has been shown to alter the dynamics of H2B in living cells (Higashi et al., 2007). Acetylation of histone tails also appears to facilitate chaperone-mediated histone exchange; *in vitro* studies showed that the transfer of H2A–H2B from nucleosomes to histone chaperone Nap1 (nucleosomes assembly protein 1) is facilitated by p300-mediated acetylation (Ito et al., 2000). Although we are only now beginning to understand the kinetics of different histone variants and FRAP analysis has yet to be carried out for the majority of the variants, it is very likely that these histones have different

mobilities compared with the canonical forms and that their incorporation has the potential to affect of histone and nucleosome stability as already suggested by biochemical approaches.

Recently the development of photoswitchable or photoactivatable tags has made them an optimal tool for studying the spatial and temporal dynamics of proteins *in vivo* (Lippincott-Schwartz et al., 2003). As the activation/conversion process is quicker than bleaching, it is more suitable than FRAP for measuring fast diffusion kinetics. Another advantage of photoactivation/conversion is that a much lower laser intensity is required for activation or conversion than with bleaching, thus substantially reducing photodamage to cells. Additionally, as the fluorescence of these proteins comes only after photoactivation, newly synthesized non-photoactivated pools are unobserved and do not complicate experimental results. This signal independence from new protein synthesis also allows the study of protein degradation of tagged molecules by 'optical pulse labelling' and monitoring of the fluorescence over time.

1.5.2. Single particle tracking to study gene positioning – Operon Lac system

While it is clear that spatial organization of chromatin in the nucleus is highly correlated with gene expression, the majority of the techniques used to study chromatin structure are unable to reveal a real dynamic view, providing instead a static analysis under a particular condition. The observation of chromatin motion requires the labelling of specific chromatin loci with techniques that are compatible with live cell imaging.

Recently taking advantage of the exploitation of bacterial repressor/operator interactions in conjugation with GFP technology, significant breakthroughs in this field have been possible. Two systems are currently in use: one is based on the *lac* operator/repressor (*lac*O/LacI) (Belmont, 2001; Belmont and Straight, 1998; Straight et al., 1996), while the second one uses tet operator/repressor (tetO/TetR) (Fuchs et al., 2002; Michaelis et al., 1997). Both systems rely on the genomic integration of the operator arrays in eukaryotic cells that express the bacterial repressor protein fused with GFP permitting therefore the tracking of specific chromosomal sites by real time fluorescence microscopy (Belmont et al., 1999; Robinett et al., 1996). The locus can be detected through the binding of the repressor protein which is fused to GFP and has a nuclear localization signal added. The tagged sequence is seen as a bright dot in the nucleus which has generally a dim background fluorescent signal due to unbound GFP-LacI repressor. The movement of this bright dot can be followed and

the measured trajectory can be analyzed to obtain information about the mechanisms by which the tagged sequence is moving.

The initial surprise from this approach was the dynamic behaviour that chromatin exhibits in both yeast and *Drosophila* nuclei (Marshall et al., 1997; Vazquez et al., 2001). These studies showed for the first time that the GFP tagged chromatin loci undergo constrained Brownian motion within a limited sub-region of the nucleus during interphase. The amplitude of these movements seemed to be dependent on position within the nucleus; the chromatin associated with nucleolus or localized at the nuclear periphery was shown to be more restricted in its movements than other more nucleoplasmic genomic regions (Chubb et al., 2002). In another study, it was shown that sites with higher levels of transcription explored larger regions (Rosa et al., 2006). Studies in CHO (chinese hamster ovary) cells showed that a specific DNA region changed its position from the periphery to the centre of the nucleus upon transcriptional induction by the transcriptional activator VP16 (Tumbar and Belmont, 2001). These observations raised several interesting questions: what is the significance of these movements? Is this mobility a result of an active energy-dependent process?

Experiments in yeast showed that early and late origins of replication were more mobile in G1 than in S phase, and that the movement in G1 was highly sensitive to ATP depletion and changes in metabolic status (Heun et al., 2001). This correlation makes it unlikely that the movement results from a simple diffusion mechanism. Therefore it was proposed that the movement reflects the action of large ATP-dependent enzymes involved in transcription or chromatin remodelling. This hypothesis is consistent with the reduced mobility detected in stationary phase cells where transcriptional activity drops substantially (DeRisi et al., 1997).

One drawback of this type of approach is the high sensitivity to photodamage and bleaching. It was shown for both yeast and mammalian cells that the movement of the tagged sequence is affected by long time-course imaging (Chuang et al., 2006; Hediger et al., 2004). Thus other types of microscopes such as two-photon microscopes (reviewed in (Svoboda and Yasuda, 2006) have been suggested as possible alternatives for imaging with improved photostability of the sample (Levi et al., 2005).

In summary, as the field of chromatin dynamics has developed, it has become increasingly clear that a large number of underlying physical and molecular phenomena are involved, and that to fully understand them, information at many different levels is required. The study of chromatin dynamics and its effect on gene expression has opened new and

exciting perspectives and one important goal of current research is to be able to relate these different levels of regulation. Advances and new strategies that allow "super" resolution in light microscopy will soon be in common use and may open the way to this type of correlative work.

1.6. The model plant *Arabidopsis thaliana*

Arabidopsis thaliana is a small dicotyledonous species and a member of the mustard (Brassicaceae) family. Over the last 30 years because of several traits that make it very advantageous for laboratory experimentation it has been extensively used for genetic, biochemical and physiological research, as well as evolution, population genetics and plant development. It has a fast life cycle of about 6 weeks, and produces numerous self progeny (~10,000 seeds/plant)**.** The space requirements are very limited (100-500 plants can be grown through their life cycle in a 20x30cm flat of soil), and it is easily grown in a greenhouse or indoor growth chamber.

With the completion of the *Arabidopsis* genome sequencing project in 2000 (Initiative, 2000), we now have available the full genome sequence, and an updated version of the genome is now maintained by The Arabidopsis Information Resource (TAIR). An extensive toolkit for manipulation has also been developed over the last decades, including efficient mutagenesis, facile transformation technology, and DNA, RNA, protein, and metabolite isolation and detection methods.

All together, these traits make *Arabidopsis* an ideal model organism for biological research and the species of choice for a large and growing community of scientists studying complex, advanced multicellular organisms.

Arabidopsis is also well suited to be used as a model organism to study chromatin organization and dynamics. It has a relatively small genome (~150 Mb) with 5 chromosomes and a simple heterochromatin organisation. Heterochromatin is restricted to pericentromeric regions of all five chromosomes and to Nucleolus Organizer Region (NOR) which are confined to chromosomes 2 and 4 (Fransz et al., 1998). In interphase nuclei, heterochromatin is organized as clearly distinguishable chromocenters visible as dark spots with phase-contrast microscopy or as bright, fluorescent domains after DAPI staining. In total 10 chromocenters can be visualised in theory; however in most interphase nuclei fewer chromocenters are visible due to their tendency to cluster (Fransz et al., 2002). The

chromocenters are possibly involved in controlling the expression of euchromatic sequences. The current model of nuclear organization states that euchromatic gene rich regions are organized into loops that are between 200kb and almost entire chromosome arms in length, which are attached to the chromocenter (Fransz et al., 2002; Fransz et al., 2003).

Since chromatin organization has an important role in controlling nuclear processes involved in development it is useful to understand the principles underlying these rearrangements. In this work we looked at how different features of chromatin organization affect three aspects of Arabidopsis development: root and root-hair development and flowering time. We will present a brief introduction of each of these aspects at the beginning of each chapter.

1.7. Thesis scope

The vast amount of information enclosed in the DNA of all eukaryotic organisms has to be highly organized and tightly controlled in order to allow the proper expression of sets of genes in space and time. The mechanism by which organisms are able to organize its DNA in such a way is a fundamental problem in biology and key to understanding the development of multicellular organisms. While a large number of factors and protein complexes are known to be involved in the regulation of chromatin states affecting transcription their biological function and repercussions on development are only now beginning to be revealed. The main goal of this thesis is to assess how different aspects of chromatin organization such as histone exchanging dynamics, histone modifications, histone variants or gene 3D nuclear positioning, play a role on various aspects of development.

We used as model system the root *of Arabidopsis thaliana*. The root of Arabidopsis has a simple organization; furthermore this thin organ (150 µm in thickness) allows microscopic studies on nuclei in an intact organ.

In recent years it has been shown that chromatin is quite dynamic, and even histones can be rapidly exchanged. In chapters 2 and 3, we examined how histone exchanging dynamics and histone acetylation affect plant cell differentiation. For that we used the well established developmental gradient of the Arabidopsis root (chapter 2) along with stem cells located at the root tip (chapter 3) to evaluate the mobility of different histone-GFP fusion proteins during cell differentiation.

Eukaryotic gene expression is also partially regulated by histone variants that can be build into a nucleosome, altering binding affinity to chromatin or affecting regulatory processes acting on DNA. H2A.Z, a highly conserved variant of histone H2A, is of particular interest because it is essential for viability in multicellular organisms and it has been implicated in many distinct and even contradictory functions. Despite the extensive evidence implicating H2A.Z in maintenance of genome stability, centromere structure and function, a role for H2A.Z in cell fate decisions has been only poorly investigated. In chapter 4, we looked at how the incorporation of the histone variant H2A.Z affects cell fate decisions during root hair development.

Finally, the physical position in the nucleus is also an emerging theme in gene regulation. In chapter 5, we analyzed the repositioning of alleles of a Polycomb target locus during an environmentally triggered silencing process involved in the control of flowering time - vernalization.

The final chapter discusses the results described in this thesis, and evaluates microscopic techniques that are currently used in studies on chromatin organization and dynamics.

1.8. References

Abbott, D.W., Ivanova, V.S., Wang, X., Bonner, W.M., and Ausio, J. (2001). Characterization of the stability and folding of H2A.Z chromatin particles: implications for transcriptional activation. J Biol Chem *276*, 41945-41949.

Abranches, R., Beven, A.F., Aragon-Alcaide, L., and Shaw, P.J. (1998). Transcription sites are not correlated with chromosome territories in wheat nuclei. J Cell Biol *143*, 5-12.

Adam, M., Robert, F., Larochelle, M., and Gaudreau, L. (2001). H2A.Z is required for global chromatin integrity and for recruitment of RNA polymerase II under specific conditions. Mol Cell Biol *21*, 6270-6279.

Ahmad, K., and Henikoff, S. (2002). The histone variant H3.3 marks active chromatin by replication-independent nucleosome assembly. Mol Cell *9*, 1191-1200.

Allfrey, V.G., Faulkner, R., and Mirsky, A.E. (1964). Acetylation and Methylation of Histones and Their Possible Role in the Regulation of Rna Synthesis. Proc Natl Acad Sci U S A *51*, 786-794.

Allis, C.D., Glover, C.V., Bowen, J.K., and Gorovsky, M.A. (1980). Histone variants specific to the transcriptionally active, amitotically dividing macronucleus of the unicellular eucaryote, Tetrahymena thermophila. Cell *20*, 609-617.

Bancaud, A., Huet, S., Daigle, N., Mozziconacci, J., Beaudouin, J., and Ellenberg, J. (2009). Molecular crowding affects diffusion and binding of nuclear proteins in heterochromatin and reveals the fractal organization of chromatin. EMBO J *28*, 3785-3798.

Bannister, A.J., and Kouzarides, T. (2005). Reversing histone methylation. Nature *436*, 1103-1106.

Barski, A., Cuddapah, S., Cui, K., Roh, T.Y., Schones, D.E., Wang, Z., Wei, G., Chepelev, I., and Zhao, K. (2007). High-resolution profiling of histone methylations in the human genome. Cell *129*, 823-837.

Belmont, A.S. (2001). Visualizing chromosome dynamics with GFP. Trends in cell biology *11*, 250-257.

Belmont, A.S., Li, G., Sudlow, G., and Robinett, C. (1999). Visualization of large-scale chromatin structure and dynamics using the lac operator/lac repressor reporter system. Methods Cell Biol *58*, 203-222.

Belmont, A.S., and Straight, A.F. (1998). In vivo visualization of chromosomes using lac operator-repressor binding. Trends in cell biology *8*, 121-124.

Berger, S.L. (2002). Histone modifications in transcriptional regulation. Curr Opin Genet Dev *12*, 142-148.

Boggs, B.A., Connors, B., Sobel, R.E., Chinault, A.C., and Allis, C.D. (1996). Reduced levels of histone H3 acetylation on the inactive X chromosome in human females. Chromosoma *105*, 303-309.

Bovery, T. (1909). Die Blastomerenkerne von Ascaris megalocephala und die Theorie der Chromosomenindividualitat. Archiv fur Zellforschung *3*, 181-286.

Brickner, D.G., Cajigas, I., Fondufe-Mittendorf, Y., Ahmed, S., Lee, P.C., Widom, J., and Brickner, J.H. (2007). H2A.Z-mediated localization of genes at the nuclear periphery confers epigenetic memory of previous transcriptional state. PLoS Biol *5*, e81.

Brown, K.E., Baxter, J., Graf, D., Merkenschlager, M., and Fisher, A.G. (1999). Dynamic repositioning of genes in the nucleus of lymphocytes preparing for cell division. Mol Cell *3*, 207-217.

Brown, K.E., Guest, S.S., Smale, S.T., Hahm, K., Merkenschlager, M., and Fisher, A.G. (1997). Association of transcriptionally silent genes with Ikaros complexes at centromeric heterochromatin. Cell *91*, 845-854.

Buchwitz, B.J., Ahmad, K., Moore, L.L., Roth, M.B., and Henikoff, S. (1999). A histone-H3-like protein in C. elegans. Nature *401*, 547-548.

Cai, Y., Jin, J., Florens, L., Swanson, S.K., Kusch, T., Li, B., Workman, J.L., Washburn, M.P., Conaway, R.C., and Conaway, J.W. (2005). The mammalian YL1 protein is a shared

subunit of the TRRAP/TIP60 histone acetyltransferase and SRCAP complexes. J Biol Chem *280*, 13665-13670.

Camahort, R., Shivaraju, M., Mattingly, M., Li, B., Nakanishi, S., Zhu, D., Shilatifard, A., Workman, J.L., and Gerton, J.L. (2009). Cse4 is part of an octameric nucleosome in budding yeast. Mol Cell *35*, 794-805.

Caron, F., and Thomas, J.O. (1981). Exchange of histone H1 between segments of chromatin. J Mol Biol *146*, 513-537.

Carr, A.M., Dorrington, S.M., Hindley, J., Phear, G.A., Aves, S.J., and Nurse, P. (1994). Analysis of a histone H2A variant from fission yeast: evidence for a role in chromosome stability. Mol Gen Genet *245*, 628-635.

Chambeyron, S., Da Silva, N.R., Lawson, K.A., and Bickmore, W.A. (2005). Nuclear re-organisation of the Hoxb complex during mouse embryonic development. Development *132*, 2215-2223.

Chen, D., Dundr, M., Wang, C., Leung, A., Lamond, A., Misteli, T., and Huang, S. (2005). Condensed mitotic chromatin is accessible to transcription factors and chromatin structural proteins. J Cell Biol *168*, 41-54.

Choi, J., Heo, K., and An, W. (2009). Cooperative action of TIP48 and TIP49 in H2A.Z exchange catalyzed by acetylation of nucleosomal H2A. Nucleic Acids Res *37*, 5993-6007.

Choi, K., Kim, S., Kim, S.Y., Kim, M., Hyun, Y., Lee, H., Choe, S., Kim, S.G., Michaels, S., and Lee, I. (2005). SUPPRESSOR OF FRIGIDA3 encodes a nuclear ACTIN-RELATED PROTEIN6 required for floral repression in Arabidopsis. Plant Cell *17*, 2647-2660.

Chow, C.M., Georgiou, A., Szutorisz, H., Maia e Silva, A., Pombo, A., Barahona, I., Dargelos, E., Canzonetta, C., and Dillon, N. (2005). Variant histone H3.3 marks promoters of transcriptionally active genes during mammalian cell division. EMBO Rep *6*, 354-360.

Chuang, C.H., Carpenter, A.E., Fuchsova, B., Johnson, T., de Lanerolle, P., and Belmont, A.S. (2006). Long-range directional movement of an interphase chromosome site. Curr Biol *16*, 825-831.

Chubb, J.R., Boyle, S., Perry, P., and Bickmore, W.A. (2002). Chromatin motion is constrained by association with nuclear compartments in human cells. Curr Biol *12*, 439-445.

Clarkson, M.J., Wells, J.R., Gibson, F., Saint, R., and Tremethick, D.J. (1999). Regions of variant histone His2AvD required for Drosophila development. Nature *399*, 694-697.

Cook, P.R. (1999). The organization of replication and transcription. Science *284*, 1790-1795.

Cosgrove, M.S., and Wolberger, C. (2005). How does the histone code work? Biochem Cell Biol *83*, 468-476.

Creyghton, M.P., Markoulaki, S., Levine, S.S., Hanna, J., Lodato, M.A., Sha, K., Young, R.A., Jaenisch, R., and Boyer, L.A. (2008). H2AZ is enriched at polycomb complex target genes in ES cells and is necessary for lineage commitment. Cell *135*, 649-661.

Dalal, Y., Wang, H., Lindsay, S., and Henikoff, S. (2007). Tetrameric structure of centromeric nucleosomes in interphase Drosophila cells. PLoS Biol *5*, e218.

de Nooijer, S., Wellink, J., Mulder, B., and Bisseling, T. (2009). Non-specific interactions are sufficient to explain the position of heterochromatic chromocenters and nucleoli in interphase nuclei. Nucleic Acids Res *37*, 3558-3568.

Deal, R.B., Kandasamy, M.K., McKinney, E.C., and Meagher, R.B. (2005). The nuclear actin-related protein ARP6 is a pleiotropic developmental regulator required for the maintenance of FLOWERING LOCUS C expression and repression of flowering in Arabidopsis. Plant Cell *17*, 2633-2646.

Dekker, J. (2006). The three 'C' s of chromosome conformation capture: controls, controls, controls. Nat Methods *3*, 17-21.

DeRisi, J.L., Iyer, V.R., and Brown, P.O. (1997). Exploring the metabolic and genetic control of gene expression on a genomic scale. Science *278*, 680-686.

Dhillon, N., Oki, M., Szyjka, S.J., Aparicio, O.M., and Kamakaka, R.T. (2006). H2A.Z functions to regulate progression through the cell cycle. Mol Cell Biol *26*, 489-501.

Dietzel, S., Schiebel, K., Little, G., Edelmann, P., Rappold, G.A., Eils, R., Cremer, C., and Cremer, T. (1999). The 3D positioning of ANT2 and ANT3 genes within female X chromosome territories correlates with gene activity. Exp Cell Res *252*, 363-375.

Downs, J.A., Allard, S., Jobin-Robitaille, O., Javaheri, A., Auger, A., Bouchard, N., Kron, S.J., Jackson, S.P., and Cote, J. (2004). Binding of chromatin-modifying activities to phosphorylated histone H2A at DNA damage sites. Mol Cell *16*, 979-990.

Draker, R., and Cheung, P. (2009). Transcriptional and epigenetic functions of histone variant H2A.Z. Biochem Cell Biol *87*, 19-25.

Dryhurst, D., Thambirajah, A.A., and Ausio, J. (2004). New twists on H2A.Z: a histone variant with a controversial structural and functional past. Biochem Cell Biol *82*, 490-497.

Eirin-Lopez, J.M., Gonzalez-Romero, R., Dryhurst, D., Ishibashi, T., and Ausio, J. (2009). The evolutionary differentiation of two histone H2A.Z variants in chordates (H2A.Z-1 and H2A.Z-2) is mediated by a stepwise mutation process that affects three amino acid residues. BMC Evol Biol *9*, 31.

Faast, R., Thonglairoam, V., Schulz, T.C., Beall, J., Wells, J.R., Taylor, H., Matthaei, K., Rathjen, P.D., Tremethick, D.J., and Lyons, I. (2001). Histone variant H2A.Z is required for early mammalian development. Curr Biol *11*, 1183-1187.

Fan, J.Y., Gordon, F., Luger, K., Hansen, J.C., and Tremethick, D.J. (2002). The essential histone variant H2A.Z regulates the equilibrium between different chromatin conformational states. Nat Struct Biol *9*, 172-176.

Fang, Y., and Spector, D.L. (2005). Centromere positioning and dynamics in living Arabidopsis plants. Mol Biol Cell *16*, 5710-5718.

Fazzio, T.G., Gelbart, M.E., and Tsukiyama, T. (2005). Two distinct mechanisms of chromatin interaction by the Isw2 chromatin remodeling complex in vivo. Mol Cell Biol *25*, 9165-9174.

Feng, Q., and Zhang, Y. (2001). The MeCP1 complex represses transcription through preferential binding, remodeling, and deacetylating methylated nucleosomes. Genes Dev *15*, 827-832.

Finch, J.T., and Klug, A. (1976). Solenoidal model for superstructure in chromatin. Proc Natl Acad Sci U S A *73*, 1897-1901.

Fischle, W., Tseng, B.S., Dormann, H.L., Ueberheide, B.M., Garcia, B.A., Shabanowitz, J., Hunt, D.F., Funabiki, H., and Allis, C.D. (2005). Regulation of HP1-chromatin binding by histone H3 methylation and phosphorylation. Nature *438*, 1116-1122.

Fransz, P., Armstrong, S., Alonso-Blanco, C., Fischer, T.C., Torres-Ruiz, R.A., and Jones, G. (1998). Cytogenetics for the model system Arabidopsis thaliana. Plant J *13*, 867-876.

Fransz, P., De Jong, J.H., Lysak, M., Castiglione, M.R., and Schubert, I. (2002). Interphase chromosomes in Arabidopsis are organized as well defined chromocenters from which euchromatin loops emanate. Proc Natl Acad Sci U S A *99*, 14584-14589.

Fransz, P., Soppe, W., and Schubert, I. (2003). Heterochromatin in interphase nuclei of Arabidopsis thaliana. Chromosome Res *11*, 227-240.

Fuchs, J., Lorenz, A., and Loidl, J. (2002). Chromosome associations in budding yeast caused by integrated tandemly repeated transgenes. J Cell Sci *115*, 1213-1220.

Furuyama, T., and Henikoff, S. (2009). Centromeric nucleosomes induce positive DNA supercoils. Cell *138*, 104-113.

Goldmark, J.P., Fazzio, T.G., Estep, P.W., Church, G.M., and Tsukiyama, T. (2000). The Isw2 chromatin remodeling complex represses early meiotic genes upon recruitment by Ume6p. Cell *103*, 423-433.

Gross, D.S., and Garrard, W.T. (1988). Nuclease hypersensitive sites in chromatin. Annu Rev Biochem *57*, 159-197.

Guillemette, B., Bataille, A.R., Gevry, N., Adam, M., Blanchette, M., Robert, F., and Gaudreau, L. (2005). Variant histone H2A.Z is globally localized to the promoters of inactive yeast genes and regulates nucleosome positioning. PLoS Biol *3*, e384.

Guillemette, B., and Gaudreau, L. (2006). Reuniting the contrasting functions of H2A.Z. Biochem Cell Biol *84*, 528-535.

Hake, S.B., and Allis, C.D. (2006). Histone H3 variants and their potential role in indexing mammalian genomes: the "H3 barcode hypothesis". Proc Natl Acad Sci U S A *103*, 6428-6435.

Hebbes, T.R., Clayton, A.L., Thorne, A.W., and Crane-Robinson, C. (1994). Core histone hyperacetylation co-maps with generalized DNase I sensitivity in the chicken beta-globin chromosomal domain. EMBO J *13*, 1823-1830.

Hediger, F., Taddei, A., Neumann, F.R., and Gasser, S.M. (2004). Methods for visualizing chromatin dynamics in living yeast. Methods Enzymol *375*, 345-365.

Heitz, E. (1928). Das heteromchromatin der moose. I Jahrb Wiss Botan *69*.

Henikoff, S., and Ahmad, K. (2005). Assembly of variant histones into chromatin. Annu Rev Cell Dev Biol *21*, 133-153.

Henikoff, S., Ahmad, K., and Malik, H.S. (2001). The centromere paradox: stable inheritance with rapidly evolving DNA. Science *293*, 1098-1102.

Henikoff, S., Ahmad, K., Platero, J.S., and van Steensel, B. (2000). Heterochromatic deposition of centromeric histone H3-like proteins. Proc Natl Acad Sci U S A *97*, 716-721.

Heun, P., Laroche, T., Shimada, K., Furrer, P., and Gasser, S.M. (2001). Chromosome dynamics in the yeast interphase nucleus. Science *294*, 2181-2186.

Higashi, T., Matsunaga, S., Isobe, K., Morimoto, A., Shimada, T., Kataoka, S., Watanabe, W., Uchiyama, S., Itoh, K., and Fukui, K. (2007). Histone H2A mobility is regulated by its tails and acetylation of core histone tails. Biochem Biophys Res Commun *357*, 627-632.

Hu, Y., Kireev, I., Plutz, M., Ashourian, N., and Belmont, A.S. (2009). Large-scale chromatin structure of inducible genes: transcription on a condensed, linear template. J Cell Biol *185*, 87-100.

Initiative, T.A.G. (2000). Analysis of the genome sequence of the flowering plant Arabidopsis thaliana. Nature *408*, 796-815.

Ito, T., Ikehara, T., Nakagawa, T., Kraus, W.L., and Muramatsu, M. (2000). p300-mediated acetylation facilitates the transfer of histone H2A-H2B dimers from nucleosomes to a histone chaperone. Genes Dev *14*, 1899-1907.

Jackson, J.D., and Gorovsky, M.A. (2000). Histone H2A.Z has a conserved function that is distinct from that of the major H2A sequence variants. Nucleic Acids Res *28*, 3811-3816.

Janicki, S.M., Tsukamoto, T., Salghetti, S.E., Tansey, W.P., Sachidanandam, R., Prasanth, K.V., Ried, T., Shav-Tal, Y., Bertrand, E., Singer, R.H.*, et al.* (2004). From silencing to gene expression: real-time analysis in single cells. Cell *116*, 683-698.

Jenuwein, T., and Allis, C.D. (2001). Translating the histone code. Science *293*, 1074-1080.

Jeppesen, P., and Turner, B.M. (1993). The inactive X chromosome in female mammals is distinguished by a lack of histone H4 acetylation, a cytogenetic marker for gene expression. Cell *74*, 281-289.

Jin, C., and Felsenfeld, G. (2007). Nucleosome stability mediated by histone variants H3.3 and H2A.Z. Genes Dev *21*, 1519-1529.

Khochbin, S., Verdel, A., Lemercier, C., and Seigneurin-Berny, D. (2001). Functional significance of histone deacetylase diversity. Curr Opin Genet Dev *11*, 162-166.

Kimura, H. (2005). Histone dynamics in living cells revealed by photobleaching. DNA Repair (Amst) *4*, 939-950.

Kimura, H., and Cook, P.R. (2001). Kinetics of core histones in living human cells: little exchange of H3 and H4 and some rapid exchange of H2B. J Cell Biol *153*, 1341-1353.

Kingston, R.E., and Narlikar, G.J. (1999). ATP-dependent remodeling and acetylation as regulators of chromatin fluidity. Genes Dev *13*, 2339-2352.

Kireeva, M.L., Walter, W., Tchernajenko, V., Bondarenko, V., Kashlev, M., and Studitsky, V.M. (2002). Nucleosome remodeling induced by RNA polymerase II: loss of the H2A/H2B dimer during transcription. Mol Cell *9*, 541-552.

Kobor, M.S., Venkatasubrahmanyam, S., Meneghini, M.D., Gin, J.W., Jennings, J.L., Link, A.J., Madhani, H.D., and Rine, J. (2004). A protein complex containing the conserved Swi2/Snf2-related ATPase Swr1p deposits histone variant H2A.Z into euchromatin. PLoS Biol *2*, E131.

Kornberg, R.D. (1974). Chromatin structure: a repeating unit of histones and DNA. Science *184*, 868-871.

Kosak, S.T., Skok, J.A., Medina, K.L., Riblet, R., Le Beau, M.M., Fisher, A.G., and Singh, H. (2002). Subnuclear compartmentalization of immunoglobulin loci during lymphocyte development. Science *296*, 158-162.

Kouzarides, T. (2007). Chromatin modifications and their function. Cell *128*, 693-705.

Krogan, N.J., Keogh, M.C., Datta, N., Sawa, C., Ryan, O.W., Ding, H., Haw, R.A., Pootoolal, J., Tong, A., Canadien, V.*, et al.* (2003). A Snf2 family ATPase complex required for recruitment of the histone H2A variant Htz1. Mol Cell *12*, 1565-1576.

Kumar, S.V., and Wigge, P.A. (2010). H2A.Z-containing nucleosomes mediate the thermosensory response in Arabidopsis. Cell *140*, 136-147.

Ladurner, A.G., Inouye, C., Jain, R., and Tjian, R. (2003). Bromodomains mediate an acetyl-histone encoded antisilencing function at heterochromatin boundaries. Mol Cell *11*, 365-376.

Langst, G., and Becker, P.B. (2004). Nucleosome remodeling: one mechanism, many phenomena? Biochim Biophys Acta *1677*, 58-63.

Lee, J.S., Smith, E., and Shilatifard, A. (2010). The language of histone crosstalk. Cell *142*, 682-685.

Lever, M.A., Th'ng, J.P., Sun, X., and Hendzel, M.J. (2000). Rapid exchange of histone H1.1 on chromatin in living human cells. Nature *408*, 873-876.

Levi, V., Ruan, Q., and Gratton, E. (2005). 3-D particle tracking in a two-photon microscope: application to the study of molecular dynamics in cells. Biophys J *88*, 2919-2928.

Li, B., Pattenden, S.G., Lee, D., Gutierrez, J., Chen, J., Seidel, C., Gerton, J., and Workman, J.L. (2005). Preferential occupancy of histone variant H2AZ at inactive promoters influences

local histone modifications and chromatin remodeling. Proc Natl Acad Sci U S A *102*, 18385-18390.

Lippincott-Schwartz, J., Altan-Bonnet, N., and Patterson, G.H. (2003). Photobleaching and photoactivation: following protein dynamics in living cells. Nat Cell Biol *Suppl*, S7-14.

Locklear, L., Jr., Ridsdale, J.A., Bazett-Jones, D.P., and Davie, J.R. (1990). Ultrastructure of transcriptionally competent chromatin. Nucleic Acids Res *18*, 7015-7024.

Louters, L., and Chalkley, R. (1985). Exchange of histones H1, H2A, and H2B in vivo. Biochemistry *24*, 3080-3085.

Maeshima, K., Hihara, S., and Eltsov, M. (2010). Chromatin structure: does the 30-nm fibre exist in vivo? Curr Opin Cell Biol *22*, 291-297.

Malik, H.S., and Henikoff, S. (2003). Phylogenomics of the nucleosome. Nat Struct Biol *10*, 882-891.

Manuelidis, L. (1985). Individual interphase chromosome domains revealed by in situ hybridization. Hum Genet *71*, 288-293.

March-Diaz, R., Garcia-Dominguez, M., Florencio, F.J., and Reyes, J.C. (2007). SEF, a new protein required for flowering repression in Arabidopsis, interacts with PIE1 and ARP6. Plant Physiol *143*, 893-901.

March-Diaz, R., Garcia-Dominguez, M., Lozano-Juste, J., Leon, J., Florencio, F.J., and Reyes, J.C. (2008). Histone H2A.Z and homologues of components of the SWR1 complex are required to control immunity in Arabidopsis. Plant J *53*, 475-487.

Margueron, R., and Reinberg, D. (2010). Chromatin structure and the inheritance of epigenetic information. Nat Rev Genet *11*, 285-296.

Marshall, W.F., Straight, A., Marko, J.F., Swedlow, J., Dernburg, A., Belmont, A., Murray, A.W., Agard, D.A., and Sedat, J.W. (1997). Interphase chromosomes undergo constrained diffusional motion in living cells. Curr Biol *7*, 930-939.

Martin-Trillo, M., Lazaro, A., Poethig, R.S., Gomez-Mena, C., Pineiro, M.A., Martinez-Zapater, J.M., and Jarillo, J.A. (2006). EARLY IN SHORT DAYS 1 (ESD1) encodes ACTIN-RELATED PROTEIN 6 (AtARP6), a putative component of chromatin remodelling complexes that positively regulates FLC accumulation in Arabidopsis. Development *133*, 1241-1252.

Mayer, C., Schmitz, K.M., Li, J., Grummt, I., and Santoro, R. (2006). Intergenic transcripts regulate the epigenetic state of rRNA genes. Mol Cell *22*, 351-361.

Meluh, P.B., Yang, P., Glowczewski, L., Koshland, D., and Smith, M.M. (1998). Cse4p is a component of the core centromere of Saccharomyces cerevisiae. Cell *94*, 607-613.

Meneghini, M.D., Wu, M., and Madhani, H.D. (2003). Conserved histone variant H2A.Z protects euchromatin from the ectopic spread of silent heterochromatin. Cell *112*, 725-736.

Michaelis, C., Ciosk, R., and Nasmyth, K. (1997). Cohesins: chromosomal proteins that prevent premature separation of sister chromatids. Cell *91*, 35-45.

Misteli, T., Gunjan, A., Hock, R., Bustin, M., and Brown, D.T. (2000). Dynamic binding of histone H1 to chromatin in living cells. Nature *408*, 877-881.

Mito, Y., Henikoff, J.G., and Henikoff, S. (2005). Genome-scale profiling of histone H3.3 replacement patterns. Nat Genet *37*, 1090-1097.

Mizuguchi, G., Shen, X., Landry, J., Wu, W.H., Sen, S., and Wu, C. (2004). ATP-driven exchange of histone H2AZ variant catalyzed by SWR1 chromatin remodeling complex. Science *303*, 343-348.

Noh, Y.S., and Amasino, R.M. (2003). PIE1, an ISWI family gene, is required for FLC activation and floral repression in Arabidopsis. Plant Cell *15*, 1671-1682.

Palmer, D.K., O'Day, K., Trong, H.L., Charbonneau, H., and Margolis, R.L. (1991). Purification of the centromere-specific protein CENP-A and demonstration that it is a distinctive histone. Proc Natl Acad Sci U S A *88*, 3734-3738.

Park, Y.J., Dyer, P.N., Tremethick, D.J., and Luger, K. (2004). A new fluorescence resonance energy transfer approach demonstrates that the histone variant H2AZ stabilizes the histone octamer within the nucleosome. J Biol Chem *279*, 24274-24282.

Phair, R.D., and Misteli, T. (2001). Kinetic modelling approaches to in vivo imaging. Nat Rev Mol Cell Biol *2*, 898-907.

Phair, R.D., Scaffidi, P., Elbi, C., Vecerova, J., Dey, A., Ozato, K., Brown, D.T., Hager, G., Bustin, M., and Misteli, T. (2004). Global nature of dynamic protein-chromatin interactions in vivo: three-dimensional genome scanning and dynamic interaction networks of chromatin proteins. Mol Cell Biol *24*, 6393-6402.

Rabl, C. (1885). Uber Zelltheilung. Morphologisches Jahrbuch *10*, 214-330.

Raisner, R.M., Hartley, P.D., Meneghini, M.D., Bao, M.Z., Liu, C.L., Schreiber, S.L., Rando, O.J., and Madhani, H.D. (2005). Histone variant H2A.Z marks the 5' ends of both active and inactive genes in euchromatin. Cell *123*, 233-248.

Raisner, R.M., and Madhani, H.D. (2006). Patterning chromatin: form and function for H2A.Z variant nucleosomes. Curr Opin Genet Dev *16*, 119-124.

Rangasamy, D., Berven, L., Ridgway, P., and Tremethick, D.J. (2003). Pericentric heterochromatin becomes enriched with H2A.Z during early mammalian development. EMBO J *22*, 1599-1607.

Robinett, C.C., Straight, A., Li, G., Willhelm, C., Sudlow, G., Murray, A., and Belmont, A.S. (1996). In vivo localization of DNA sequences and visualization of large-scale chromatin organization using lac operator/repressor recognition. J Cell Biol *135*, 1685-1700.

Robinson, P.J., Fairall, L., Huynh, V.A., and Rhodes, D. (2006). EM measurements define the dimensions of the "30-nm" chromatin fiber: evidence for a compact, interdigitated structure. Proc Natl Acad Sci U S A *103*, 6506-6511.

Rosa, A., Maddocks, J.H., Neumann, F.R., Gasser, S.M., and Stasiak, A. (2006). Measuring limits of telomere movement on nuclear envelope. Biophys J *90*, L24-26.

Roth, S.Y., Denu, J.M., and Allis, C.D. (2001). Histone acetyltransferases. Annu Rev Biochem *70*, 81-120.

Saha, A., Wittmeyer, J., and Cairns, B.R. (2006). Chromatin remodelling: the industrial revolution of DNA around histones. Nat Rev Mol Cell Biol *7*, 437-447.

Santisteban, M.S., Kalashnikova, T., and Smith, M.M. (2000). Histone H2A.Z regulats transcription and is partially redundant with nucleosome remodeling complexes. Cell *103*, 411-422.

Santos-Rosa, H., Schneider, R., Bannister, A.J., Sherriff, J., Bernstein, B.E., Emre, N.C., Schreiber, S.L., Mellor, J., and Kouzarides, T. (2002). Active genes are tri-methylated at K4 of histone H3. Nature *419*, 407-411.

Sarcinella, E., Zuzarte, P.C., Lau, P.N., Draker, R., and Cheung, P. (2007). Monoubiquitylation of H2A.Z distinguishes its association with euchromatin or facultative heterochromatin. Mol Cell Biol *27*, 6457-6468.

Schalch, T., Duda, S., Sargent, D.F., and Richmond, T.J. (2005). X-ray structure of a tetranucleosome and its implications for the chromatin fibre. Nature *436*, 138-141.

Schardin, M., Cremer, T., Hager, H.D., and Lang, M. (1985). Specific staining of human chromosomes in Chinese hamster x man hybrid cell lines demonstrates interphase chromosome territories. Hum Genet *71*, 281-287.

Schubeler, D., Francastel, C., Cimbora, D.M., Reik, A., Martin, D.I., and Groudine, M. (2000). Nuclear localization and histone acetylation: a pathway for chromatin opening and transcriptional activation of the human beta-globin locus. Genes Dev *14*, 940-950.

Schwartz, B.E., and Ahmad, K. (2005). Transcriptional activation triggers deposition and removal of the histone variant H3.3. Genes Dev *19*, 804-814.

Schwarz, P.M., and Hansen, J.C. (1994). Formation and stability of higher order chromatin structures. Contributions of the histone octamer. J Biol Chem *269*, 16284-16289.

Seo, S., Herr, A., Lim, J.W., Richardson, G.A., Richardson, H., and Kroll, K.L. (2005). Geminin regulates neuronal differentiation by antagonizing Brg1 activity. Genes Dev *19*, 1723-1734.

Shogren-Knaak, M., Ishii, H., Sun, J.M., Pazin, M.J., Davie, J.R., and Peterson, C.L. (2006). Histone H4-K16 acetylation controls chromatin structure and protein interactions. Science *311*, 844-847.

Simonis, M., Kooren, J., and de Laat, W. (2007). An evaluation of 3C-based methods to capture DNA interactions. Nat Methods *4*, 895-901.

Solovei, I., Grandi, N., Knoth, R., Volk, B., and Cremer, T. (2004). Positional changes of pericentromeric heterochromatin and nucleoli in postmitotic Purkinje cells during murine cerebellum development. Cytogenet Genome Res *105*, 302-310.

Sterner, D.E., and Berger, S.L. (2000). Acetylation of histones and transcription-related factors. Microbiol Mol Biol Rev *64*, 435-459.

Strahl, B.D., and Allis, C.D. (2000). The language of covalent histone modifications. Nature *403*, 41-45.

Straight, A.F., Belmont, A.S., Robinett, C.C., and Murray, A.W. (1996). GFP tagging of budding yeast chromosomes reveals that protein-protein interactions can mediate sister chromatid cohesion. Curr Biol *6*, 1599-1608.

Strohner, R., Wachsmuth, M., Dachauer, K., Mazurkiewicz, J., Hochstatter, J., Rippe, K., and Langst, G. (2005). A 'loop recapture' mechanism for ACF-dependent nucleosome remodeling. Nat Struct Mol Biol *12*, 683-690.

Sun, F.L., Cuaycong, M.H., and Elgin, S.C. (2001). Long-range nucleosome ordering is associated with gene silencing in Drosophila melanogaster pericentric heterochromatin. Mol Cell Biol *21*, 2867-2879.

Sutherland, H., and Bickmore, W.A. (2009). Transcription factories: gene expression in unions? Nat Rev Genet *10*, 457-466.

Suto, R.K., Clarkson, M.J., Tremethick, D.J., and Luger, K. (2000). Crystal structure of a nucleosome core particle containing the variant histone H2A.Z. Nat Struct Biol *7*, 1121-1124.

Svoboda, K., and Yasuda, R. (2006). Principles of two-photon excitation microscopy and its applications to neuroscience. Neuron *50*, 823-839.

Tagami, H., Ray-Gallet, D., Almouzni, G., and Nakatani, Y. (2004). Histone H3.1 and H3.3 complexes mediate nucleosome assembly pathways dependent or independent of DNA synthesis. Cell *116*, 51-61.

Talbert, P.B., and Henikoff, S. (2010). Histone variants--ancient wrap artists of the epigenome. Nat Rev Mol Cell Biol *11*, 264-275.

Thatcher, T.H., and Gorovsky, M.A. (1994). Phylogenetic analysis of the core histones H2A, H2B, H3, and H4. Nucleic Acids Res *22*, 174-179.

Thomas, J.O., and Rees, C. (1983). Exchange of histones H1 and H5 between chromatin fragments. A preference of H5 for higher-order structures. Eur J Biochem *134*, 109-115.

Tumbar, T., and Belmont, A.S. (2001). Interphase movements of a DNA chromosome region modulated by VP16 transcriptional activator. Nat Cell Biol *3*, 134-139.

Turner, B.M. (2002). Cellular memory and the histone code. Cell *111*, 285-291.

van Daal, A., White, E.M., Elgin, S.C., and Gorovsky, M.A. (1990). Conservation of intron position indicates separation of major and variant H2As is an early event in the evolution of eukaryotes. J Mol Evol *30*, 449-455.

Vazquez, J., Belmont, A.S., and Sedat, J.W. (2001). Multiple regimes of constrained chromosome motion are regulated in the interphase Drosophila nucleus. Curr Biol *11*, 1227-1239.

Verschure, P.J., van der Kraan, I., Manders, E.M., Hoogstraten, D., Houtsmuller, A.B., and van Driel, R. (2003). Condensed chromatin domains in the mammalian nucleus are accessible to large macromolecules. EMBO Rep *4*, 861-866.

Volpi, E., Mittendorfer, B., Rasmussen, B.B., and Wolfe, R.R. (2000). The response of muscle protein anabolism to combined hyperaminoacidemia and glucose-induced hyperinsulinemia is impaired in the elderly. J Clin Endocrinol Metab *85*, 4481-4490.

White, J., and Stelzer, E. (1999). Photobleaching GFP reveals protein dynamics inside live cells. Trends Cell Biol *9*, 61-65.

Wieland, G., Orthaus, S., Ohndorf, S., Diekmann, S., and Hemmerich, P. (2004). Functional complementation of human centromere protein A (CENP-A) by Cse4p from Saccharomyces cerevisiae. Mol Cell Biol *24*, 6620-6630.

Wirbelauer, C., Bell, O., and Schubeler, D. (2005). Variant histone H3.3 is deposited at sites of nucleosomal displacement throughout transcribed genes while active histone modifications show a promoter-proximal bias. Genes Dev *19*, 1761-1766.

Woodcock, C.L., Grigoryev, S.A., Horowitz, R.A., and Whitaker, N. (1993). A chromatin folding model that incorporates linker variability generates fibers resembling the native structures. Proc Natl Acad Sci U S A *90*, 9021-9025.

Ye, Q., Callebaut, I., Pezhman, A., Courvalin, J.C., and Worman, H.J. (1997). Domain-specific interactions of human HP1-type chromodomain proteins and inner nuclear membrane protein LBR. J Biol Chem *272*, 14983-14989.

Zhang, H., Roberts, D.N., and Cairns, B.R. (2005). Genome-wide dynamics of Htz1, a histone H2A variant that poises repressed/basal promoters for activation through histone loss. Cell *123*, 219-231.

Zilberman, D., Coleman-Derr, D., Ballinger, T., and Henikoff, S. (2008). Histone H2A.Z and DNA methylation are mutually antagonistic chromatin marks. Nature *456*, 125-129.

Zofall, M., Fischer, T., Zhang, K., Zhou, M., Cui, B., Veenstra, T.D., and Grewal, S.I. (2009). Histone H2A.Z cooperates with RNAi and heterochromatin factors to suppress antisense RNAs. Nature *461*, 419-422.

Zofall, M., Persinger, J., Kassabov, S.R., and Bartholomew, B. (2006). Chromatin remodeling by ISW2 and SWI/SNF requires DNA translocation inside the nucleosome. Nat Struct Mol Biol *13*, 339-346.

Chapter 2

Auxin regulates chromatin dynamics and histone acetylation in root development

The work described in this chapter is entirely my own with the exception of the immunofluorescence on Col-0 and *hag1-6* which were kindly provided by Professor Nobuko Ohmido. This work has been submitted for publication as:

Auxin regulates chromatin dynamics and histone acetylation in root development.

Stefanie Rosa, Vardis Ntoukakis, Nobuko Ohmido, Ali Pendle, Rita Abranches and Peter Shaw

Chapter2:

Auxin regulates chromatin dynamics and histone acetylation in root development

2.1. Abstract

The mechanism whereby the same genome can give rise to different cell types with different gene expression profiles is a fundamental problem in biology and the key to understanding the development of multicellular organisms. It is clear that chromatin organization and dynamics vary with altered gene expression in different cell types, but there is little evidence yet from whole organisms linking chromatin dynamics with development. Here we use the well-defined development pathway in Arabidopsis roots to show that as cells progress from meristematic to fully differentiated, core histones become less mobile and more strongly bound to chromatin. Furthermore we show that this transition is mediated by changes in histone acetylation, and that auxin maintains meristem competency of Arabidopsis root cells by regulating histone acetylation during development.

2.2. Introduction

Epigenetic mechanisms that control chromatin organization are now known to regulate changes in gene activity. Chromatin organization within the nucleus is mediated by structural chromatin proteins, the most prominent of which are the core and linker histones, basic proteins that are responsible for the vast degree of packaging of the DNA within the nucleus of all eukaryotes. The nucleosome, consisting of an octamer of core histones (H2A, H2B, H3 and H4) complexed with DNA, has long been considered a very stable building block of chromatin; recent data, however, has shown that even core histones are constantly being exchanged within chromatin, allowing the access of proteins like polymerases to DNA for gene expression, and that different levels of cell differentiation may be associated with altered histone dynamics (Meshorer et al., 2006; Phair and Misteli, 2000). There is little data, however, about the regulation of histone dynamics during differentiation of a multicellular organism.

The Arabidopsis root is an excellent model system to study cell differentiation since there is a very well established developmental gradient from the growing tip towards the mature parts of the root (Dolan et al., 1993). The meristem or division zone consists of actively dividing undifferentiated cells that emerge from stem cells located at the root tip. When cell division ceases, cells first start to increase in length, forming the elongation zone; subsequently the appearance of root hairs demarcates the differentiation zone where cells assume their final fate and are fully differentiated (Fig. 2.1).

The communication between developing cells and undifferentiated cells has an important role in determining cell differentiation. The control of post-embryonic root growth is known to be tightly regulated by the plant hormone auxin. The importance of auxin in root formation was demonstrated in tissue culture experiments, in which a high ratio between auxin and the plant hormone cytokinin resulted in the formation of roots (Skoog and Miller, 1957).

Auxin signaling can be divided broadly into three aspects that contribute to its complexity: the spatio-temporal pattern of its biosynthesis, its directional transport and tissue-specific responses.

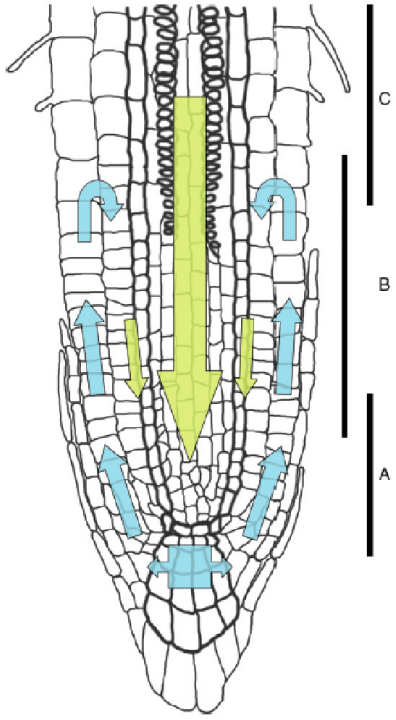

Figure 2.1. The proximal-distal organization of the Arabidopsis root and the "inverted fountain" of auxin movement.
(A) Division zone. (B) Elongation zone. (C) Differentiation zone. The arrows highlight the transport-mediated "reflux" of auxin. (Teale et al., 2005)

Auxin can be synthesized in the roots, however its physiological significance remains unclear (Ljung et al., 2001). Auxin is in fact primarily synthesized in young aerial organs and transported in a polar fashion towards the root tip which represents the major sink tissue (Palme and Galweiler, 1999).

From its sites of biosynthesis, auxin is actively transported by influx and efflux carrier proteins. In Arabidopsis, the most studied auxin transporters are the *PINFORMED* (*PIN*) genes, which form a family of eight members, most of which seem to facilitate auxin efflux (Paponov et al., 2005). PINs are located in the plasma membrane and show polar localization. The polarity of PIN localization correlates well with the direction of auxin transport (Vanneste and Friml, 2009) and on the root tip it determines the establishment of the so called "inverted fountain" movement of auxin (Overvoorde et al., 2010) (Fig. 2.1).

As it reached the sites of action, auxin is perceived by the TRANSPORT INHIBITOR RESPONSE 1 (TIR1) family of receptors (Dharmasiri et al., 2005; Kepinski and Leyser, 2005). TIR1 encodes a F-box subunit of the ubiquitin ligase complex SCFTIR1 (SKP1, CDC53/CULLIN, F-box); when auxin binds to the TIR1 receptor, it stabilizes the interaction between TIR1 and the AUXIN/INDOLE-3- ACETIC ACID (Aux/IAA) proteins (Tan et al., 2007). This interaction results in Aux/IAA ubiquitination and subsequent 26S-proteasome mediated degradation. The Aux/IAA proteins act as auxin response inhibitors by forming heterodimers with the ARF (AUXIN RESPONSE FACTOR) transcription factors, thereby preventing activation of auxin-responsive genes (Mockaitis and Estelle, 2008). The TIR1-mediated Aux/IAA protein degradation releases the ARFs from their inhibitory effect, prompting activation of the auxin-responsive genes, among which are also the Aux/IAA genes (Benjamins and Scheres, 2008; Gray et al., 2001). Degradation of the Aux/IAA proteins and consequent ARF activity depends on auxin concentration: high levels of auxin cause Aux/IAA degradation, whereas, at low auxin levels, these proteins are stable and interact with the ARFs (Mockaitis and Estelle, 2008). This mechanism, together with regulated stability of Aux/IAA proteins, provides a self-regulatory loop for auxin-induced gene expression (Benjamins and Scheres, 2008).

In roots, meristem maintenance was shown to be under the control of a cytokinin-auxin antagonistic interaction (Dello Ioio et al., 2007). While accumulation of auxin promotes cell division, high concentrations of cytokinins promote cell differentiation. Experiments involving applications of cytokinin have shown a decrease in meristem size as a consequence of a progressive decrease in the number of meristematic cells (Dello Ioio et al., 2007). Application of auxins on the other hand, results in an increase of meristem size (Dello

Ioio et al., 2008). The molecular mechanism underlying this antagonistic interaction has been also revealed. These two hormones were shown to control in opposite ways the expression of *SHY2* (SHORT HYPOCOTYL 2) gene (Dello Ioio et al., 2008), a member of the auxin/indole-3-acetic acid (Aux/IAA) auxin-inducible gene family (Tian et al., 2003) that acts as auxin-response inhibitor by preventing activation of auxin-responsive genes (Benjamins and Scheres, 2008).

In researching the control of meristem maintenance much advance has been made on the genetic networks controlling this process. Little is known however about the cellular characteristics of meristematic cells and how chromatin mechanisms control cell proliferation and cell differentiation.

In this chapter we studied the overall changes in histone-DNA interactions during cell differentiation using the well-defined developmental pathway in the Arabidopsis root.

2.3. Materials and Methods

2.3.1. Plant lines and growth conditions

Mutants and transgenic lines used in this study come from the following sources: *hag1-6* mutant (Kornet and Scheres, 2009); RHD6-GFP (Menand et al., 2007); RSL4-GFP (Yi et al., 2010); PIN1-GFP (Benkova et al., 2003), PIN2-GFP (Xu and Scheres, 2005) and PIN7-GFP (Blilou et al., 2005). Mutants and transgenic lines were in Columbia (Col) background.

Seeds were surface sterilized in 5% v/v sodium hypochlorite for 5 minutes and rinsed three times in sterile distilled water. Seeds were then plated on to Murashige and Skoog medium (pH 5.8) supplemented with 1% w/v sucrose and 0.5% w/v Phytagel. Seeds were stratified at 4°C for 48 hours in the darkness and then grown in continuous light at 25°C in vertically oriented Petri dishes. The roots were observed after 3 to 5 days of incubation, depending on the experiment. For analysis of TSA and IAA effect on meristem size, plants were initially germinated in non-supplemented media for 3 days and then transferred overnight to new plates containing the respective supplements.

2.3.2. Supplemented growth media

Before pouring into plates, molten media was supplemented with stock solutions of trichostatin A (TSA) and 3-Indoleacetic acid (IAA). For IAA supplemented media a final concentration of 0.3 nM was used. IAA was obtained from Sigma™ (catalogue #A-3903). Final concentrations of 100 ng/ml of TSA on the media were used for the experiments described here. TSA was obtained from Sigma™ (catalogue # T8552).

2.3.3. Constructs and plant transformation

The cDNA clones of H2B (At1g49950), H2A (At5g67580) and H4 (At3g49850) were amplified from whole seedling cDNA with primers containing attB1 and attB2 sites. The PCR products were cleaned using a PCR purification column (QIAQuick; Qiagen) and recombined into pDONR 207 (Invitrogen) by BP reaction (Gateway technology, Invitrogen). All plasmid inserts were verified by sequencing. Histone entry clones were then recombined by LR reaction Gateway technology, Invitrogen) into the plant destination vector GFP-N-bin (gift from Ben Trewaskis, MPI, Germany), which contains GFP fusion at the N-terminus and a constitutive 35S promoter. LR reactions were performed in accordance with the Invitrogen manual.

The multisite gateway system (Invitrogen) was used for the PAGFP construct. The 2.5 Kb region immediately upstream of the start site of the *SCARECROW* coding region was amplified with PCR primers containing recombination sequences and cloned into pDONR P4-P1R vectors (Invitrogen). The H2B (At1g49950) cDNA coding region was amplified and cloned into pDONR P2R-P3 and PAGFP tag cloned into pDONR 207 without the stop codon. After all plasmid inserts were verified by sequencing, a MultiSite Gateway reaction (Invitrogen) was then performed with the three resulting pDONR plasmids and the binary vector pGWB multisite (the destination binary vector pGWB multisite was a gift from M. Tomlinson (John Innes Centre, Norwich, UK) and was generated by replacing the R1-CmR-ccdB-R2 cassette of pGWB1 into R4-CmR-ccdB-R3 (pGWB1 was from Tsuyoshi Nakagawa, Shimane Univ., Japan)).

The binary plasmid pNLS:MS2CP:GFP, containing the bacteriophage MS2 coat protein (a gift from Adrian Sambade, John Innes Centre, Norwich, UK) was also used to generate transgenic stable Arabidopsis lines.

Agrobacterium tumefaciens strain GV3103 was used for plant transformation by the floral dipping method as described (Clough and Bent, 1998). T1 plants were screened on MS and agar plates without sucrose and containing 50 µg/ml kanamycin for the histone-GFP constructs, and 50 µg/ml hygromycin and 50 µg/ml kanamycin for the PAGFP fusion construct. MS2CP plants were screened with Basta selection on soil.

2.3.4. Microscopy

Optical sections of roots were collected with a Zeiss 510 Meta confocal microscope. For visualization of roots stained with propidium iodide an excitation line of 488nm was used and signal was detected at wavelengths of 580-700nm. For observation of GFP expression we used a 488 nm excitation line and BP filter 505-550 nm. Immunofluorescence imaging was performed using a Nikon Eclipse 600 epifluorescence microscope equipped with a Hamamatsu Orca ER cooled CCD digital camera and a Prior Proscan x–z stage. The following wavelengths were used for fluorescence detection: excitation 340-380 nm and emission 425-475 nm for DAPI and excitation 490-510 nm and emission 520-550 nm for Alexa488. For all experiments series of optical sections with z-steps of 0.2 µm were collected using MetaMorph software (Universal Imaging). Images were processed with the ImageJ program (http://rsb.info.nih.gov/ij/) or Adobe Photoshop CS.

2.3.5. FRAP

For FRAP experiments on histone proteins, a pre-scan was acquired followed by a bleaching pulse of 5 iterations (speed 200–500 pixel/ms) using a spot 1 µm in radius. At all imaging time-points series of optical sections (15-20 slices) with z-steps of 1 µm were collected. One z-stack (512x512 pixels) was collected every 60 seconds. For imaging, the laser power was attenuated to 1% of the bleach intensity. FRAP recovery curves were generated from background subtracted images and normalized for the loss of fluorescence due to imaging and bleach pulse – double normalization (Phair et al., 2004). We additionally normalized for the variation on the bleaching depth as follows:

$$I(norm) = \frac{I_t - I_{tbleach}}{1 - I_{tbleach}}$$

Where,

$I_{tbleach}$, is the fluorescent intensity after double normalization at the bleach point.

Images were processed with ImageJ program (http://rsb.info.nih.gov/ij/).

Mobile fractions and half-life were calculated as averages by individually fitting the FRAP recoveries of each nucleus to a single exponential function. The standard Student's *t*-test was used to determine the statistical significance of results. All quantitative values represent averages from at least 10 cells. For the exponential fitting and statistical analysis we used the GraphPad Prism 5 software.

For FRAP on MS2CP-GFP lines faster settings were used. Image quality was reduced to 256x256 pixels and imaging was performed on a bi-directional scanning mode (with pixel time 0.8 µsec). Five pre-scans were taken before a bleaching pulse of 1 iteration 100% laser power (488 nm) followed by 60 scans with 1% laser power. No time delays or Z-stacks were taken. All values were then normalized accordingly.

2.3.6. *De novo* synthesis and cell division rates

For calculation of *de novo* synthesis z-stacks of cells expressing H2B-GFP protein were taken (z-steps of 0.5 µm) followed by photobleaching of entire nuclei with a 488 laser line at 100% power (5 iterations). One z-stack was collected straight after bleaching and a final one after 1h. De novo synthesis was expressed as followed:

$$\%Intensity = \frac{I_{after1h} - I_{afterbleach}}{I_{beforebleach}} \times 100$$

For calculation of cell division rates pSCR::PAGFP-H2B plants were photoactivated using a quick pulse (~3 seconds) of 405 nm laser (30%) on a defined region containing one single nucleus. A single image was then taken to confirm the appearance of GFP signal. Plants were then put back to grow on MS plates or MS + TSA overnight. The number of cell divisions that had taken place during that period was calculated based on the number of cells showing GFP signal.

2.3.7. Root Meristem Size Analysis

Meristem size was expressed as the number of cells in the cortex files extending from the quiescent centre to the first elongated cortex cell. Values represent the mean with standard error (n=15). Measurements were performed 5 days after germination. Seedlings were stained with 20 mg/ml propidium iodide and observed on a confocal microscope. The standard Student's *t*-test was used to determine the statistical significance of results.

2.3.8. Immunofluorescence

The Arabidopsis roots were fixed for 60 min with 4% (w/v) formaldehyde freshly made from paraformaldehyde (PFA) in PBS buffer. After washing in PBS for 5 min, the roots were digested in a mixture of 1% Dolicalase, 0.5% Cellulase, 0.025 % Pectolyase at 37°C for 45-60 min. After enzyme treatment, roots were washed in PBS three times for 5 minutes each and squashed between poly-L Lysine slides (Polysine, VWR international) and coverslips in PBS. After freezing the slides in liquid N_2, the coverslips were removed and the samples were air-dried. Slides were incubated for 15 min in detergent solution (0.5% Triton X-100 in PBS). Slides were washed three times with PBS for 5 min each and incubated in 0.1 N HCL for 15 min. Then the slides were washed three times with PBS, blocked with 4% BSA in PBS for 30 min, followed by histone antibody staining.

Anti-H2BAc(K20) antibody from rabbit (1:200) (Cell Signalling, Switzerland) was used as a primary antibody in 1% BSA in PBS. The slides were incubated at 4°C overnight with the primary antibody in a humid box. After washing the slides in PBS for 5 min each, anti-rabbit IgG A488 conjugate (Invitrogen) was applied as secondary antibody and slides were incubated for 1 hour in a humid dark box at 37°C. After washing the slides 3 times in PBS for 5 min each, the specimens were counter-stained with 1 μg/ml DAPI and mounted in Vectashield (Vector Lab.).

For quantification of acetylation signal, total integrated intensity of antibody signal was measured using ImageJ software and divided by total intensity of DAPI signal. The standard Student's *t*-test was used to determine the statistical significance of results.

2.3.9. Western Blot

Root extracts from Col-0 and Col-0 plants grown overnight in the presence of TSA or IAA, were made by grinding roots in SDS-PAGE loading buffer (Invitrogen) in the presence of 0.05 M DTT and heated to 70 °C for 10 min. Electrophoresis was performed using precast 4-12% gradient gels (Invitrogen) according to manufacturers' instructions. Proteins were transferred to PVDF membranes (Thermo Scientific) using NuPage transfer buffer (Invitrogen) for Western blotting. The PVDF membrane was blocked with 3% BSA (Sigma) in tris-buffered saline containing 1% Tween-20 (Sigma) (TBS-T) for 2h with gentle shaking. Anti-H4Ac (AbD Serotec) antibody was then added at a concentration of 1:800 for 60

minutes. Blots were washed thoroughly three times in TBS-T, for 10 minutes each with further shaking and finally labelled with a peroxidase-conjugated secondary antibody anti-rabbit (Sigma-Aldrich) at a 1:20000 dilution and detected using the ECL reagent (GE Healthcare). Membranes were stained with Coomassie Brilliant Blue R-250.

2.4. Results

2.4.1. Histone dynamics in Arabidopsis root development

To visualize H2B in living cells, Arabidopsis lines stably expressing H2B-GFP under a constitutive promoter were established (Fig. 2.2a). Mitotic figures showed that all H2B-GFP proteins were associated with chromosomes (Fig. 2.2b), confirming that the expressed protein was correctly incorporated into chromatin and behaved like endogenous H2B protein.

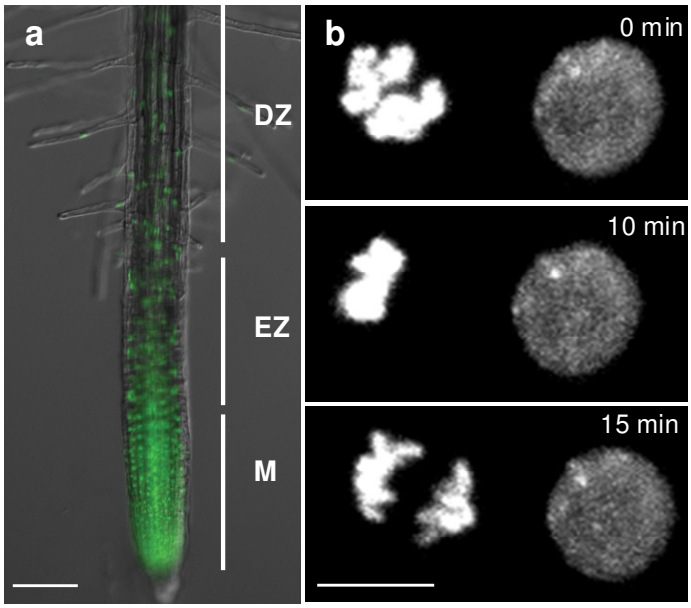

Figure 2.2. Expression of H2B-GFP in Arabidopsis roots.

(a) Arabidopsis root expressing H2B-GFP protein fusion in the different developmental zones (M – division zone; EZ – elongation zone; DZ – differentiation zone), scale bar represents 100 μm. **(b)** Cell division showing complete incorporation of H2B-GFP in the chromatin. The nucleus on the left is undergoing division while the one in the right is in G2 stage, scale bar represents 5 μm.

We then characterized the dynamics of H2B exchange in the different developmental regions of Arabidopsis root by fluorescence recovery after photobleaching (FRAP) (Fig. 2.3a). The FRAP data for H2B-GFP showed that the half-time (t1/2) for recovery in the division zone was significantly less than that in the elongation or differentiation zones (11.35 min in the division zone, 13.73 min in the elongation zone, 16.73 min in the differentiation zone) (Fig. 2.3b; Table 2.1). Quantitative analysis of the FRAP data also showed that the size of the mobile H2B fraction was highest in the division zone and decreased successively in the elongation zone and the differentiation zone (51.56%, 41.46% and 21.19% respectively) (Fig. 2.3c).

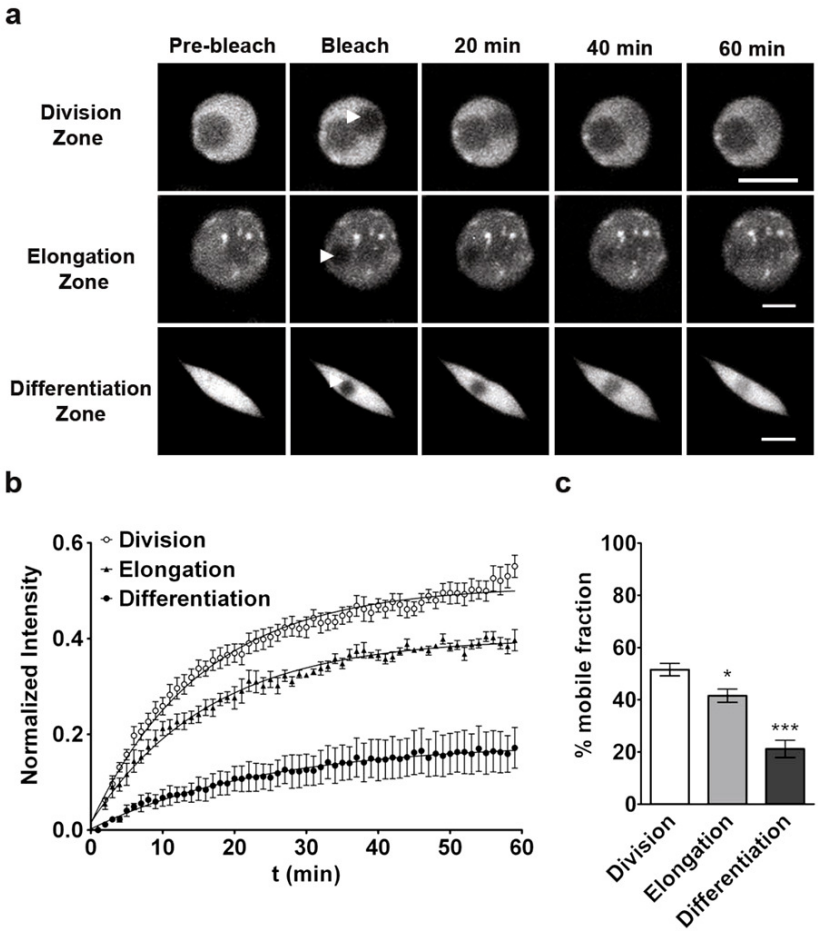

Figure 2.3. FRAP analysis of H2B-GFP reveals higher mobility in meristematic cells.

(a) Representative fluorescence changes in nuclei expressing H2B-GFP in different developmental zones of the root. A region of 2 µm in diameter was bleached and recovery followed over 60 min. Scale bars: 5 µm. **(b)** Quantitative analysis of FRAP experiments within the different developmental zones. Values represent means ± s.e. from at least 10 cells. **(c)** Estimated mobile fractions. Values represent mean ± s.e. from at least 10 cells. (Student's *t* test, **P*< 0.05; ***P*< 0.01; ****P*< 0.001).

Table 2.1. FRAP table for half time recovery in minutes (min) for the different histone-GFP lines at the different developmental zones of the root. Values represent averages ± s.e..

	Division (min)	Elongation (min)	Differentiation (min)
H2B-GFP	11.35±1.36	13.73±2.56	16.73±2.45
H2A-GFP	10.48±1.39		20.37±2.02
H4-GFP	11.93±2.80		13.20±2.10

To exclude the possibility that the observed differences in histone mobility reflected differences in rates of protein synthesis, the *de novo* expression rates of H2B-GFP were measured. Entire nuclei of cells expressing H2B-GFP were photobleached and the recovery of the fluorescence signal, due to newly synthesised H2B-GFP proteins, was measured. The synthesis rate observed for cells in the different zones was very small and comparable between the different zones (Fig. 2.4a), showing that the different exchange kinetics of H2B-GFP in the different zones cannot be accounted for by differential *de novo* expression rates. To rule out possible differences in the properties of the nucleoplasm that might affect protein mobility between nuclei at different stages of development, we analysed the mobility of a non-chromatin-binding protein of a similar size to H2B from the capsid of the virus MS2 (MS2CP-GFP). We observed no differences in the FRAP curves for this protein within the different developmental zones (Fig. 2.4b), showing that general differences in protein mobility in the different cell types cannot explain the different mobilities of H2B-GFP. To determine whether the changes in dynamics were limited to H2B or are a general property of all core histones, we also measured the exchange dynamics of H2A and H4 using GFP fusion proteins to these histones. In all cases, the overall recovery kinetics were faster in the cells of the division zone (Fig. 2.4c-d; Table 2.1) as observed for H2B.

These results show that, as root cells progress from the meristematic region through the elongation region to the differentiation region, histones become generally less dynamic and more strongly bound to chromatin i.e. that global histone mobility is reduced upon differentiation in this multicellular organism. Similar results have been previously reported for mammalian cultured cells undergoing differentiation (Meshorer et al., 2006). Together these results support the idea that global chromatin remodelling is a central feature of the cellular differentiation process.

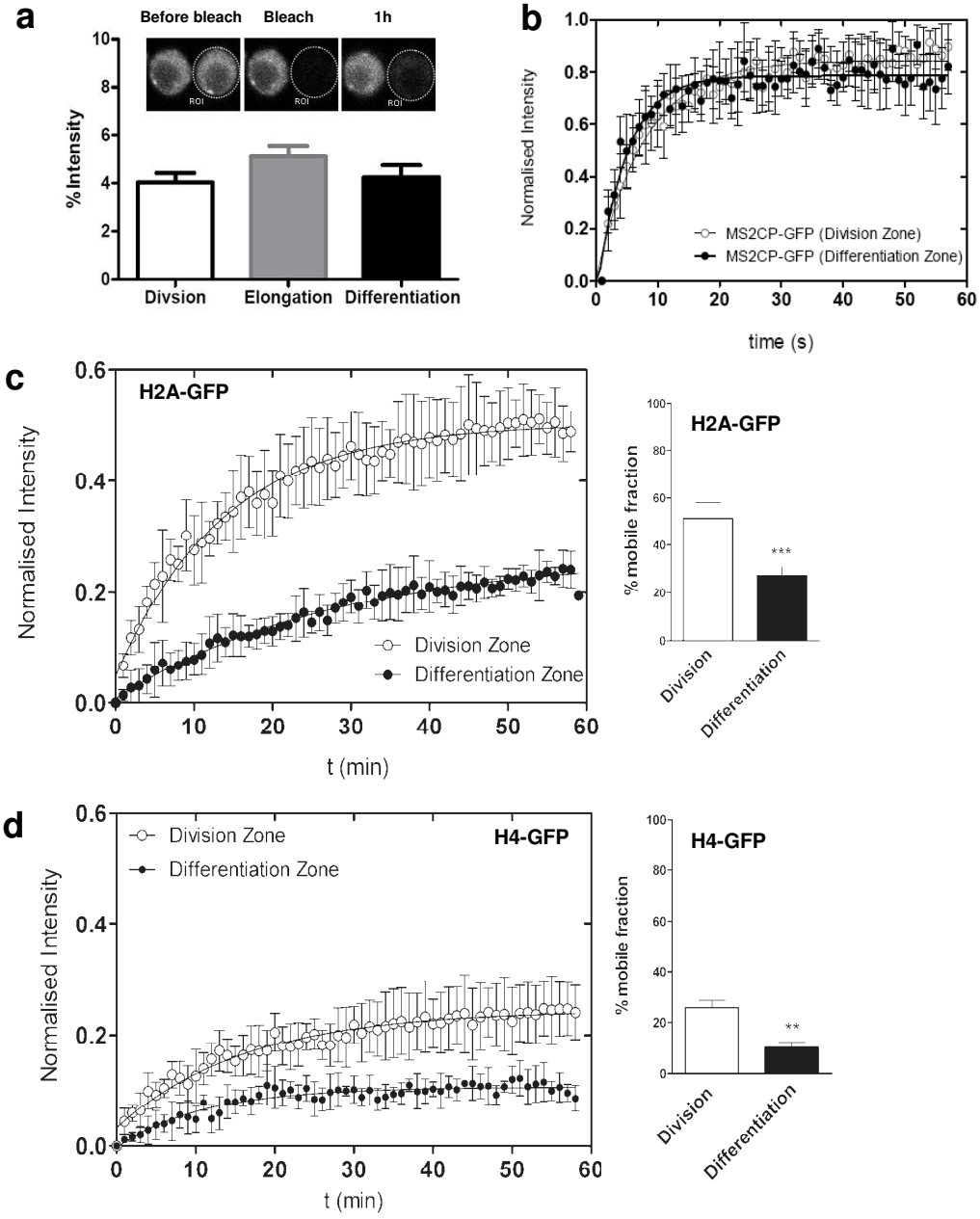

Figure 2.4. Controls for FRAP experiments on root developmental zones.

(a) *De novo* synthesis rates calculated as a percentage of initial intensities for H2B-GFP protein after a period of 1h in the different developmental zones showing no significant differences on the expression rates. Values represent mean±s.e. (n=6-8). **(b)** FRAP curves for a non-chromatin-binding protein (MS2CP-GFP), showing similar recoveries within the different developmental regions. Values represent mean±s.e. from at least 10 cells. **(c)** FRAP data for H2A-GFP Left: recovery kinetics over a period of 60min in division zone (empty circles) and differentiation zone (black circles). Right: estimated mobile fractions of division zone (white), and differentiation zone (black). **(d)** FRAP data for H4-GFP Left: recovery kinetics over a period of 60min in division zone (empty circles) and differentiation zone (black circles). Right: estimated mobile fractions of division zone (white), and differentiation zone (black). (Student's *t* test, $^{**}P < 0.01$; $^{***}P < 0.001$).

2.4.2. H2B mobility is regulated by histone acetylation

Posttranslational modification of histones by acetylation has been shown to strongly affect chromatin structure. Typically, acetylation occurs within N-terminal histone tails and is thought to modulate the interactions between the tails and the DNA, leading to increased accessibility of target genes to transcription (Kadonaga, 1998; Strahl and Allis, 2000). Histone acetylation levels are controlled by the balance between histone deacetylase and histone acetyl transferase activity.

To assess the role of histone acetylation in histone mobility we manipulated the acetylation levels using two different strategies, to either increase or decrease acetylation, and analysed the resulting mobility of H2B-GFP by FRAP. As there are about 20 histone deacetylases in the Arabidopsis genome, to inhibit histone deacetylase activity we used trichostatin A (TSA), a well characterised inhibitor of histone deacetylases (HDACs) (Yoshida et al., 1990). On the other hand, the major histone acetyl-transferase (HAT) mutant is *hag1-6* (Kornet and Scheres, 2009), and decreased histone acetylation levels were achieved by crossing the H2B-GFP line with this mutant.

The results from these two complementary strategies showed that in nuclei in the division zone, hypoacetylation in the *hag1-6* mutant reduced the mobility of H2B-GFP whereas hyperacetylation by TSA treatment had no effect on histone exchange (Fig. 2.5a-b). On the other hand, in nuclei in the differentiation zone, hyperacetylation by TSA significantly increased H2B-GFP mobility while hypoacetylation in the *hag1-6* mutant did not further reduce histone mobility (Fig. 2.5c-d). These experiments show that histone acetylation levels directly affect histone dynamics.

These data agree with the proposal from mammalian cells of a relation between acetylation of core histone tails and nucleosome relaxation (Misteli et al., 2000). Importantly, the manipulation of the acetylation levels by TSA or *hag1-6* did not affect the mobility of H2B in the same way in all cells but specifically depended on their state of differentiation.

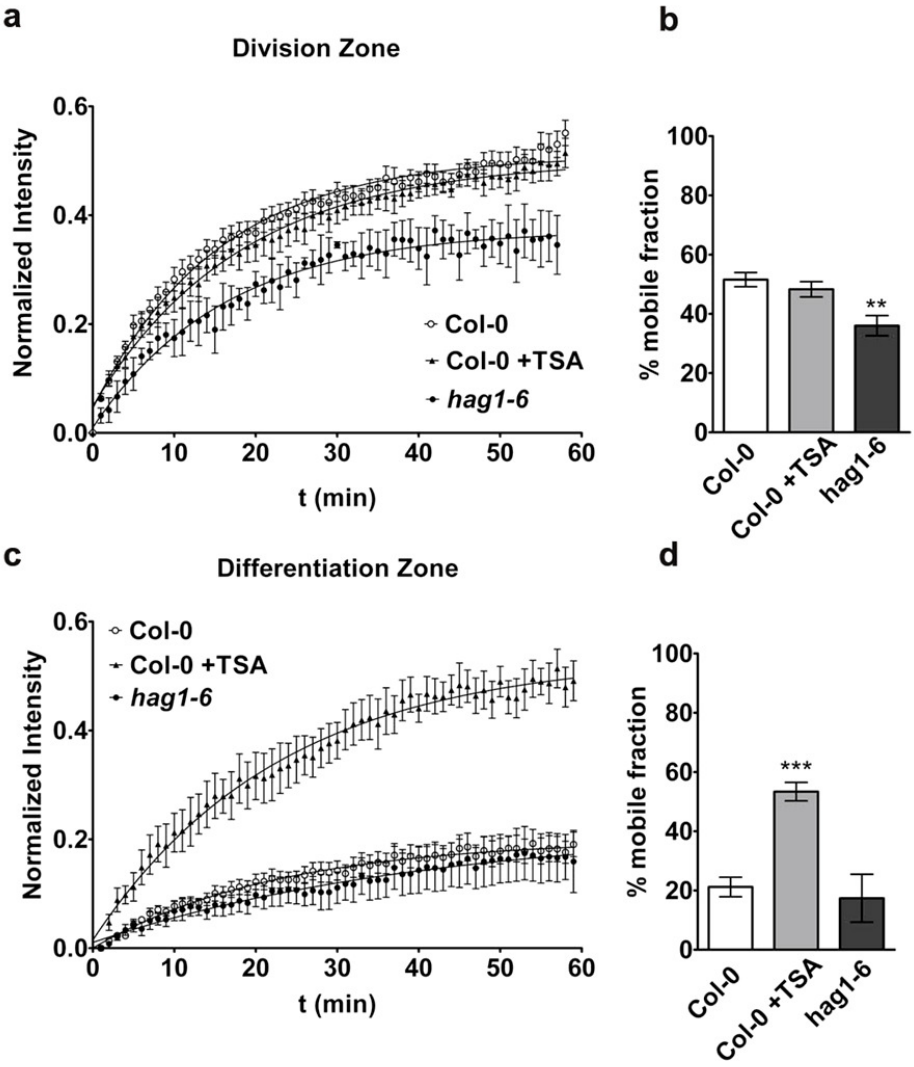

Figure 2.5. H2B mobility is regulated by acetylation.

FRAP curves for H2B-GFP in the division zone **(a, b)** and differentiation zone **(c, d)** on 4-day-old Col-0 plants (empty circles), *hag1-6* mutant (black circles) and on overnight TSA (100ng/ml) treated plants (triangles). Estimated mobile fractions on division **(b)** and differentiation **(d)** zones for the described treatments. Values represent mean±s.e.m. from at least 10 cells. (Student's *t* test, $^{**}P < 0.01$; $^{***}P < 0.001$).

2.4.3. Histone acetylation affects root development and meristem size

We next examined whether inducing changes in histone acetylation, and thus histone dynamics, caused changes in development, by quantifying the numbers of meristem cells. It has been previously shown (Kornet and Scheres, 2009) that the *hag1-6* mutant has shorter roots and smaller meristems. We showed that this phenotype is due to smaller numbers of meristem cells, and that the phenotype could not be rescued by TSA treatment (Fig. 2.6e-f and h). On the other hand, TSA induced an increase in meristem cell number in wild-type plants (Fig. 2.6b, h). In principle, the increase in meristem cell number by hyperacetylation

could be caused either by an increased rate of cell division in the meristematic cells or by a delay in differentiation. To address this question we used a line expressing H2B fused with a photoactivatable GFP marker. We specifically photoactivated a single nucleus in the meristem of each plant and counted the number of cell divisions after a period of 12h in wild-type control plants and wild-type treated with TSA (Fig. 2.7a). The results showed no increase in cell division rate upon TSA treatment (Fig. 2.7b). These observations strongly suggest that the increased levels of histone acetylation following TSA treatment delay cell differentiation in the root meristem, resulting in a higher meristem cell number.

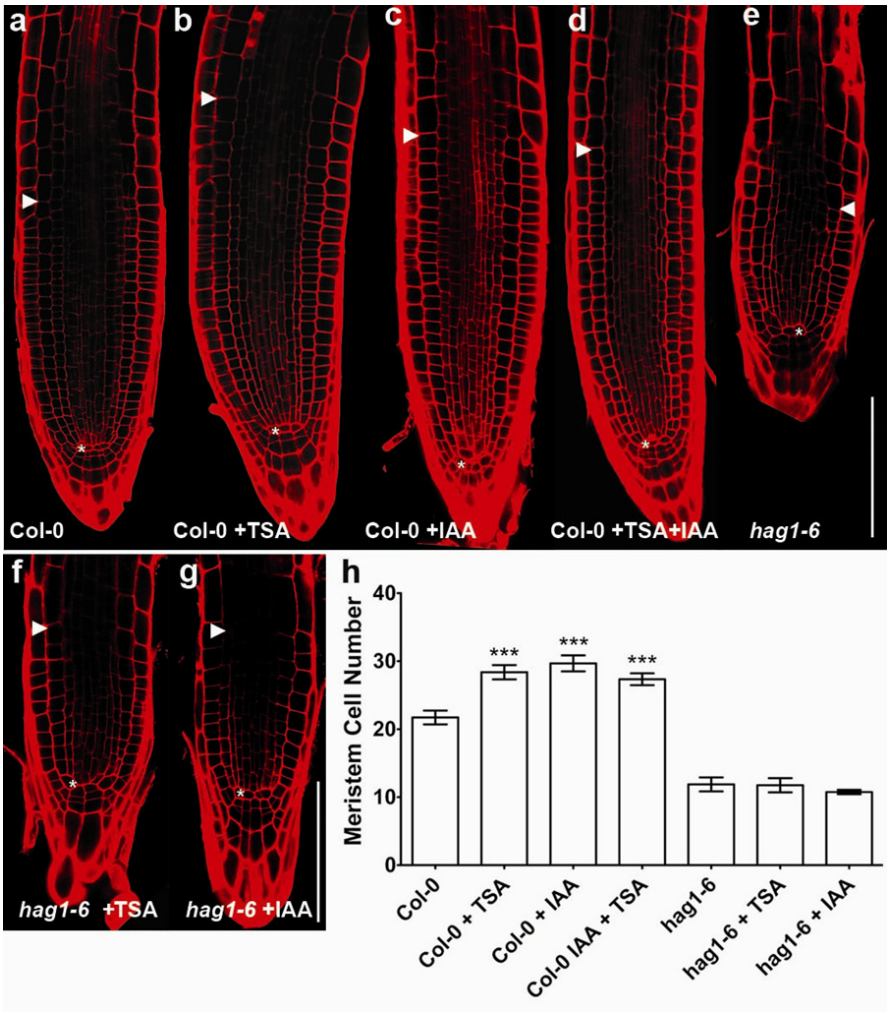

Figure 2.6. Histone acetylation affects root development and meristem size.
a-g, 4 day-old root meristems of, wild-type plants **(a)** wild-type plants treated overnight with 100 ng/ml TSA **(b)** wild-type plants treated overnight with 0.3 nM IAA **(c)** wild-type plants treated with TSA and IAA overnight **(d),** *hag1-6* mutant **(e),** *hag1-6* mutant treated overnight with TSA **(f),** *hag1-6* mutant treated overnight with IAA **(g)**. **h,** Root meristem cell number of plants depicted in a-g. Root meristem size is expressed as the number of cortex cells in a file extending from the quiescent centre (asterisk) to the first elongated cortex cells (white arrowheads). Scale bars: 100 µm. Data are shown as mean±s.e. (n=8-10). (Student's t test, ***P< 0.001).

We further examined two specific GFP based markers of cell differentiation, RHD6-GFP and RSL4-GFP, to monitor changes in expression patterns after TSA treatment. RHD6 and RSL4 are transcription factors involved in root-hair development (Yi et al., 2010). RHD6 is expressed only in the meristem whereas RSL4 is specifically expressed in the elongation zone (Fig. 2.7c, e). Following TSA treatment the cells from the differentiation zone expressed the meristematic marker (RHD6) (Fig. 2.7d), whereas the marker for the elongation zone (RSL4) had its expression reduced to fewer cells (Fig. 2.7f). Together these results reinforce the finding that the levels of histone acetylation have a major role in regulating cell differentiation and development.

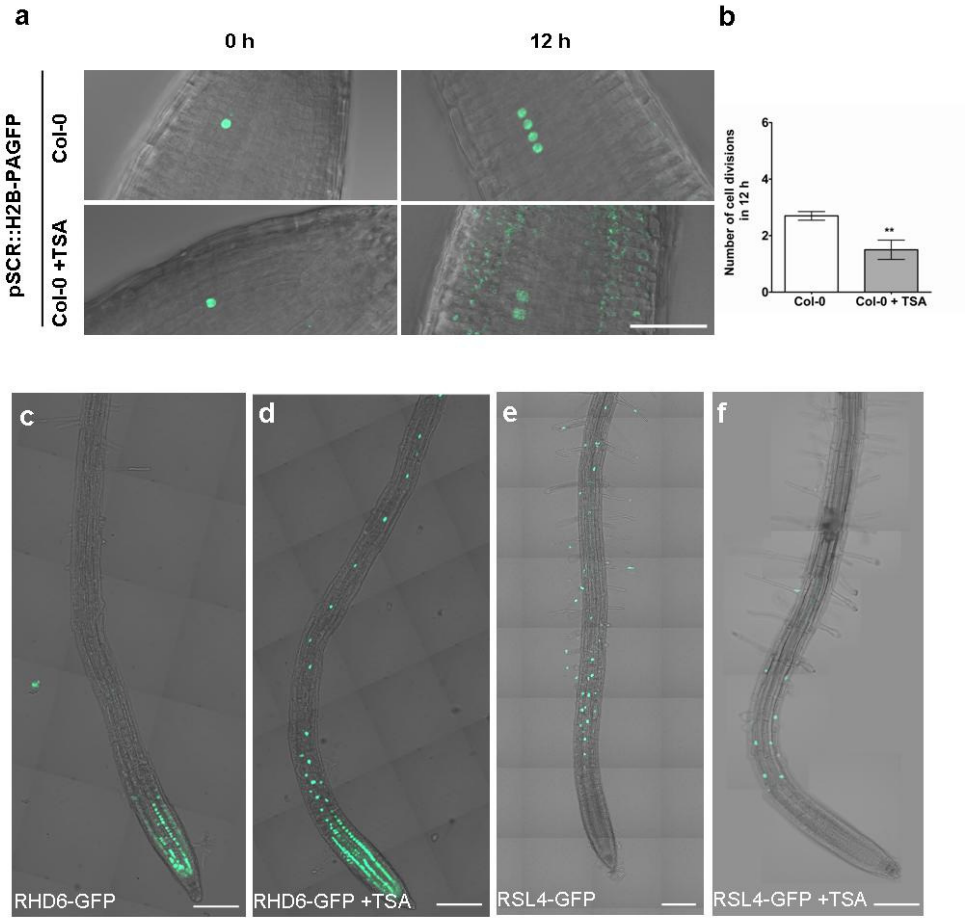

Figure 2.7. TSA effects on cell division and on the expression of root developmental markers.

a, Single nuclei of 4-day-old wild-type plants expressing H2B-PAGFP were photoactivated and cell divisions observed after 12h in control situation and after treatment with 100 ng/ml TSA. **b,** Number of cell division counted during a period of 12h, values represent means± s.e. (n= 10). 3-day-old wild-type roots expressing RHD6-GFP **(c-d)** and RSL4-GFP **(e-f)**. After overnight incubation with TSA (100 ng/ml) expression of RHD6-GFP was extended to the cell in the differentiation zone **(d)**, while RSL4-GFP expression was reduced to fewer cells in the elongation zone **(f)**. Scale bars represent 100 µm. (Student's *t* test, $^{**}P < 0.01$).

2.4.4. Auxins control histone acetylation levels and histone exchange

These results show that establishing the correct histone acetylation level is necessary for the proper differentiation of the developing roots. This raises the question of how such levels are established and maintained during Arabidopsis development. The plant hormone auxin is a key regulator of root development, and it is known that there is a gradient of auxin in the root (Overvoorde et al., 2010). A recent model is that auxin promotes cell division, whereas cytokinins control the switch from meristematic to differentiated cells by inhibiting auxin responses (Dello Ioio et al., 2007; Moubayidin et al., 2009). We applied exogenous auxin to wild-type roots overnight, and, as with TSA, showed an increase in meristem cell number (Fig. 2.6c, h). Similar to *hag1-6*, mutants of the *AUX/IAA* auxin response-related genes have very short primary roots and reduced meristem cell number (Hamann et al., 2002; Tian and Reed, 1999). We therefore determined whether the root phenotype of *hag1-6* mutant plants could be complemented by exogenous application of IAA (Fig. 2.6g-h); IAA was unable to induce an increase in meristem cell number in this mutant, which lacks a major histone acetyltransferase. In addition, when added together, IAA and TSA do not have a synergistic effect on meristem size (Fig. 2.6d, h). Taken together these results provide evidence that the effect of auxin on the meristem size is dependent on histone acetylation.

It had been shown that auxin gradient is dependent on the distribution of auxin efflux facilitators (PINs) (Friml, 2010; Grieneisen et al., 2007). In order to rule out the possibility that histone acetylation affects auxin distribution we monitored the effect of TSA on the expression of PIN1, PIN2 and PIN7. No differences in the distribution of PINs were observed following TSA treatment (Fig. 2.8).

As an independent confirmation that auxins can increase histone acetylation levels we performed immunofluorescence on IAA or TSA treated wild-type roots with an antibody against H2BK20ac (Fig. 2.9a-b). The results showed that both TSA and IAA induce increased levels of acetylation of H2B. The increase in acetylation was not restricted to H2B, but was also confirmed on histone H4 by western blotting (Fig. 2.9d). We then determined whether exogenous auxin application could increase H2B mobility. Photobleaching experiments on H2B-GFP plants grown overnight in the presence of IAA showed a significant increase in the mobility of H2B-GFP in the cells from the differentiation zone as previously seen for TSA (Fig. 2.9c).

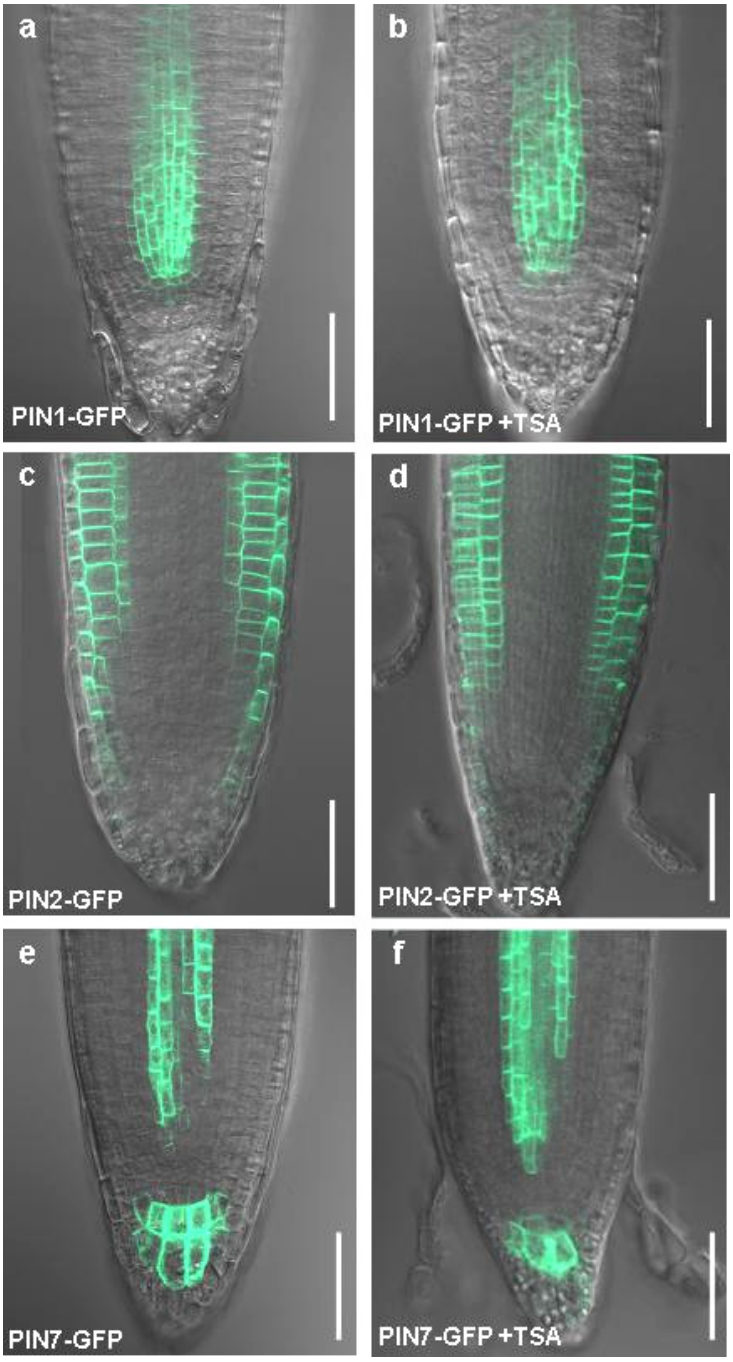

Figure 2.8. Histone hyperacetylation by TSA does not affect distribution of PINs.

Four-day old wild-type root meristems expressing PIN1-GFP **(a)**, PIN2-GFP **(c)** and PIN7-GFP **(e)**. No changes on PIN distribution were observed after overnight incubation with TSA (100 ng/ml) **(b, d, f)**. Scale bars represent 50µm.

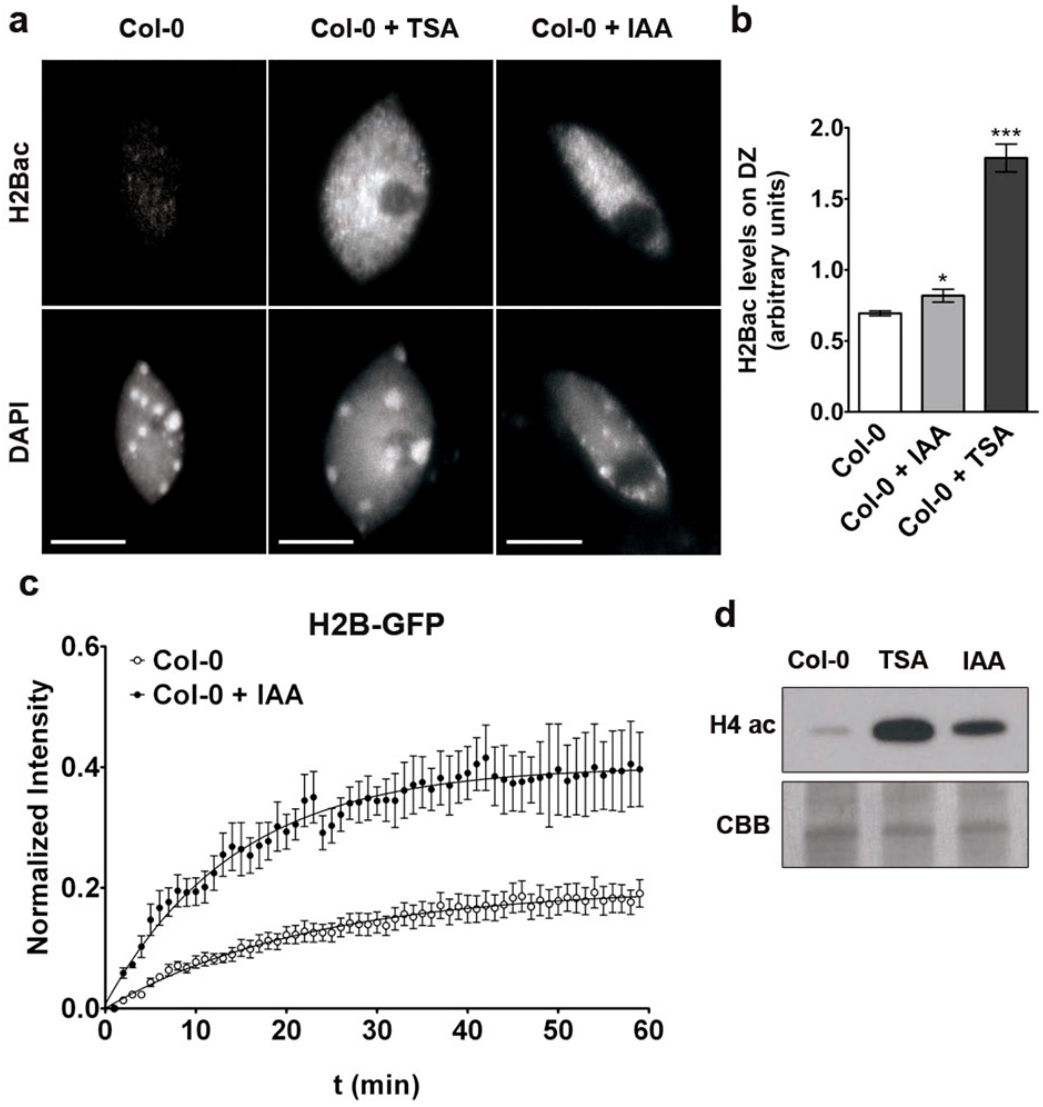

Figure 2.9. Auxins control histone acetylation levels and histone exchange.

(a) Representative immunolabeling images of Arabidopsis nuclei from the differentiation zone with an antibody against H2BK20ac, in wild-type plants showing an increase in the acetylation levels after treatment with TSA and IAA. Scale bars: 5 µm. (**b**) Quantitative analysis of immunolabeling experiment depicted in a. Values represent means ± s.e. from 10 cells. (**c**) FRAP curves for H2B-GFP in the differentiation zone on Col-0 plants showing and increase in mobility after treatment with IAA. Values represent means ± s.e. from at least 10 cells. (**d**) Western blot for H4ac in protein extracts from whole Col-0 roots showing an increase in the acetylation levels after overnight treatment with TSA and IAA. Comassie Brilliant Blue (CBB) showing equal loading.

2.5. Discussion

The process by which plants retain a population of dividing undifferentiated cells preventing them from differentiation is a fundamental question in biology and important for understanding plant growth and development. Here, we show that in the Arabidopsis root, meristematic cells are characterized by relatively weaker and more dynamic histone-DNA interactions. As root cells progress from the meristem towards the differentiation zone, histones become less mobile and more strongly bound to the chromatin. To account for our FRAP results, these changes must affect chromatin globally, and cannot simply be caused by changes in a subset of genes whose expression changes with differentiation.

Our studies further demonstrate that the changes in histone stability during root development are caused at least in part by changes in histone acetylation levels. We also found that altering stability via manipulation of acetylation levels, can affect aspects of root development. We observed that, consistent with a short root phenotype *hag1-6* (Kornet and Scheres, 2009) has a reduced number of meristematic cells, and that these cells are characterized by a less dynamic chromatin. Also hyperacetylation by TSA causes not only an increase on meristem size but also the expression of a meristem marker (*RHD6*) in cells from the differentiation zone together with a decrease of histone mobility in those cells. These results reveal a coordinate role for histone acetylation and histone stability in determining meristem competency and root development.

Finally we observed that the plant hormone auxin can directly affect histone acetylation levels and histone stability. We propose that the higher concentrations of auxin present in the root meristem are responsible for the higher histone exchange rates observed in these cells, acting by increasing the levels of histone acetylation. These results are consistent with a report where a loss-of-function mutation in PICKLE, a putative chromatin remodelling factor thought to function in cooperation with a histone deacetylase, allows the transcription of meristematic genes involved in lateral root initiation (Fukaki et al., 2006). In addition, application of a histone deacetylase inhibitor was found to suppress the lateral root defects seen in the *slr-1* (SOLITARY-ROOT) mutant (Fukaki et al., 2006). Another report, indicates that the transcriptional co-repressor TOPLESS mediates auxin-induced transcriptional repression, probably via recruitment of HDACS to chromatin (Szemenyei et al., 2008). While these studies suggest an involvement of histone modifications in auxin response, no direct link between histone acetylation levels and auxin was shown. However, a recent report has shown that auxin treatment is followed by a decrease in histone acetylation on a specific

CDK inhibitor gene involved in the control of cell proliferation (Anzola et al., 2010). Our analysis of auxin effects on histone dynamics and meristem activity suggests that this mechanism might represent a negative feedback loop to restrict the expression of CDK inhibitors to the meristem allowing a control of cell proliferation.

In summary our results show that high global levels histone acetylation and thus histone mobility in the genome regulate the maintenance of meristem competence, and that these acetylation levels are controlled by auxin.

2.6. Acknowledgments

We thank Michael Lenhard, Silvia Costa and Silke Robatzek for critical comments and Liam Dolan, Adrien Sicard, José Feijó and Lars Ostergaard for comments and advice.

2.7. References

Anzola, J.M., Sieberer, T., Ortbauer, M., Butt, H., Korbei, B., Weinhofer, I., Mullner, A.E., and Luschnig, C. (2010). Putative Arabidopsis transcriptional adaptor protein (PROPORZ1) is required to modulate histone acetylation in response to auxin. Proc Natl Acad Sci U S A *107*, 10308-10313.

Benjamins, R., and Scheres, B. (2008). Auxin: the looping star in plant development. Annu Rev Plant Biol *59*, 443-465.

Benkova, E., Michniewicz, M., Sauer, M., Teichmann, T., Seifertova, D., Jurgens, G., and Friml, J. (2003). Local, efflux-dependent auxin gradients as a common module for plant organ formation. Cell *115*, 591-602.

Blilou, I., Xu, J., Wildwater, M., Willemsen, V., Paponov, I., Friml, J., Heidstra, R., Aida, M., Palme, K., and Scheres, B. (2005). The PIN auxin efflux facilitator network controls growth and patterning in Arabidopsis roots. Nature *433*, 39-44.

Clough, S.J., and Bent, A.F. (1998). Floral dip: a simplified method for Agrobacterium-mediated transformation of Arabidopsis thaliana. Plant J *16*, 735-743.

Dello Ioio, R., Linhares, F.S., Scacchi, E., Casamitjana-Martinez, E., Heidstra, R., Costantino, P., and Sabatini, S. (2007). Cytokinins determine Arabidopsis root-meristem size by controlling cell differentiation. Curr Biol *17*, 678-682.

Dello Ioio, R., Nakamura, K., Moubayidin, L., Perilli, S., Taniguchi, M., Morita, M.T., Aoyama, T., Costantino, P., and Sabatini, S. (2008). A genetic framework for the control of cell division and differentiation in the root meristem. Science (New York, NY *322*, 1380-1384.

Dharmasiri, N., Dharmasiri, S., and Estelle, M. (2005). The F-box protein TIR1 is an auxin receptor. Nature *435*, 441-445.

Dolan, L., Janmaat, K., Willemsen, V., Linstead, P., Poethig, S., Roberts, K., and Scheres, B. (1993). Cellular organisation of the Arabidopsis thaliana root. Development *119*, 71-84.

Friml, J. (2010). Subcellular trafficking of PIN auxin efflux carriers in auxin transport. Eur J Cell Biol *89*, 231-235.

Fukaki, H., Taniguchi, N., and Tasaka, M. (2006). PICKLE is required for SOLITARY-ROOT/IAA14-mediated repression of ARF7 and ARF19 activity during Arabidopsis lateral root initiation. Plant J *48*, 380-389.

Gray, W.M., Kepinski, S., Rouse, D., Leyser, O., and Estelle, M. (2001). Auxin regulates SCF(TIR1)-dependent degradation of AUX/IAA proteins. Nature *414*, 271-276.

Grieneisen, V.A., Xu, J., Maree, A.F., Hogeweg, P., and Scheres, B. (2007). Auxin transport is sufficient to generate a maximum and gradient guiding root growth. Nature *449*, 1008-1013.

Hamann, T., Benkova, E., Baurle, I., Kientz, M., and Jurgens, G. (2002). The Arabidopsis BODENLOS gene encodes an auxin response protein inhibiting MONOPTEROS-mediated embryo patterning. Genes Dev *16*, 1610-1615.

Kadonaga, J.T. (1998). Eukaryotic transcription: an interlaced network of transcription factors and chromatin-modifying machines. Cell *92*, 307-313.

Kepinski, S., and Leyser, O. (2005). The Arabidopsis F-box protein TIR1 is an auxin receptor. Nature *435*, 446-451.

Kornet, N., and Scheres, B. (2009). Members of the GCN5 histone acetyltransferase complex regulate PLETHORA-mediated root stem cell niche maintenance and transit amplifying cell proliferation in Arabidopsis. Plant Cell *21*, 1070-1079.

Ljung, K., Bhalerao, R.P., and Sandberg, G. (2001). Sites and homeostatic control of auxin biosynthesis in Arabidopsis during vegetative growth. Plant J *28*, 465-474.

Menand, B., Yi, K., Jouannic, S., Hoffmann, L., Ryan, E., Linstead, P., Schaefer, D.G., and Dolan, L. (2007). An ancient mechanism controls the development of cells with a rooting function in land plants. Science *316*, 1477-1480.

Meshorer, E., Yellajoshula, D., George, E., Scambler, P.J., Brown, D.T., and Misteli, T. (2006). Hyperdynamic plasticity of chromatin proteins in pluripotent embryonic stem cells. Dev Cell *10*, 105-116.

Misteli, T., Gunjan, A., Hock, R., Bustin, M., and Brown, D.T. (2000). Dynamic binding of histone H1 to chromatin in living cells. Nature *408*, 877-881.

Mockaitis, K., and Estelle, M. (2008). Auxin receptors and plant development: a new signaling paradigm. Annu Rev Cell Dev Biol *24*, 55-80.

Moubayidin, L., Di Mambro, R., and Sabatini, S. (2009). Cytokinin-auxin crosstalk. Trends Plant Sci *14*, 557-562.

Overvoorde, P., Fukaki, H., and Beeckman, T. (2010). Auxin control of root development. Cold Spring Harb Perspect Biol *2*, a001537.

Palme, K., and Galweiler, L. (1999). PIN-pointing the molecular basis of auxin transport. Curr Opin Plant Biol *2*, 375-381.

Paponov, I.A., Teale, W.D., Trebar, M., Blilou, I., and Palme, K. (2005). The PIN auxin efflux facilitators: evolutionary and functional perspectives. Trends Plant Sci *10*, 170-177.

Phair, R.D., Gorski, S.A., and Misteli, T. (2004). Measurement of dynamic protein binding to chromatin in vivo, using photobleaching microscopy. Methods Enzymol *375*, 393-414.

Phair, R.D., and Misteli, T. (2000). High mobility of proteins in the mammalian cell nucleus. Nature *404*, 604-609.

Skoog, F., and Miller, C.O. (1957). Chemical regulation of growth and organ formation in plant tissues cultured in vitro. Symp Soc Exp Biol *11*, 118-130.

Strahl, B.D., and Allis, C.D. (2000). The language of covalent histone modifications. Nature *403*, 41-45.

Szemenyei, H., Hannon, M., and Long, J.A. (2008). TOPLESS mediates auxin-dependent transcriptional repression during Arabidopsis embryogenesis. Science *319*, 1384-1386.

Tan, X., Calderon-Villalobos, L.I., Sharon, M., Zheng, C., Robinson, C.V., Estelle, M., and Zheng, N. (2007). Mechanism of auxin perception by the TIR1 ubiquitin ligase. Nature *446*, 640-645.

Teale, W.D., Paponov, I., Ditengou, F., and Palme, K. (2005). Auxin and the developing root of Arabidopsis thaliana. Physiologia Plantarum *123*, 130-138.

Tian, Q., Nagpal, P., and Reed, J.W. (2003). Regulation of Arabidopsis SHY2/IAA3 protein turnover. Plant J *36*, 643-651.

Tian, Q., and Reed, J.W. (1999). Control of auxin-regulated root development by the Arabidopsis thaliana SHY2/IAA3 gene. Development *126*, 711-721.

Vanneste, S., and Friml, J. (2009). Auxin: a trigger for change in plant development. Cell *136*, 1005-1016.

Xu, J., and Scheres, B. (2005). Dissection of Arabidopsis ADP-RIBOSYLATION FACTOR 1 function in epidermal cell polarity. Plant Cell *17*, 525-536.

Yi, K., Menand, B., Bell, E., and Dolan, L. (2010). A basic helix-loop-helix transcription factor controls cell growth and size in root hairs. Nat Genet *42*, 264-267.

Yoshida, M., Kijima, M., Akita, M., and Beppu, T. (1990). Potent and specific inhibition of mammalian histone deacetylase both in vivo and in vitro by trichostatin A. J Biol Chem *265*, 17174-17179.

Chapter 3

Histone exchange in plant stem cells

The work described in this chapter is entirely my own.

Chapter 3:

Histone exchange in plant stem cells

3.1. Abstract

During plant development cells progress through different states as they evolve from stem cells to fully differentiated cells. There is evidence this transition can be accompanied by changes in chromatin state. It is now known from research into mammalian cell cultures that in pluripotent stem cells a significant fraction of histones is only loosely associated with chromatin. However nothing is known about the involvement of histones in the differentiation of plant stem cells. Here we used two-photon photoactivation to show that in stem cells from the root – the quiescent centre (QC) and initial cells - the mobility of the core histone H2B is reduced in these cells when compared with the surrounding cells of the meristem. Additionally, we show that histone acetylation controls maintenance of QC cells in the developing root. Hypercaetylation by TSA not only induces QC division but also the loss of expression of QC markers. We propose that plant stem cells have very immobile chromatin but they keep the potential to divide and differentiate into more dynamic states, and that these states are regulated by histone acetylation.

3.2. Introduction

The development of a multicellular organism demands the proper differentiation of pluripotent stem cells into a variety of specialized cell types. Plants have a remarkable ability to generate new organs from founder cells in their apical meristems. Their bodies derive from populations of dividing cells called meristems, which contain stem cells. It has been shown by clonal analysis that the ultimate source of cells in the *Arabidopsis thaliana* root meristem is the quiescent centre (QC), a group of cells that divides infrequently and that originate all tissue systems of the root (Kidner et al., 2000). The QC cells are also surrounded by other types of stem cells – initial cells – that divide more often to regenerate themselves and produce cells that give rise to all the different tissues that make up the root body (van den Berg et al., 1997; Wildwater et al., 2005). The main body of the root has therefore a simple

radial organization (Dolan et al., 1993). It consists of concentric tissue layers with different functional properties; from outside to inside, these are the epidermis, cortex, endodermis, pericycle, and the centrally located stele (Fig. 3.1).

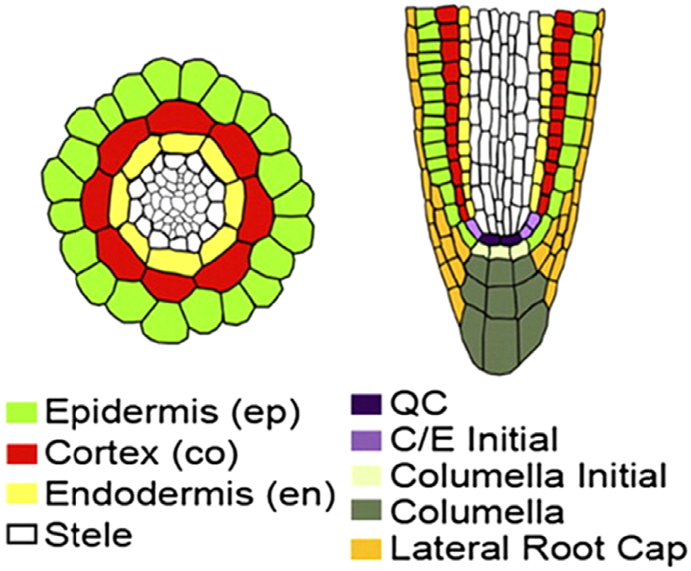

Figure 3.1. A schematic diagram showing tissues in Arabidopsis root meristem. (Heo et al., 2011)

Because initials can be replaced by QC cell division, the former can be considered to be short-term stem cells (Kidner et al., 2000). The exact role of the QC remains still unclear, though it is known that it maintains a stem cell state in adjacent cells and acts as a long-term stem cell pool itself. Ablation of the QC causes rapid differentiation of the root cap stem cells (van den Berg et al., 1997). Also, in Arabidopsis mutants which do not maintain a QC, the root meristem is eventually exhausted and all cells cease to divide (Aida et al., 2004; Sabatini et al., 2003).

QC specification was shown to be induced by an auxin-dependent patterning system. The auxin maximum in this system specifies QC position playing a critical role on its specification (Sabatini et al., 1999). In addition to auxin, two distinct transcription factor activities have previously been associated with QC specification. PLETHORA (PLT) and SHORTROOT/SCARECROW (SHR/SCR) appear to be required for different aspects of QC specification (Aida et al., 2004). SCR and SHR are also known for their role in creating and specifying the endodermis layer during embryogenesis, and maintaining endodermis identity in later stages of root development (Di Laurenzio et al., 1996; Helariutta et al., 2000; Nakajima et al., 2001).

Although QCs and plant stem cells generally have been extensively analyzed over the past decade many questions are still unsolved. The concept of "stem cells" has deeply captivated the attention of both scientists and the general public, at least partly because of the theoretical potential in medicine and tissue engineering. However whether the founder cells in plants are equivalent to the pluripotent stem cells in animals is still a matter of debate amongst plant scientists (Laux, 2003).

In chapter 2 we showed that histone-DNA interactions are weaker in undifferentiated meristematic cells. Also, research on mammalian pluripotent stem cells has demonstrated that a significant fraction of histones and other chromatin proteins is only loosely associated with chromatin (Meshorer et al., 2006). And, it has been proposed that this hyperdynamic binding of histone proteins is necessary for keeping differentiation options open.

In this chapter we studied the overall changes in histone dynamics during differentiation of plant stem cells.

3.3. Materials and Methods

3.3.1. Plant lines and growth conditions

Mutants and transgenic lines used in this study come from the following sources: H2A.Z-GFP (Kumar and Wigge, 2010); WOX5::GFP (Blilou et al., 2005); DR5::GFP (Ottenschlager et al., 2003). Transgenic lines were in Columbia (Col) background.

Seeds were surface sterilized, stratified and grown under the conditions described on Chapter 2. The roots were observed after 3 to 5 days of growth, depending on the experiment. For analysis of TSA and IAA effects, plants were initially germinated in non-supplemented media for 3 days and then transferred to new plates containing the respective supplements.

3.3.2. Supplemented growth media

Plates supplemented with trichostatin A (TSA) and 3-Indoleacetic acid (IAA) were prepared as described in Chapter 2.

3.3.3. Constructs and plant transformation

The H2B-PAGFP construct was cloned using the multisite gateway system (Invitrogen) as described in Chapter 2. *Agrobacterium tumefaciens* strain GV3103 was used for plant transformation by the floral dipping method as described (Clough and Bent, 1998). T1 plants were screened on MS and agar plates without sucrose and containing 50 µg/ml hygromycin and 50 µg/ml kanamycin.

3.3.4. Microscopy

Optical sections of roots were collected with a Zeiss 510 Meta confocal microscope. Roots were stained with propidium iodide as described on Chapter 2, and GFP expression analysed using a 488 nm excitation line and BP filter 505-550 nm.
Images were processed with the ImageJ program (http://rsb.info.nih.gov/ij/) or Adobe Photoshop CS.

3.3.5. Two-photon FRAP

Two-photon photo-activation experiments were performed on an Ultima two-photon laser scanning microscope (Prairie Technologies). Live images were acquired using either Olympus 60x 0.9NA water immersion objectives at 512x512 resolution and 1µm steps.
We chose to acquire data by two-photon microscopy because by single-photon confocal microscopy photo-activation of small areas induced photoconversion of the entire nucleus of the cells of interest, probably because of the optical properties of the root tip itself. Because the total lack of initial fluorescence makes it impossible to identify the regions of interest for photoactivation an initial pre-activation was necessary. This faint pre-activation was achieved by scanning the root tip at 850nm wavelength, 50% power and with a pixel time of 5.6 µs. One or two scans were necessary depending on signal.

Photoactivation of PAGFP in live tissue was carried out by defining simultaneously several regions-of-interest (ROI) that covered half of each nucleus in the different Z-positions. We then pulsed the ROIs with a 710 nm light at 30% power with a pixel time of 8.8 µs. We repeated this cycle two times, and then started imaging.

For imaging a Z-stack was collected at 925 nm (at 50% power, 8.8 µs/pixel). One z-stack (512x512 pixels) was collected every 60 seconds for 1h. To generate fluorescence decay curves background levels were initially subtracted from the images. Data was then corrected for the loss of fluorescence due to imaging and normalized as described by Phair et al. (Phair et al., 2004). We additionally normalized for the proportion of activated molecules as follows:

$$I_{norm}(t) = \frac{I(t) - I_{final}}{1 - I_{final}}$$

Where,

I_{final}, is the intensity of the activated region (ROI) at the end of the experiment considering a situation in which all molecules are mobile (on our case because half of the nucleus was photoactivated this value is 0.5).

Mobile fractions and half-lives were calculated by individually fitting the FRAP recoveries of each nucleus to a single exponential decay function and averaging. The standard Student's *t*-test was used to determine the statistical significance of results. All quantitative values represent averages from at least 10 cells. For the exponential fitting and statistical analysis we used the GraphPad Prism 5 software. Images were processed with the ImageJ program (http://rsb.info.nih.gov/ij/).

3.4. Results

3.4.1. Reduced mobility of Histone 2B in pluripotent plant stem cells

The faster recovery kinetics of H2B-GFP in meristematic nuclei described in the previous chapter suggested that as cells start to differentiate, the histone-DNA interactions become stronger, thus making the histones less dynamic. We next asked whether the mobility of histone proteins would be even higher in undifferentiated pluripotent stem cells. For these experiments and given that stem cells in the root are located in the middle of the tissue at a depth of circa 50 µm, two-photon imaging was required. Additionally, in order to improve the signal-to-noise ratio we used a photoactivatable marker, the photoactivatable GFP (PAGFP) (Patterson and Lippincott-Schwartz, 2002). As a result, instead of a conventional photobleaching experiment we analysed the kinetic properties of H2B in stem cells by fluorescence loss after photoactivation which is characterized by an exponential decay.

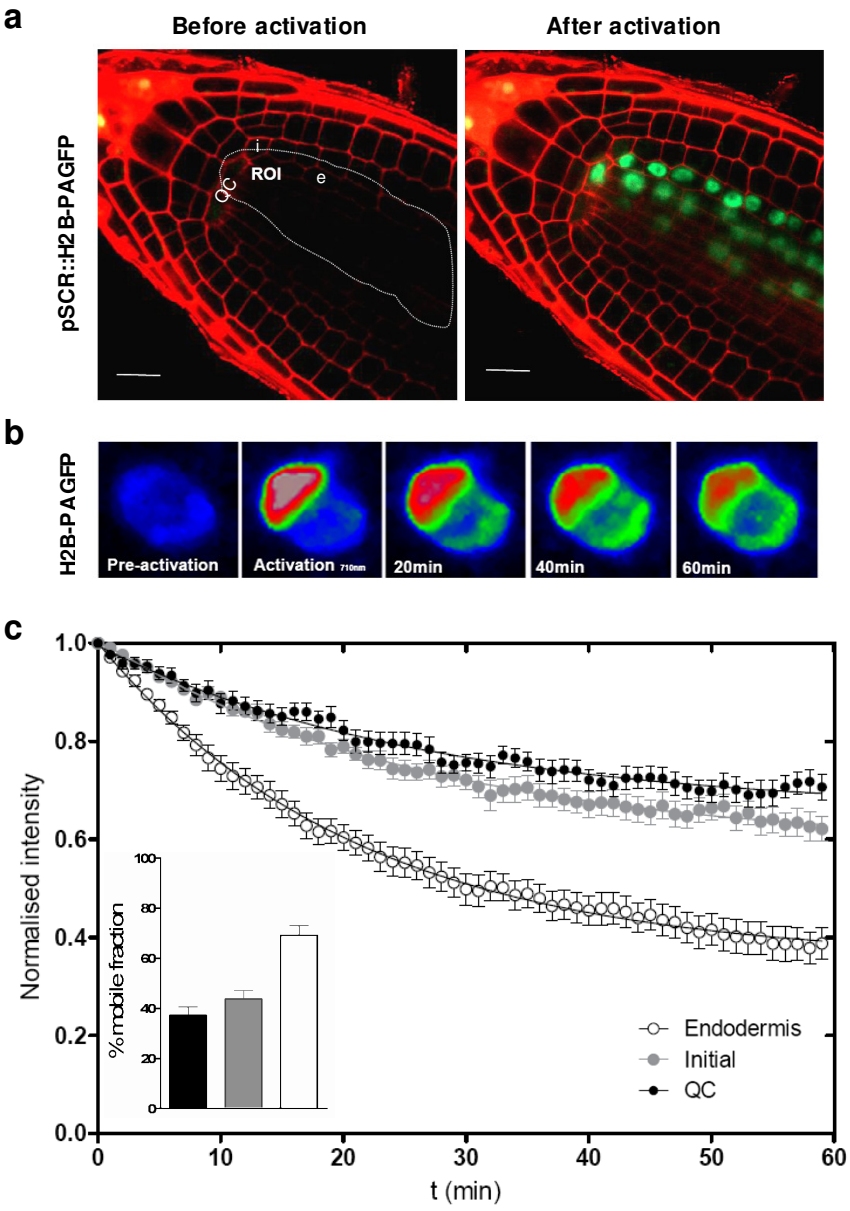

Figure 3.2. Reduced H2B-PAGFP mobility on pluripotent plant stem cells is revealed by two-photon FRAP.

(a) Longitudinal optical section of Arabidopsis stem cell niche in roots expressing H2B-PAGFP construct. This construct was expressed under the control of the promoter of SCARECROW which drives expression on QC cells, initials and endodermis. 4-day old seedlings were stained with propidium iodide and the GFP signal was activated under pulses of a 710 nm wavelength laser. The following abbreviations are used: QC, quiescent centre; i, initial cell; e, endodermis; ROI, region of interest. Scale bars represents 10 μm. **(b)** Representative fluorescence changes in a nucleus from the endodermis expressing H2B-PAGFP. Half of each nucleus was photo-activated and the loss of fluorescence within the activated area was measured with a wavelength of 850 nm. **(c)** Decay curves for H2B-PAGFP fluorescence within the different cell types; Insert: Estimated mobile fractions. Values represent mean±s.e. from at least 20 cells.

By placing the H2B-PAGFP construct under the control of a root cell specific promoter (pSCR), we were able to express our constructs simultaneously in QC cells (QC), endodermis/cortex initials (i), and on root endodermis (e) (Fig. 3.2a). This setup allowed us to compare, in vivo and in one organism, the dynamics of a histone protein in pluripotent stem cells as they progress into more differentiated states.

Photoactivation of PAGFP was carried out at a wavelength of 710 nm whereas 950 nm was used for imaging. In these experiments half of each nucleus was photoactivated as shown in Fig. 3.2b.

In contrast to our initial predictions we observed that for undifferentiated stem cells (QC and initial cells) the fluorescence decay was significantly slower than in the differentiated cells (endodermis) (Fig. 3.2c). The half-time for decay was 18.77 min after activation for the QC cell, 18.32 min in the initials and only 13.62 min in cells from the endodermis (Table 3.1). A similar pattern of mobility is shown by the size of the mobile pools, QCs and initials showed reduced mobile pools (37.22% and 43.70% respectively) in contrast with the cells from endodermis that showed a large pool of mobile histones (69.15%) (Fig. 3.2c). These results show that H2B is less mobile and more strongly bound to chromatin in “real” stem cells than in the adjacent differentiated cells of the meristem. It is the meristematic cells that show the fastest exchange, probably as a sign of very active and less condensed chromatin.

Table 3.1. Two-photon measurements for the half time recovery in minutes (min) for the H2B-PAGFP at the different cell types and developmental zones of the root. Values represent averages ± s.e..

	Half life (min)
QC	18.77±2.87
Initials	18.32±2.56
Endodermis	13.62±1.22
Elongation	13.83±1.21
Differentiation	16.96±1.05

To check the reliability of two-photon photoactivation experiments in relation to the photobleaching data presented in the previous chapter we carried out photoactivation in the different developmental zones of the root (Fig. 3.3). The results obtained by photoactivation were similar to the ones obtained by photobleaching. Therefore the differences of mobility observed for the stem cells are valid and significant. It is also important to notice that the values shown here for H2B dynamics on the endodermis are very similar to the ones obtained for the epidermis (Chapter 2). These observations suggest that the degree of global histone exchange is related with the state of differentiation rather than to differences between specific cell types.

Our observations for plant stem cells were quite different from results from animal stem cells (Meshorer et al., 2006). In contrast to animals, plant stem cells showed less mobile chromatin, in which histones are stably associated with the DNA. Is only when cells move out from the stem cell niche and acquire a meristematic characteristic that the chromatin becomes more open and histones become significantly more mobile. These differences are interesting but they also raise a number of questions about what the concept of stem cell really means in plants.

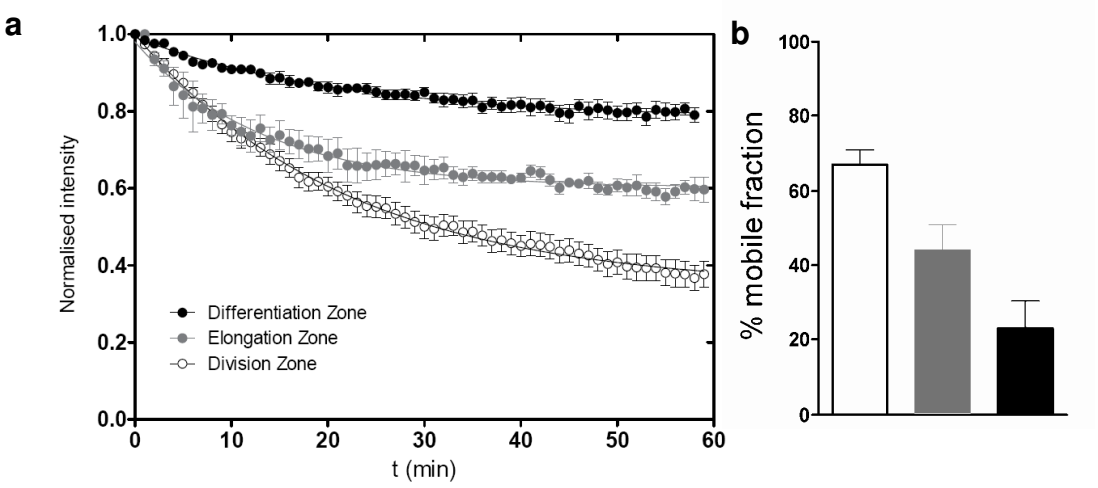

Figure 3.3. Two-photon FRAP curves for H2B at the different developmental zones.

(a) Recovery kinetics over a period of 60min in division zone (empty circles), elongation zone (grey circles) and differentiation zone (black circles). **(b)** Estimated mobile fractions of division zone (white), elongation zone (grey) and differentiation zone (black). Values represent mean±s.e..

3.4.2. Histone acetylation controls QC maintenance

In the previous chapter we showed that histone acetylation plays a major role in regulating cell differentiation and development. We therefore asked whether histone acetylation has any effect on the normal development of the stem cell niche.

To identify the effect of histone acetylation on the development of the stem cells we analysed the structure of the root tip on plants treated with TSA. We consistently observed QC divisions on plants treated overnight with TSA (Fig. 3.4a-b).

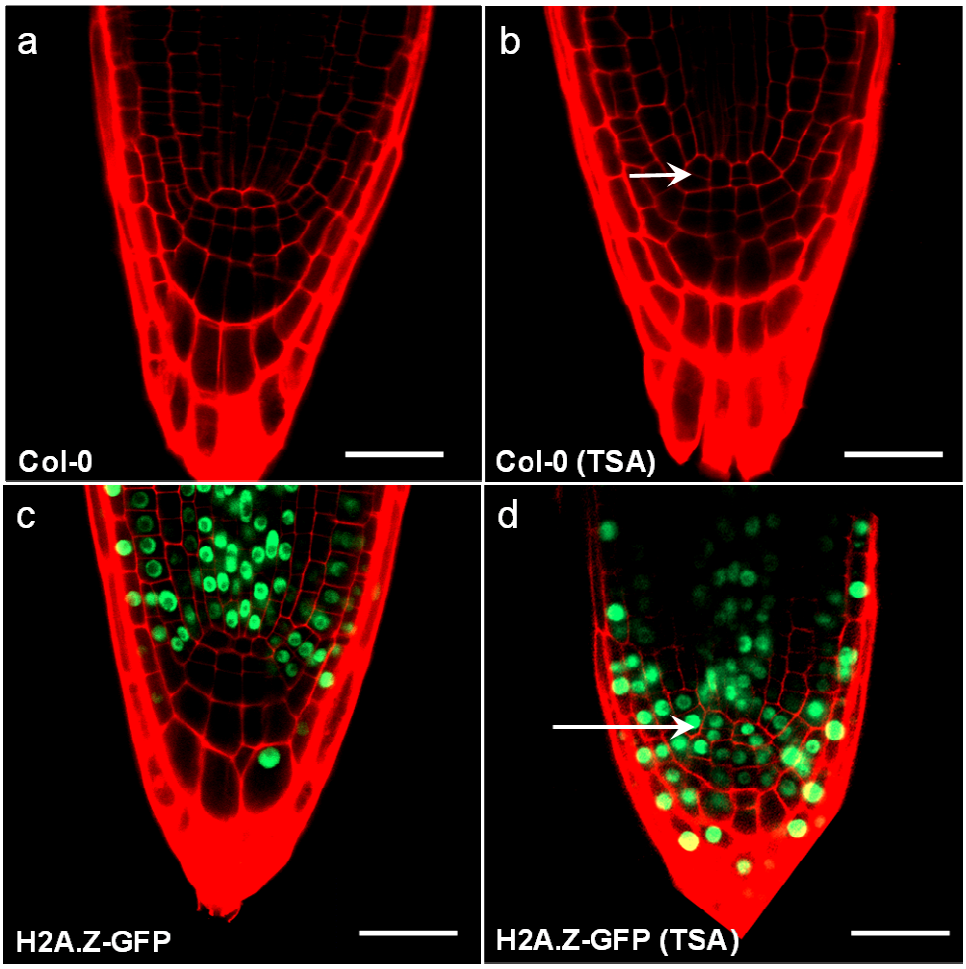

Figure 3.4. Histone hyperacetylation by TSA induces division and activity of QC cells.

Longitudinal optical sections of Arabidopsis stem cell niche in 4-day-old wild-type **(a, b)** and H2A.Z-GFP expressing roots **(c-d)**. **(a)** Col-0. **(b)** Col-0 root after incubation with 100 ng/ml TSA for 12h, showing division of QC cells (arrow). **(c)** Col-0 plant expressing H2AZ-GFP. **(d)** Col-0 H2A.Z-GFP root after TSA treatment showing expression of H2A.Z-GFP in QC cells (arrow). Scale bars: 20 µm.

Interestingly we also detected that histone hyperacetylation by TSA induces an ectopic expression of H2A.Z on QC cells (Fig. 3.4b). This histone variant was shown to be associated with replication activity (Costas et al., 2011) and is absent from QCs (Fig. 3.4a). Additionally this variant is mainly expressed in meristematic tissue, as it will be discussed in Chapter 4. Together these results suggest that increasing histone acetylation levels in the QC cells increases their replicative activity as observed by the expression of H2A.Z and as a result they re-enter the cell cycle and start to divide, similarly to a meristematic cells.

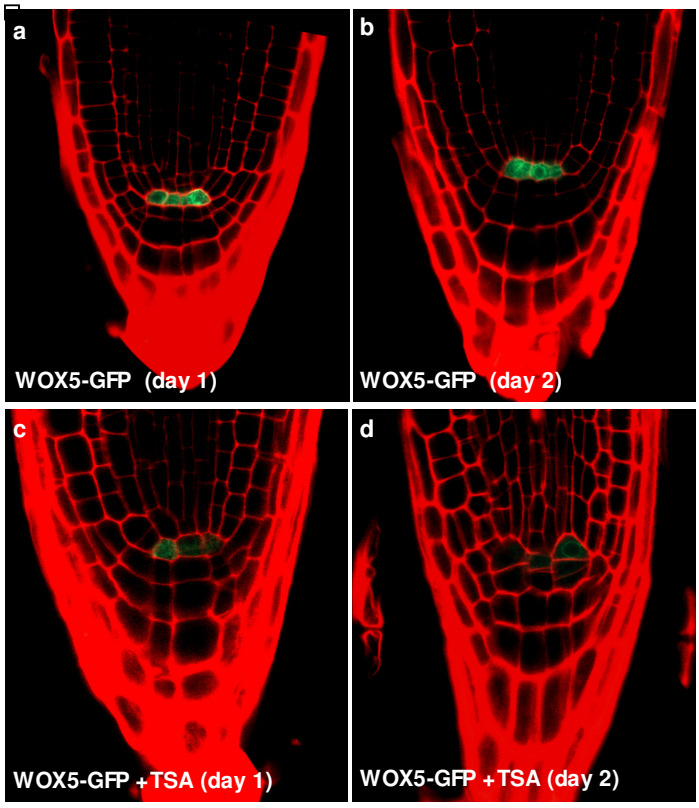

Figure 3.5. Effect of Histone hyperacetylation on the expression of WOX5 QC marker.

Gradual decrease in WOX5::GFP signal in control conditions **(a, b)** and after treatment with TSA (100 ng/ml) during one day **(c)** and 3 days **(d)**.

These observations were further supported by the fact that the specific QC marker WOX5 (WUSCHEL RELATED HOMEOBOX 5) transcription factor had its expression reduced on the presence of TSA (Fig. 3.5).

3.4.3. Histone hyperacetylation does not affect auxin maxima at QCs

It has been shown that QC maintenance is associated with an auxin maximum at the root tip (Sabatini et al., 1999). To investigate whether the altered QC development observed after TSA treatment was related with changes on the auxin levels we monitored relative auxin content in root tips of living Arabidopsis seedlings by means of the auxin reporter DR5::GFP (Ottenschlager et al., 2003). No changes were observed in auxin maxima after either TSA or IAA treatment (Fig. 3.6). These results suggest that histone acetylation directly affects QC maintenance and exerts its effects downstream of auxins.

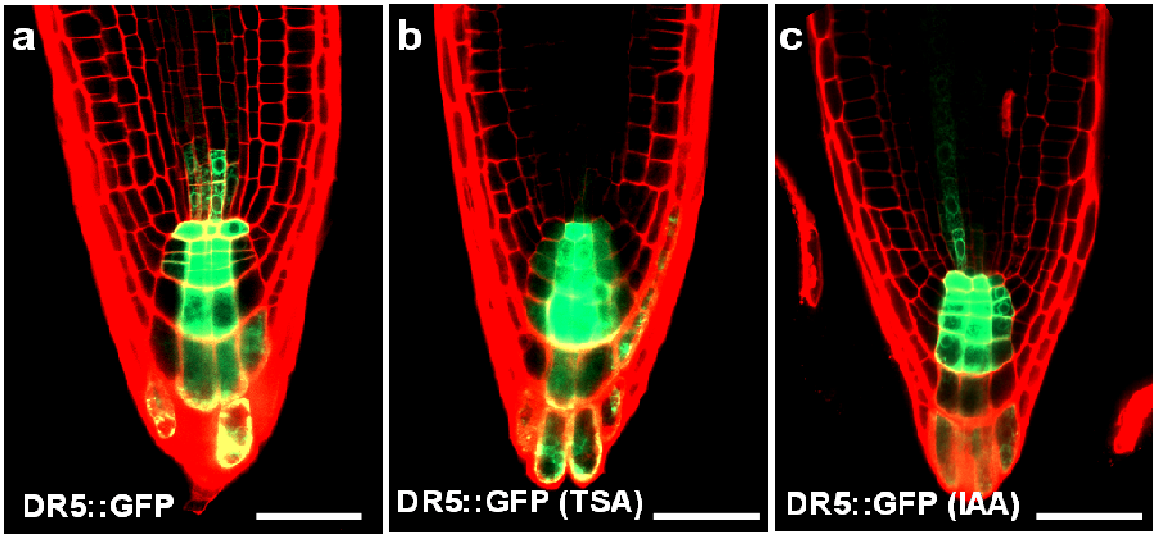

Figure 3.6. Histone hyperacetylation by TSA does not affect QC auxin maxima.

(a) Expression of DR5::GFP auxin response reporter in roots of 4-day-old seedlings.
(b) DR5::GFP expression in the presence of 100 ng/ml TSA, for 12h.
(c) DR5::GFP expression in the presence of 0.3ng/ml IAA for 12h.

3.5. Discussion

In Chapter 2 we demonstrated that during differentiation of root cell types the overall histone-DNA interactions become stronger and histones less mobile. Here we described that the overall state of the chromatin in plant stem cells is less dynamic with strong histone-DNA

interactions. The low mobilities observed for root stem cells are unexpected as these cells are pluripotent. However this aspect may reflect the very specialised function of these cells.

Root stem cells, and especially QCs, divide very infrequently, being mostly responsible for sending signals controlling differentiation of their neighbouring cells. Therefore to fulfil this role, these cells might need the activity of fewer genes. Transcriptome analysis of the Arabidopsis QC cells did not reveal a significantly smaller number of genes expressed in these cells in comparison to other cell types (Nawy et al., 2005). However, it should also be noticed that the marker used to isolate QC protoplasts, AGL42 (AGAMOUS-LIKE 42), was not shown to be enriched in the data set. Thus this study might not have been accurate enough to reveal such a reduced number of expressed genes or the isolation of protoplasts itself might have effects on the specific transcriptional profiles of the cells.

Although we do not yet have direct data showing that histone mobility is controlled by histone acetylation levels in stem cells, we predict that QC identity is associated with low levels of histone acetylation. Evidence for this is the induction of cell division and loss of the QC marker (WOX5) in those cells after TSA treatment. In a similar way it was shown by Kornet and Scheres (Kornet and Scheres, 2009) that the histone acetyltranferase GCN5 (for general control nonderepressible 5) is essential for root stem cell maintenance, supporting the idea that histone acetylation plays an important role in root and stem cell development. These results are further supported by the relation that has been reported in Arabidopsis between histone acetylation and DNA replication (Jasencakova et al., 2000). If DNA replication is associated with high levels of histone acetylation then it is likely that cells such as QCs or differentiated cells (as shown in Chapter 2), that are not dividing, have low levels of histone acetylation, and thus why these cells have low histone mobilities.

Our results are also consistent with the analysis of DNA methylation of Arabidopsis root by Lorvellec (Lorvellec, 2007). In this study they revealed that during the differentiation of root cells the overall DNA methylation levels increase and more importantly that the nuclei from stem cell niche were hypermethylated, in particular those of QCs and endodermis/cortex initials. Given that DNA methylation is normally associated with hypoacetylated histones, these results support the idea that in plant stem cells histones are poorly acetylated as we predicted from our FRAP data.

On the other hand our results contrast with what was already known for animal stem cells (Meshorer et al., 2006). Embryonic animal stem cells were shown to have hyperdynamic chromatin proteins and this state was proved to be essential for their function as pluripotent cells. Interestingly it was also shown that in nuclei of mammalian blastulas and embryonic

stem cells the chromatin is hypomethylated and that it becomes more methylated with the progress of cell differentiation (Jaenisch, 1997; Lei et al., 1996). Therefore with respect to their overall histone dynamics as well as patterns of DNA methylation and histone acetylation, animal stem cells resemble more the Arabidopsis root cells from the division zone rather than the QCs and initials. These observations might define fundamental differences between plant and animal stem cells. However it is important to notice that these studies were carried out on animal cell cultures and it would be interesting to see how the chromatin of animal stem cells behaves in the context of a multicellular organism.

In chapter 2 we made an association between histone mobility, levels of histone acetylation and the auxin gradient on the root. Surprisingly here the auxin maximum present at the QCs does not correlate with high mobility of histones and with high levels of histone acetylation as we predict for these cells. This puzzling result suggests that there are other activities, independent of auxin, necessary for stem cell specification and the low histone mobilities observed in these cells. For instance it has recently been shown that ethylene is part of a signalling pathway that modulates cell division in the quiescent center (Ortega-Martinez et al., 2007). Typically all developmental processes in plants are coordinated by overlapping activities of more than one hormone and stem cell maintenance is certainly no exception.

3.6. Acknowledgments

I would like to thank José Feijó and Nuno Moreno for the help with the Multiphoton microscope at the Gulbenkian Institute and to Vardis Ntoukakis for comments and advice.

3.7. References

Aida, M., Beis, D., Heidstra, R., Willemsen, V., Blilou, I., Galinha, C., Nussaume, L., Noh, Y.S., Amasino, R., and Scheres, B. (2004). The PLETHORA genes mediate patterning of the Arabidopsis root stem cell niche. Cell *119*, 109-120.

Blilou, I., Xu, J., Wildwater, M., Willemsen, V., Paponov, I., Friml, J., Heidstra, R., Aida, M., Palme, K., and Scheres, B. (2005). The PIN auxin efflux facilitator network controls growth and patterning in Arabidopsis roots. Nature *433*, 39-44.

Clough, S.J., and Bent, A.F. (1998). Floral dip: a simplified method for Agrobacterium-mediated transformation of Arabidopsis thaliana. Plant J *16*, 735-743.

Costas, C., de la Paz Sanchez, M., Stroud, H., Yu, Y., Oliveros, J.C., Feng, S., Benguria, A., Lopez-Vidriero, I., Zhang, X., Solano, R.*, et al.* (2011). Genome-wide mapping of Arabidopsis thaliana origins of DNA replication and their associated epigenetic marks. Nat Struct Mol Biol *18*, 395-400.

Di Laurenzio, L., Wysocka-Diller, J., Malamy, J.E., Pysh, L., Helariutta, Y., Freshour, G., Hahn, M.G., Feldmann, K.A., and Benfey, P.N. (1996). The SCARECROW gene regulates an asymmetric cell division that is essential for generating the radial organization of the Arabidopsis root. Cell *86*, 423-433.

Dolan, L., Janmaat, K., Willemsen, V., Linstead, P., Poethig, S., Roberts, K., and Scheres, B. (1993). Cellular organisation of the Arabidopsis thaliana root. Development *119*, 71-84.

Helariutta, Y., Fukaki, H., Wysocka-Diller, J., Nakajima, K., Jung, J., Sena, G., Hauser, M.T., and Benfey, P.N. (2000). The SHORT-ROOT gene controls radial patterning of the Arabidopsis root through radial signaling. Cell *101*, 555-567.

Heo, J.O., Chang, K.S., Kim, I.A., Lee, M.H., Lee, S.A., Song, S.K., Lee, M.M., and Lim, J. (2011). Funneling of gibberellin signaling by the GRAS transcription regulator scarecrow-like 3 in the Arabidopsis root. Proc Natl Acad Sci U S A *108*, 2166-2171.

Jaenisch, R. (1997). DNA methylation and imprinting: why bother? Trends Genet *13*, 323-329.

Jasencakova, Z., Meister, A., Walter, J., Turner, B.M., and Schubert, I. (2000). Histone H4 acetylation of euchromatin and heterochromatin is cell cycle dependent and correlated with replication rather than with transcription. Plant Cell *12*, 2087-2100.

Kidner, C., Sundaresan, V., Roberts, K., and Dolan, L. (2000). Clonal analysis of the Arabidopsis root confirms that position, not lineage, determines cell fate. Planta *211*, 191-199.

Kornet, N., and Scheres, B. (2009). Members of the GCN5 histone acetyltransferase complex regulate PLETHORA-mediated root stem cell niche maintenance and transit amplifying cell proliferation in Arabidopsis. Plant Cell *21*, 1070-1079.

Kumar, S.V., and Wigge, P.A. (2010). H2A.Z-containing nucleosomes mediate the thermosensory response in Arabidopsis. Cell *140*, 136-147.

Laux, T. (2003). The stem cell concept in plants: a matter of debate. Cell *113*, 281-283.

Lei, H., Oh, S.P., Okano, M., Juttermann, R., Goss, K.A., Jaenisch, R., and Li, E. (1996). De novo DNA cytosine methyltransferase activities in mouse embryonic stem cells. Development *122*, 3195-3205.

Lorvellec, M. (2007). Chromatin organization during Arabidopsis root development. PhD Thesis, Wageningen University, Netherlands.

Meshorer, E., Yellajoshula, D., George, E., Scambler, P.J., Brown, D.T., and Misteli, T. (2006). Hyperdynamic plasticity of chromatin proteins in pluripotent embryonic stem cells. Developmental cell *10*, 105-116.

Nakajima, K., Sena, G., Nawy, T., and Benfey, P.N. (2001). Intercellular movement of the putative transcription factor SHR in root patterning. Nature *413*, 307-311.

Nawy, T., Lee, J.Y., Colinas, J., Wang, J.Y., Thongrod, S.C., Malamy, J.E., Birnbaum, K., and Benfey, P.N. (2005). Transcriptional profile of the Arabidopsis root quiescent center. Plant Cell *17*, 1908-1925.

Ortega-Martinez, O., Pernas, M., Carol, R.J., and Dolan, L. (2007). Ethylene modulates stem cell division in the Arabidopsis thaliana root. Science (New York, NY *317*, 507-510.

Ottenschlager, I., Wolff, P., Wolverton, C., Bhalerao, R.P., Sandberg, G., Ishikawa, H., Evans, M., and Palme, K. (2003). Gravity-regulated differential auxin transport from columella to lateral root cap cells. Proc Natl Acad Sci U S A *100*, 2987-2991.

Patterson, G.H., and Lippincott-Schwartz, J. (2002). A photoactivatable GFP for selective photolabeling of proteins and cells. Science (New York, NY *297*, 1873-1877.

Phair, R.D., Gorski, S.A., and Misteli, T. (2004). Measurement of dynamic protein binding to chromatin in vivo, using photobleaching microscopy. Methods in enzymology *375*, 393-414.

Sabatini, S., Beis, D., Wolkenfelt, H., Murfett, J., Guilfoyle, T., Malamy, J., Benfey, P., Leyser, O., Bechtold, N., Weisbeek, P.*, et al.* (1999). An auxin-dependent distal organizer of pattern and polarity in the Arabidopsis root. Cell *99*, 463-472.

Sabatini, S., Heidstra, R., Wildwater, M., and Scheres, B. (2003). SCARECROW is involved in positioning the stem cell niche in the Arabidopsis root meristem. Genes Dev *17*, 354-358.

van den Berg, C., Willemsen, V., Hendriks, G., Weisbeek, P., and Scheres, B. (1997). Short-range control of cell differentiation in the Arabidopsis root meristem. Nature *390*, 287-289.

Wildwater, M., Campilho, A., Perez-Perez, J.M., Heidstra, R., Blilou, I., Korthout, H., Chatterjee, J., Mariconti, L., Gruissem, W., and Scheres, B. (2005). The

RETINOBLASTOMA-RELATED gene regulates stem cell maintenance in Arabidopsis roots. Cell *123*, 1337-1349.

Chapter 4

H2A.Z controls a position-dependent cell fate switch in Arabidopsis

The work described in this chapter was carried out in collaboration with Vardis Ntoukakis. I have been directly involved in all the confocal microscopy imaging including, FRAP, *de novo* synthesis measurements and total nuclei fluorescence determinations.

Chapter 4:

H2A.Z controls a position-dependent cell fate switch in Arabidopsis

4.1. Abstract

During development plant cells frequently need to assess positional information if organ and tissue formation are to occur. In the Arabidopsis root epidermis, cells differentiate into alternating files of hair cells and non-hair cells. This pattern is controlled by the position-dependent expression of the homoeodomain transcription factor GLABRA 2 (GL2). Previous work showed that this position-dependent cell-fate switch relies on alternative states of chromatin organization at the *GL2* locus. This raises the question of what mechanism leads to the different chromatin states. Here, we show that an ATP dependent chromatin remodelling complex, PIE1, is involved in the position-dependent cell-fate decision. PIE1 is responsible for the exchange of the canonical histone H2A with the histone variant H2A.Z. We show that H2A.Z incorporation is higher in non-hair cells, and that mutants of PIE1 complex, where H2A.Z incorporation is diminished, develop ectopic roots hairs as a result of mis-regulation of *GL2* expression. Furthermore, we show that WEREWOLF (WER), a MYB transcription factor that directly binds to the GL2 promoter, controls this position-dependent incorporation of H2A.Z. Our results suggest that the dynamic redistribution of H2A.Z may represent a general mechanism for cell fate switching in plants.

4.2. Introduction

The root epidermis of Arabidopsis is made up of columns of two distinct cell types – hair and non-hair cells. This organization is established during embryogenesis and is maintained throughout the development of the Arabidopsis root suggesting a mechanism that propagates the patterning (Berger et al., 1998; Costa and Shaw, 2006; Lin and Schiefelbein, 2001). The establishment of the patterning relies on positional information and requires the activity of GLABRA2 (GL2) — a homeodomain transcription factor (Berger et al., 1998; Di Cristina et al., 1996; Lin and Schiefelbein, 2001). Cell fate specification of epidermal cells is

established in the meristem, and is controlled by the cell position in relation to the underlying cortical cells (Berger et al., 1998). Atrichoblasts (future non-hair cells) overlay a single cortical cell and express GL2, which negatively regulates root hair formation. On the other hand, trichoblasts (future hair cells) overlay the cleft between two cortical cells and do not express GL2 (Fig. 4.1).

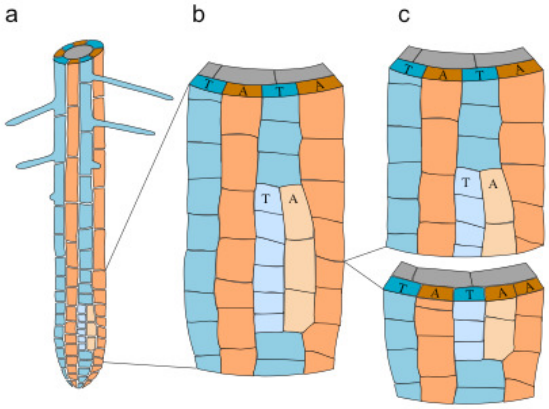

Figure 4.1. Schematic representation of Arabidopsis root epidermis organisation.

a, Longitudinal files of atrichoblasts (orange), which differentiate into non-hair cells, alternate with files of trichoblasts (blue), which differentiate into hair cells. **b**, **c** Close-up sections of a region of the root (a), showing that trichoblasts overlay two cortical cells (grey), while atrichoblasts overlay a single cortical cell. An epidermal T clone is represented in lighter colours. These clones are formed when an epidermal cell divides transversely originating two files of cells with the same clonal origin but with different fates determined by their position relative to the underlying cortical cells. (Costa and Shaw, 2006)

The molecular mechanism that generates and transduces the positional information to epidermal cells is still poorly understood. It is known that the *SCRAMBLED* (*SCM*) gene which encodes a receptor-like kinase is involved in this process (Chevalier et al., 2005; Kwak et al., 2005). This receptor is expressed in all plant tissues including the root epidermis, where in the presence of an unknown signal localized at the cleft between two cortical cells it causes the repression of *GL2* expression (Kwak and Schiefelbein, 2007). This cell fate switch is especially evident when a transversal division occurs that misplaces an epidermal cell from its initial position (T-clones) (Fig 4.1 b,c). In this situation the cells that occupy a new position in relation to the cortical cells acquire a new fate.

We know many of the components of the regulatory network controlling GL2 expression and subsequently fate specification of Arabidopsis root epidermal cells. GL2 is positively regulated by *WERWOLF* (*WER*), GLABRA3 (GL3), ENHANCER OF GLABRA3

(EGL3) and TRANSPARENT TESTA GLABRA1 (TTG1). *WER* gene encodes a member of the R2R3 MYB class of transcriptional regulators (Lee and Schiefelbein, 1999) and is required for non-hair cell specification. It is expressed in developing non-hair cells where it binds the GL2 promoter (Koshino-Kimura et al., 2005; Lee and Schiefelbein, 1999). GL3 and EGL3 encode bHLH transcription factors (Bernhardt et al., 2003). TTG1 encodes a WD40 repeat protein (Walker et al., 1999). In contrast, *CAPRICE* (*CPC*) encodes a R3 Myb protein that helps to specify hair cell fate in the root by acting as a negative regulator of *GL2* (Wada et al., 2002; Wada et al., 1997). Despite its function in promoting hair cell formation, CPC is expressed in non-hair cell files (Wada et al., 2002). Nevertheless it has been shown that CPC protein is localised within nuclei of all epidermal cells which implies that this protein moves from non-hair cells to hair cells (Wada et al., 2002). Mutations in *CPC* cause a reduction in the number of root hairs as a consequence of the expression of GL2 in all epidermal cells.

In addition to *GL2*, *WER*, *GL3*, *EGL3*, *TTG1* and *CPC*, hundreds of genes are differentially expressed between atrichoblasts and trichoblasts cells (Birnbaum et al., 2003; Brady et al., 2007; Deal and Henikoff, 2010; Won et al., 2009). These differences in gene expression could only partially be attributed to trimethylation of histone H3 at lysines 4 and 27 (Deal and Henikoff, 2010), indicating the involvement of an alternative mechanism in the regulation of gene expression between the two types of cells. It has been previously shown that changes in positional information are accompanied by rapid changes in chromatin accessibility of the genomic region around the *GL2* locus (Costa and Shaw, 2006). Such a major rearrangement in chromatin organization during cell fate switching suggests the involvement of chromatin remodelling complex as an alternative mechanism controlling cell specification.

In this chapter we investigated the presence of such chromatin remodelers during epidermal cell specification.

4.3. Materials and Methods

4.3.1. Plant lines and growth conditions

Mutants and transgenic lines used in this study come from the following sources: *arp6-1* mutant (Deal et al., 2005); *esd1-2* mutant (Martin-Trillo et al., 2006); *sw6-1* mutant

(Choi et al., 2007); *yaf9-1* mutant (Choi et al., 2011); scm-2 (Kwak et al., 2005); wer (Masucci et al., 1996); H2A.Z-GFP (Kumar and Wigge, 2010); H2B-GFP (Chapter 2); H3.1 and h3.3 (Ingouff et al., 2007; Ingouff et al., 2010) pWER:GFP ; pGL2:GFP ; pCPC:GFP were described previously (Lin and Schiefelbein, 2001; Ryu et al., 2005; Wada et al., 2002). Mutants and transgenic lines were in Columbia (Col) background.

Seeds were sterilized for 5 minutes in 5% v/v sodium hypochlorite and rinsed three times in sterile distilled water. Seeds were then plated on to Murashige and Skoog medium (pH 5.8) supplemented with 1% w/v sucrose and 0.5% w/v Phytagel. Next, seeds were stratified for 48h at 4°C in a dark room and finally transferred to grown in continuous light at 25°C in vertically oriented Petri dishes. Roots were observed after 3 to 5 days of incubation, depending on the experiment.

4.3.2. Supplemented growth media

For MG132 supplemented media a final concentration of 100µM was used in liquid MS media for 6h. MG132 was obtained from Sigma-Aldrich.

4.3.3. Constructs and plant transformation

Arabidopsis *arp6-1* plants were transformed as described previously (Clough and Bent, 1998) using the binary vector pGWB10 containing the *ARP6* gene under the control of its own promoter (Kumar and Wigge, 2010). Homozygous single-insertion transformants were selected in the T3 generation and ARP6 accumulation was confirmed by western blots.

4.3.4. Microscopy

For longitudinal analysis of root epidermis seedlings were stained with 20 mg/ml propidium iodide (Sigma) and observed on a Zeiss 510 Meta confocal microscope. For visualization of propidium iodide an excitation line of 488nm was used and signal was detected at wavelengths of 580-700nm. For observation of GFP expression we used a 488 nm excitation line and BP filter 505-550 nm. Images were processed with the ImageJ program (http://rsb.info.nih.gov/ij/) or Adobe Photoshop CS3.

4.3.5. FRAP

A Zeiss confocal LSM 510 was used for all photobleaching experiments. Photobleaching and quantification was performed as described in Chapter 2. For FRAP experiments on H2A.Z-GFP under *arp6-1* background image size was reduced to 256x256 pixels and imaging was performed with a bi-directional scanning mode (with pixel dwell time 0.8 µsec). Five pre-scans were taken before a bleaching pulse of 1 iteration 100% laser power (488 nm) followed by 60 scans with 1% laser power. No time delays or Z-stacks were taken.

4.3.6. *De novo* synthesis

For calculation of *de novo* synthesis, z-stacks (steps of 0.5 µm) of nuclei expressing H2A.Z-GFP protein were collected followed by photobleaching of the entire nucleus with the 488 laser line at 100% power. One z-stack was acquired after photobleaching and a further one after 1h. The quantification of de novo synthesis was calculated as described in Chapter 2.

4.3.7. Total Fluorescence

For determination of fluorescence intensity per nucleus of cells expressing H2A.Z-GFP we collected z-stacks, with a z-step of 0.2 µm. The stack was than processed on ImageJ software (http://rsb.info.nih.gov/ij/), where a Z-max projection was followed by the quantification of the mean grey value within each nucleus. The same settings were used between experiments.

4.3.8. Root-hair measurement

Root hairs phenotypes were evaluated by visualizing the roots of 7-day-old seedlings under a Leica M10 dissecting microscope. Pictures of root hairs measuring approximately 3 mm to the root tip were collected by a Nikon N995 digital camera. The digital images were used directly for root-hair density measurement by ImageJ (http://rsb.info.nih.gov/ij/).

4.3.9. Transversal Sections

Roots were fixed in 1x PBS, 4% paraformaldehyde, 2.5% glutaraldehyde, 0.1% Triton X-100 for 20 min, and then overnight in 1xPBS, 4% paraformaldehyde, at 4 °C. After dehydration, whole roots were stained with a solution of 0.2% (w/v) Eosin Y (Sigma) diluted

in absolute ethanol, embedded in Epon and 1 mm sections were prepared and stained with a solution of 0.05% (w/v) of toluidine blue (Sigma).

4.4. Results

4.4.1. PIE1(Arp6) controls root hair development

To identify possible chromatin remodelers controlling epidermal cell specification in Arabidopsis root we screened mutants of chromatin remodelling complexes for defective root hair phenotypes. We identified one mutant with an aberrant number of root hairs, *arp6-1*. This mutant has been previously characterised as a member of actin-related protein (ARP) family in Arabidopsis (Choi et al., 2005; Deal et al., 2005). ARP6 is a peripheral subunit of the PIE1 (SWR1 in yeast) chromatin remodelling complex which regulates transcription through the deposition of the H2A.Z histone variant at target genes (Krogan et al., 2003; Mizuguchi et al., 2004).

In the *arp6-1* mutant the number of root hairs is significantly higher than in wild-type plants (Fig. 4.2a; Fig. 4.3a-b), while the number of trichomes is reduced (Fig. 4.2b). Both of these phenotypes were complemented in transgenic plants of the *arp6-1* mutant expressing the functional ARP6 protein tagged with a C-terminal FLAG epitope under the control of the native ARP6 promoter (Fig. 4.2a-b). Most importantly, the increased number of root hairs in the *arp6-1* mutant can be attributed to ectopic root hairs (Fig. 4.2c) that lead to increased number of hair files without altering the total number of epidermal cell files (Fig. 4.2d) and the root structure (Fig. 4.3c). A similar phenotype was observed with an additional allele of ARP6, *esd1-2* (Martin-Trillo et al., 2006), and two mutants of other subunits of the PIE1 complex *swc6*-1(Lazaro et al., 2008) and *yaf9-1* (Meagher et al., 2005)(Fig. 4.3a-b).

4.4.2. H2A.Z-GFP patterning in the meristem transition zone

In order to confirm the role of PIE1 complex in controlling cell specification we use a previously described Arabidopsis line expressing the HTA11:GFP, one of the 3 H2A.Z encoding genes, under the control of its endogenous HTA11 promoter (Kumar and Wigge, 2010). In accordance with previous Affymetrix GeneChip expression data (Hennig et al.,

2003; Zimmermann et al., 2004) suggesting that HTA11 expression was linked to S phase, HTA11:GFP was expressed exclusively in the meristem zone of Col-0 roots and is progressively excluded from the fully differentiated parts of the root (Fig.4.5a).

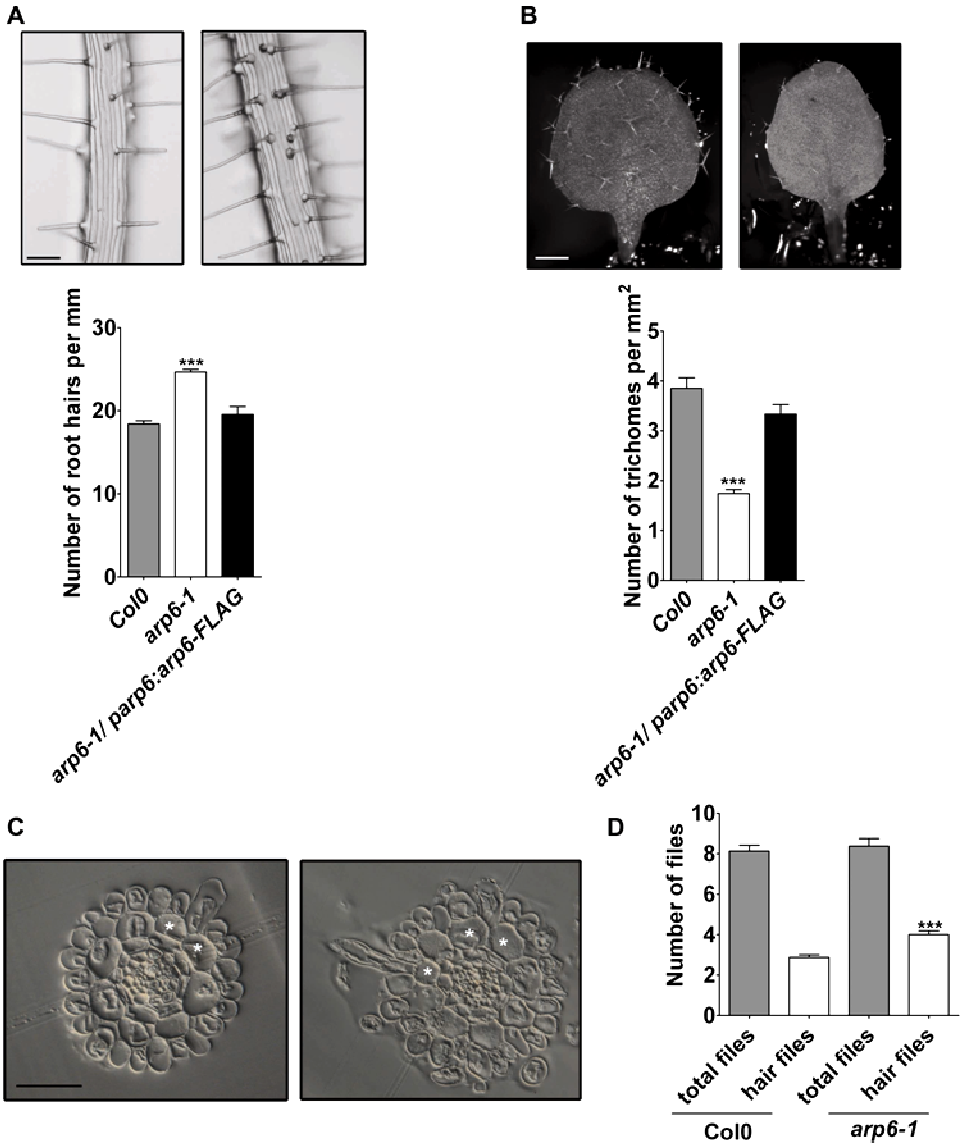

Figure 4.2. A mutant of the PIE1complex (*Arp6*) has altered root hair numbers.

Root hair phenotype of *arp6-1* plants and its complementation with ARP6 genomic DNA (*arp6-1*/arp6:arp6-FLAG), scale bar: 100 µm. Quantification of root hair density (mean ± s.e.; n=30) is shown at the bottom. Asterisks indicate statistically significant differences (P<0.001). **(b)** Trichome phenotype of *arp6-1* plants. Images showing adaxial surface of leaves, scale bar: 1 mm. Quantification of trichome (mean ± s.e.; n=30) density is shown at the bottom. Asterisks indicate statistically significant differences (P<0.001). **(c)** Transverse sections of root meristems showing the presence of ectopic root hairs in *arp6-1* mutant. The hair cell observed in *arp6-1* is facing a single cortical cell (marked with a start). **(d)** Quantification of ectopic hair formation. (values represent mean±s.e.; P<0.001).

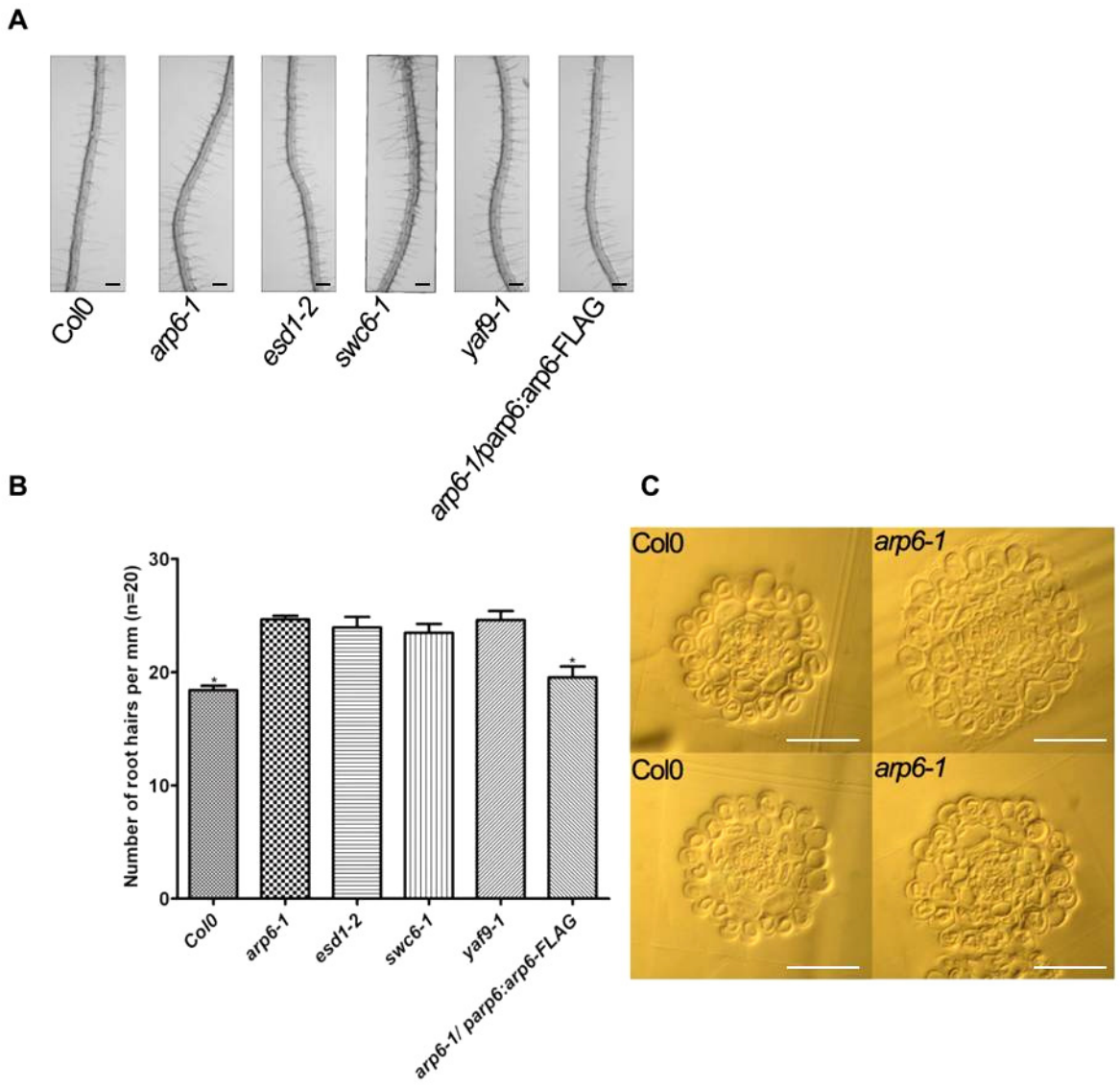

Figure 4.3. Mutants of PIE1 complex show increased root hair density.

(a) Root hair phenotype of mutants on different sub-units of PIE1 complex. **(b)** Quantification of root hair density of PIE1 complex mutants (mean ± s.e.; n=30). Scale bars: 100µm. Asterisks indicate statistically significant differences (*P<0.01). **(c)** Transverse sections of root meristems of Col-0 and *arp6-1* plants, showing a similar structural and tissue organization. Scale bars: 50µm.

More detailed examination revealed an interesting pattern of HTA11:GFP accumulation in the meristem transition zone of Col-0 roots (Fig. 4.4a). The levels of HTA11:GFP were noticeable higher in atrichoblast cells compared to trichoblasts, as demonstrated by the quantification of total fluorescence per nucleus (Fig. 4.4a). The higher levels of HTA11:GFP in atrichoblast cells only occurred in the meristem transition zone and

not in the other zones of Col-0 roots (Fig. 4.5b). Interestingly this region overlaps with the region where *GL2* was shown to have alternate chromatin conformations in atrichoblasts and trichoblasts (Costa and Shaw, 2006), suggesting that differential incorporation of H2A.Z might account for the different conformational states. In contrary to Col-0, HTA11:GFP accumulation in *arp6-1* mutant was generally lower and most importantly the patterning evident in the meristem transition zone of Col-0 was lost in the mutant (Fig. 4.4b).

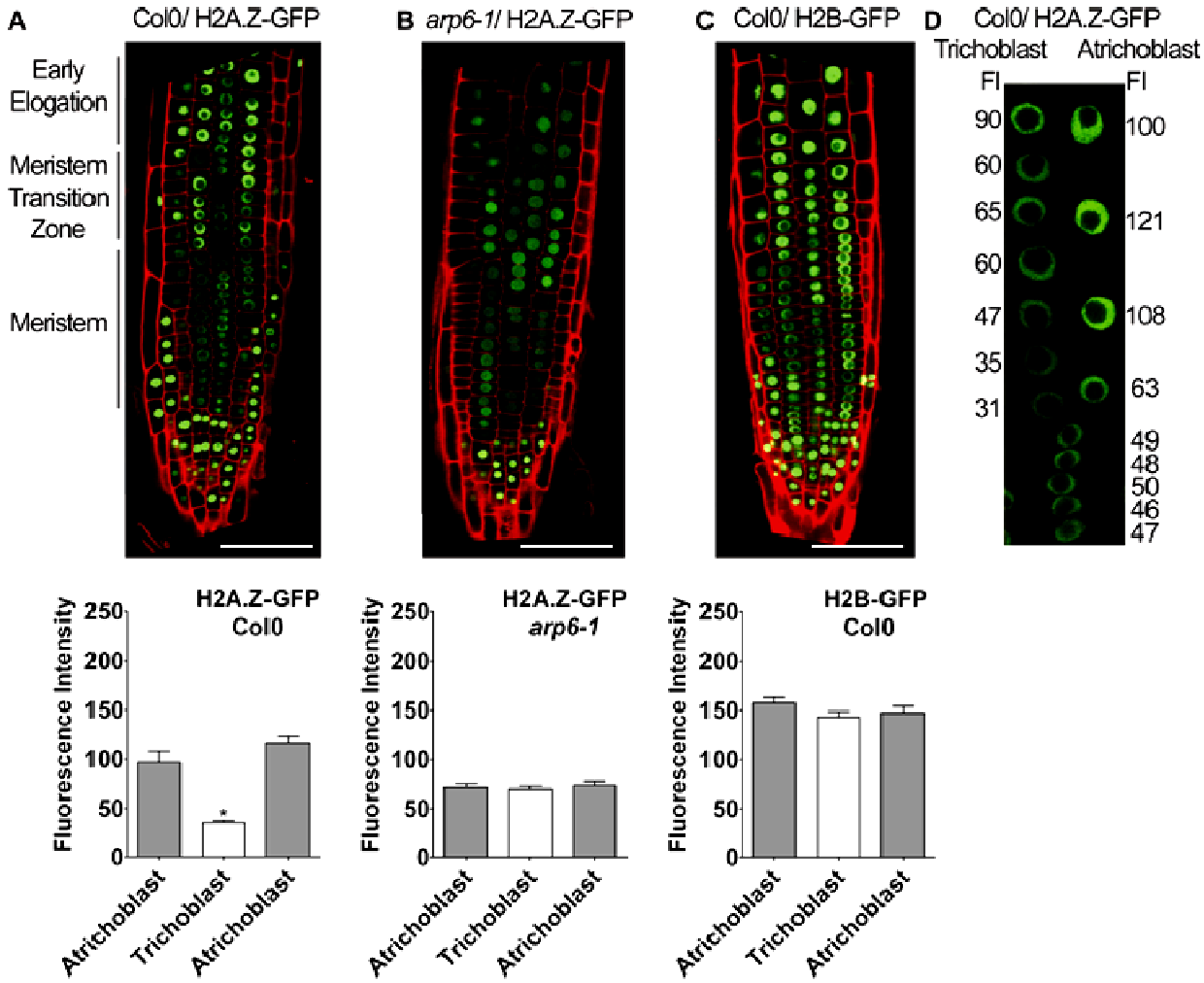

Figure 4.4. H2A.Z-GFP pattering is specific to the on meristem transition zone and defined by positional information.

Four day-old root meristems of **(a)** wild-type plants expressing H2A.Z-GFP **(b)** *arp6-1* mutant expressing H2A.Z-GFP **(c)** wild-type plants expressing H2B-GFP. Scale bar: 100 µm. Graphs show quantification of GFP signal of the corresponding histone on nuclei from the meristem transition zone (mean ± s.e.; n=10). Asterisks indicate statistically significant differences (*P<0.01). Scale bars: 50 µm **(d)** Quantification of fluorescence intensity (FI) after a division of an epidermal cells along the longitudinal plane (T-clone). Values represent mean fluorescent values of GFP signal.

In order to confirm that HTA11:GFP patterning observed in Col-0 was specific for this histone variant and not a general aspect of chromatin in the meristem transition zone we looked at the expression of other histone-GFP lines. Neither the canonical histones H2B and H3.1 nor the H3.3 variant (Ingouff et al., 2007; Ingouff et al., 2010) showed any obvious pattern at the meristem transition zone (Fig. 4.4c, Fig. 4.5c-d). Taken together, these results suggest that the differential accumulation of HTA11 in trichoblast and atrichoblast cells is a specific characteristic of the meristem transition zone and is dependent on the PIE1 complex.

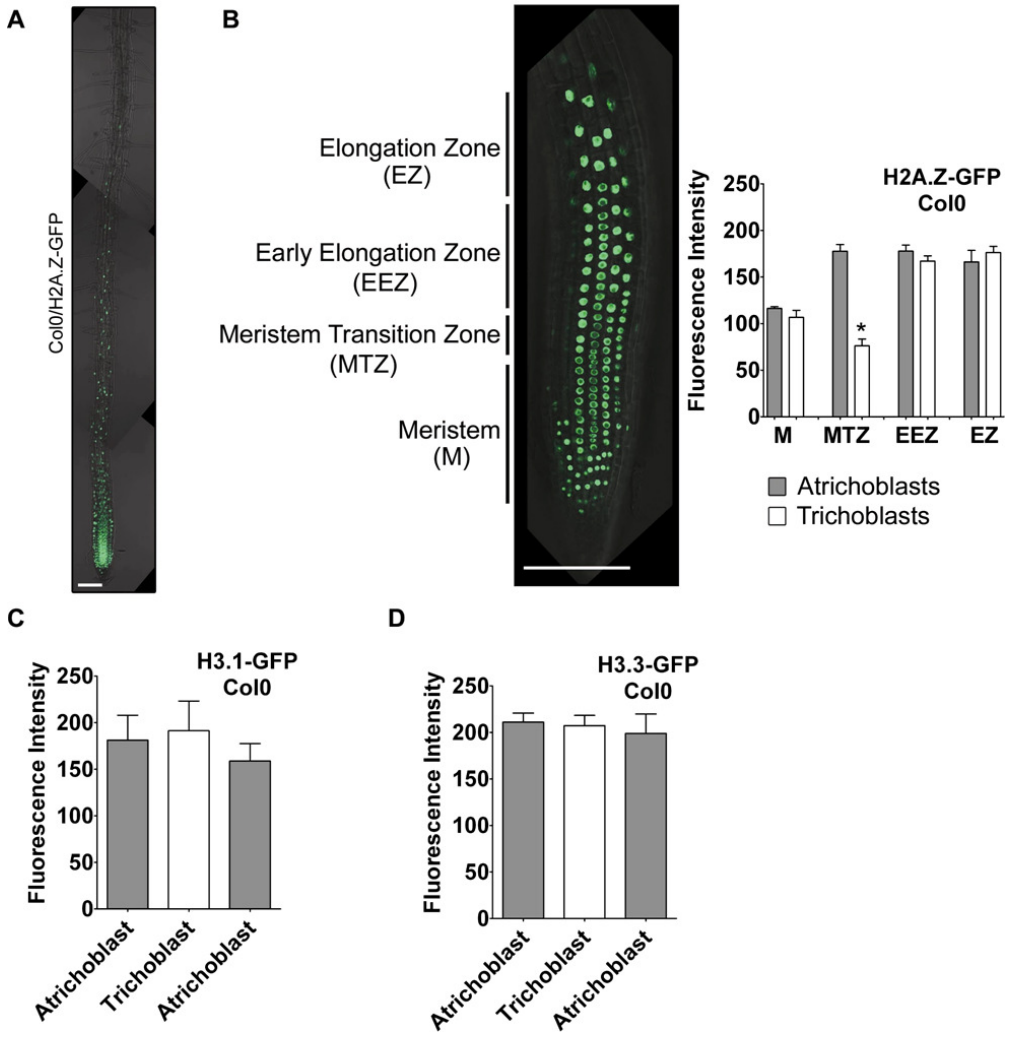

Figure 4.5. H2A.Z-GFP patterning is specific to meristem transition zone.

(a) 4 day-old wild-type root showing H2A.Z-GFP expression in the meristem, elongation zone and early developmental zone. Scale bar: 100 µm. **(b)** 4 day-old wild-type root showing H2A.Z-GFP patterning in meristem transition zone. On the right, quantification of H2A.Z-GFP signal (trichoblasts vs atrichoblats) along the different zones of development. (*P<0.01). **(c)** Quantification of H3.1-GFP signal on nuclei from the meristem transition zone (mean ± s.e.; n=20). **(d)** Quantification of H3.3-GFP signal on nuclei from the meristem transition zone (mean ± s.e.; n=20).

To further analyse the role of positional information in controlling HTA11:GFP deposition and cell specification, we determined whether the patterns of HTA11:GFP expression could be altered in response to changes in positional information by examining longitudinal divisions of epidermal cells (T-clones) (Fig.4.4d). In T clones the parallel files of cells deriving from a single epidermal cell had a rapid change on HTA11:GFP accumulation. A gradual increase of HTA11:GFP accumulation was detected in the atrichoblast cells. On the contrary, in the trichoblast cells the HTA11:GFP accumulation was decreased and gradually recovered. As cells of the same clonal origin in the two parallel files start elongating the differences in HTA11:GFP accumulation diminished. This indicates that HTA11:GFP accumulation is quickly re-adjusted in response to a new positional cue after a T-clone division.

4.4.3. Dynamics of H2A.Z-GFP patterning

We then asked how such patterning could be maintained. In principle it could be a consequence of differential protein synthesis or differential degradation. To distinguish between these possibilities we performed photobleaching experiments. First, we determined the rates of *de novo* production of HTA11:GFP in the two cell types by entirely photobleaching nuclei in the meristem transition zone and observing the recovery of fluorescence (Fig. 4.6a), which must be due to *de novo* synthesis. There was generally a recovery of about 3-7% within an hour; however there were no significant differences between atrichoblast and trichoblast cells. This shows that the *de novo* production cannot account for the difference between the two cell types, and suggested that the presence of a HTA11:GFP patterning was a consequence of differential protein degradation. To test this hypothesis we quantified total nuclear intensity in the presence of the proteasome inhibitor MG132. We observed that after 6 hours of treatment with MG132, HTA11:GFP was accumulated in high level in both types of cells and the initial differences in fluorescence between atrichoblast and trichoblast cells was diminished (Fig. 4.6b). In addition, no differences were observed on *de novo* synthesis upon MG132 treatment between the two cell types (Fig. 4.6a). These data suggests a model where differences on the rates of HTA11:GFP degradation rather than the rates of *de novo* protein production can explain the HTA11:GFP patterning between the two cell types in the meristem transition zone.

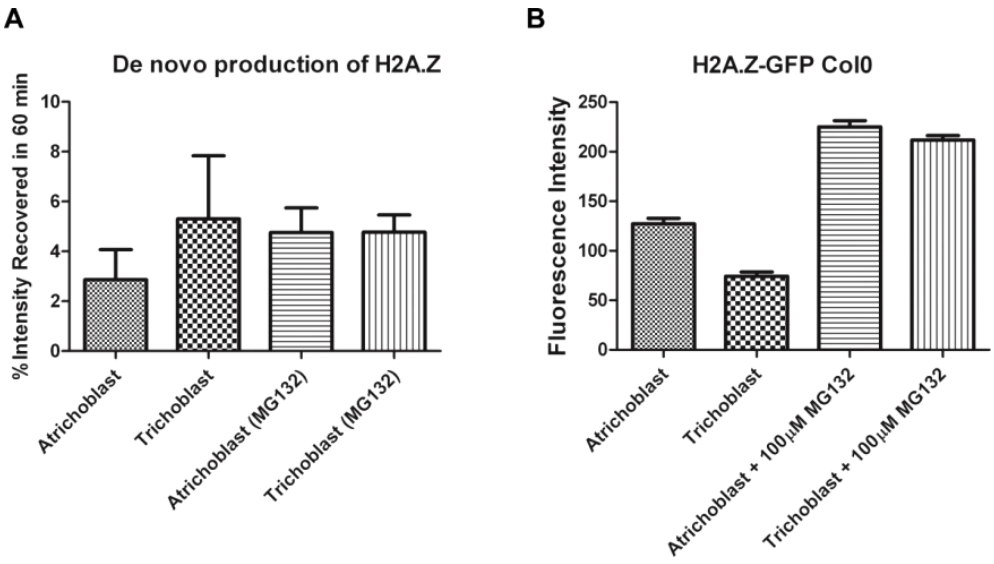

Figure 4.6. H2A.Z-GFP patterning is stabilised by different degradation rates between trichoblasts and atrichoblasts.

(a) *De novo* synthesis rates calculated as a percentage of initial intensities for H2A.Z-GFP protein after a period of 1h in the meristem transition zone showing no significant differences on the expression rates. Values represent mean ± s.e. (n=8). **(b)** Quantification of H2A.Z-GFP signal on nuclei of trichoblast and atrichoblast from the meristem transition zone of control plants and plants treated for 1h with MG132 showing the loss of H2A.Z-GFP pattering in the presence of the drug inhibitor (mean ± s.e.; n=10).

The proposed model does not answer the question of why HTA11 degradation is higher on trichoblast cells leading to lower accumulation of the protein in comparison to atrichoblast cells. We postulated that H2A.Z incorporated into chromatin is protected from degradation, whereas unincorporated H2A.Z is subject to proteasomal degradation. Thus we predicted that, in the transition zone, atrichoblasts should have a larger pool of immobile, incorporated H2A.Z, whereas trichoblasts, with a lower overall level of H2A.Z, should have a smaller immobile pool. To test this assumption we performed fluorescence recovery after photobleaching (FRAP) to determine pools of immobile histone molecules (or stably incorporated into the chromatin). In these experiments only a small portion of the nucleus was photobleached and the fluorescence recovery of the GFP-tagged histones was monitored. As predicted, we showed that atrichoblast cells at the meristem transition zone have a much larger immobile pool of HTA11 histone (Fig. 4.7a-b), explaining the higher levels of fluorescence intensity observed in these cells in comparison to trichoblast cells. Additionally, we show that there are no the differences in immobile pools for other histones such as canonical H2B, which did not show a fluorescence patterning (Fig. 4.7c-d).

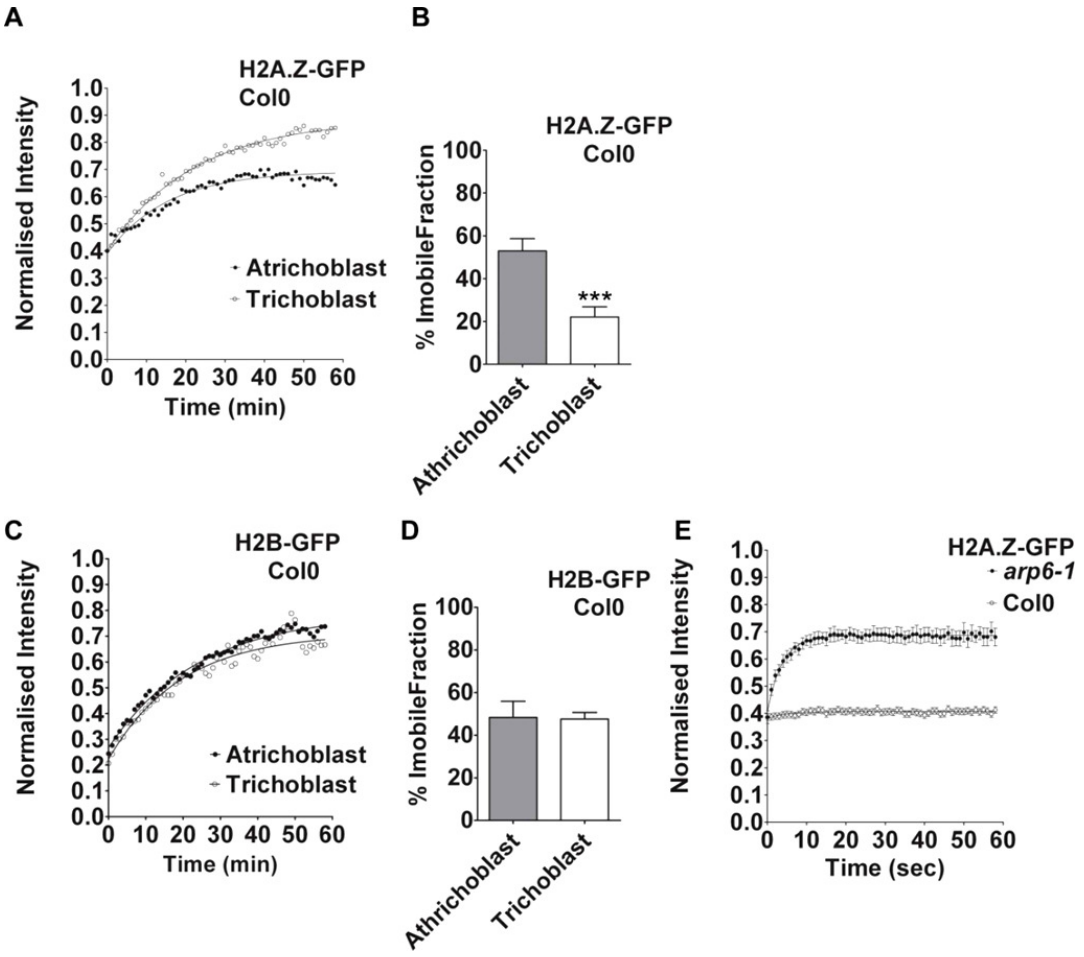

Figure 4.7. FRAP analysis of H2A.Z-GFP reveals higher immobile pool in atrichoblast cells.

(a) FRAP curves for H2A.Z-GFP on trichoblasts and atrichoblasts present in the meristem transition zone of Col-0 plants. Values represent a typical recovery for each cell type. **(b)** Estimated immobile fractions for FRAP experiment depicted on a. Values represent mean ± s.e. from 20 cells. ($P<0.001$) **(c)** Quantitative analysis of FRAP experiments of H2B-GFP on trichoblast and atrichoblast cells present in the meristem transition zone of Col-0 plants. Values represent a typical recovery for each cell type. **(d)** Estimated immobile fractions for FRAP experiment depicted on c. Values represent mean ± s.e. from 20 cells. **(e)** FRAP curves for H2A.Z-GFP in *arp6-1* and Col-0 plants. Values represent means ± s.e. from 20 cells.

We also performed FRAP experiments in *arp6-1* mutant plants expressing HTA11:GFP. In these plants the HTA11:GFP accumulation was lower than the Col-0 plants and the fluorescence patterning of HTA11:GFP was lost (Fig. 4.4b). As expected, in the *arp6-1* mutant the PIE1 complex fails to properly incorporate HTA11:GFP into chromatin. Thus the fluorescence recoveries of HTA11:GFP are much faster in the *arp6-1* mutant (ten seconds) than in the Col-0 plants (one hour). These results validate a model where the inability to properly incorporate HTA11 into chromatin results in rapid degradation of the histones, failure to perceive a positional cue and consequently an incorrect developmental output.

4.4.4. Genetic interactions of *PIE1*(*Arp6*) with *WER*, *GL2* and *CPC*

Cell fate specification during epidermal root patterning is known to be dependent on a complex transcription factor network that regulates the expression of *GL2*. To determine the genetic position of *PIE1* (*ARP6*) in relation to this network we analysed *WER*, *CPC* and *GL2* expression in the *arp6-1* mutant. We first investigated the role of *arp6-1* mutant in the spatial expression patterning of *WER*. Arabidopsis lines expressing the transcriptional reporter construct for *WER* (*pWER:GFP*) were crossed with the *arp6-1* mutant and homozygous lines were subsequently analysed. Similarly to the wild-type WER expression in *arp6-1* mutant was restricted to atrichoblast cells (Fig. 4.8a). This observation is in some way contra-intuitive with *arp6-1* phenotype; however we occasionally observed *WER* expression in root hairs (Fig. 4.9). This result suggests that although *WER* is correctly expressed on *arp6-1* mutant it fails to trigger *GL2* expression and consequently a *WER*-expressing cell can develop into a hair-cell. In contrast, of homozygous crosses of Arabidopsis lines expressing a transcriptional reporter construct of *GL2* (*pGL2::GFP*) and *CPC* (*pCPC::GFP*) with the *arp6-1* mutant revealed an abnormal expression of the two constructs (Fig. 4.8b-c). In the case of *pGL2::GFP*, we observed that the expression in atrichoblast files is often disrupted along the file by 2-3 cells in which *GL2* activity is lost. On the other hand, *CPC* expression in the *arp-6-1* mutant was patchy, being seen in both types of cells. These results place *ARP6* downstream of *WER* and upstream *GL2* and *CPC*.

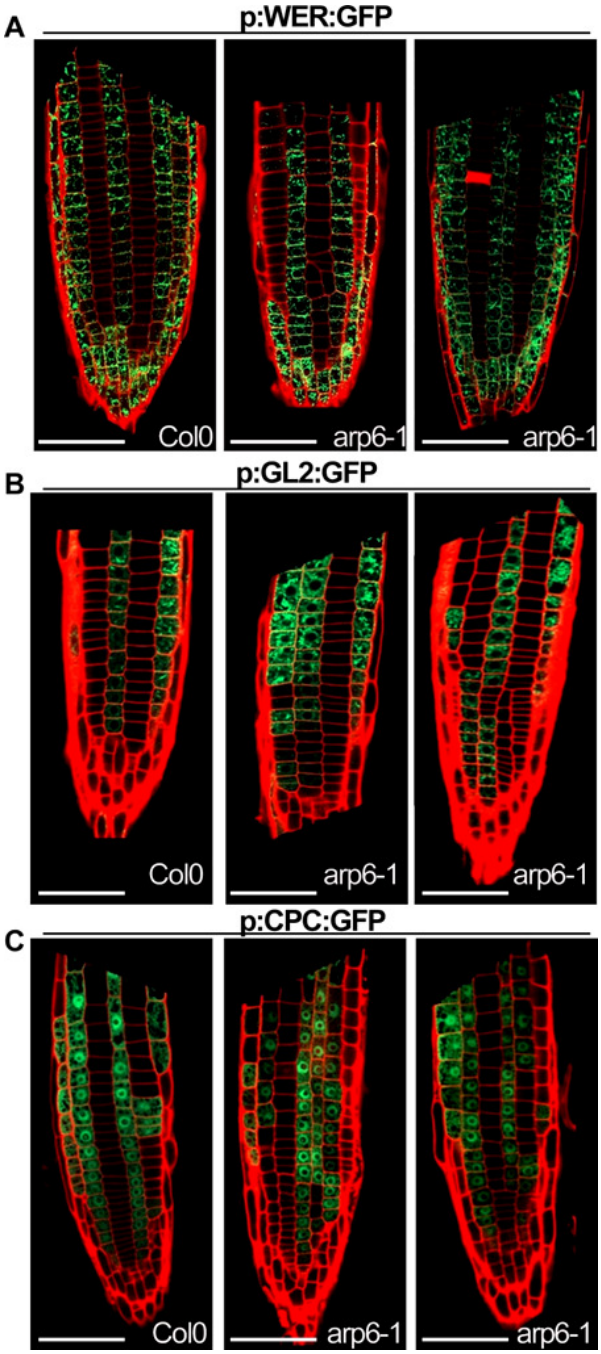

Figure 4.8. Genetic interactions of *PIE1*(*Arp6*) with *WER*, *GL2* and *CPC*.

(a) Expression of pWER:GFP reporter construct on Col-0 plants (left panel) and on *arp6-1* plants (middle and right panels). **(b)** Expression of pGL2:GFP reporter construct on Col-0 plants (left panel) and on *arp6-1* plants (middle and right panels), showing loss of GFP signal on some atrichoblast cell. **(c)** Expression of pCPC:GFP reporter construct on Col-0 plants (left panel) and on *arp6-1* plants (middle and right panels), showing GFP signal on trichoblast cells. Scale bars: 50 µm.

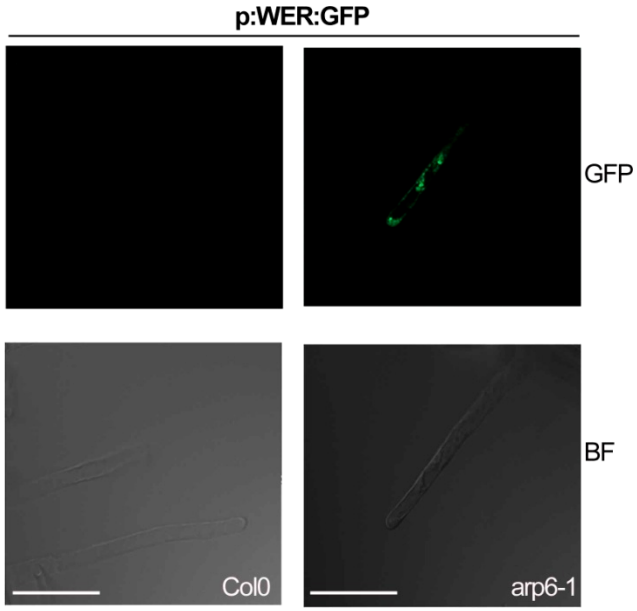

Figure 4.9. WERWOLF does not stop hair formation on *arp6-1* mutant.

Brightfield (BF) and fluorescent images of root hairs containing a pWER:GFP reporter construct on a Col-0 hair cells (left panels) and on *arp6-1* plants (right panels), showing presence of GFP signal on the mutant. Scale bars: 40µm.

4.4.5. WER transcription factor is necessary for H2A.Z-GFP patterning

Because *WER* expression was unaffected in the *arp6-1* mutant, we predicted that the function of *WER* transcription factor was upstream of PIE1 complex. To further test this hypothesis we determined the pattern of HTA11:GFP accumulation in the meristem transition zone of *SCM* and *WER* mutants. SCM is a receptor like kinase that drives the repression of *WER* expression in the trichoblast cells (Kwak and Schiefelbein, 2007). SCM (*scm-1*) and WER (*wer*) mutant Arabidopsis lines were crossed with the lines expressing the HTA11:GFP. HTA11 is equally accumulated in atrichoblasts and trichoblasts cells in the meristem transition zone of both mutants and therefore HTA11 patterning is lost in these mutants (Fig. 4.10a-b). These results suggest that the transmission of a positional clue by the receptor like kinase SCM through WER transcription factor determines the differential activity of PIE1 complex between the two cell types.

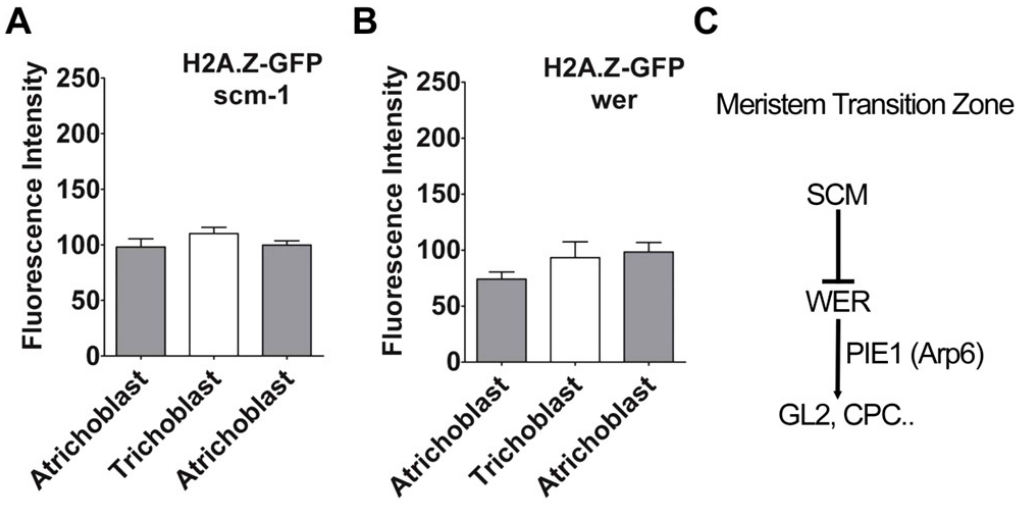

Figure 4.10. *WER* and *SCM* are necessary for H2A.Z-GFP patterning on meristem transition zone.

(a) Quantification of H2A.Z-GFP signal on nuclei of trichoblast and atrichoblast cells from the meristem transition zone of 4 day-old root meristems of *scm-1* plants showing loss of H2A.Z-GFP pattering (mean ± s.e.; n=20). **(b)** Quantification of H2A.Z-GFP signal on nuclei of trichoblast and atrichoblast cells from the 4 day-old root meristems of *wer* plants expressing H2A.Z-GFP showing loss of H2A.Z-GFP pattering (mean ± s.e.; n=20). **(c)** A simplified model that accounts for the role of PIE1(ARP6). It is proposed WER guides PIE1(ARP6) to target genes such as *GL2*, where it proceeds to the incorporation of H2A.Z and consequently promotes gene expression.

4.5. Discussion

Over the last few years, it has become evident in plants and animals that correct interpretation of positional signals and subsequent correct cell specification is vital for organ and tissue formation (Dolan and Okada, 1999; Wolpert, 2003). In plants the patterning of the Arabidopsis root epidermis with alternating files of hair cells and non-hair cells has been used as a model system to study cell fate specification. Although substantial progress has been made in identifying genes differentially expressed in the two cell files little is known about the mechanism underlying these differences. Chromatin modification by histone H3 trimethylation at lysines 4 and 27 cannot fully explain these differences in gene expression (Deal and Henikoff, 2010). Histone acetylation also plays a crucial role in the expression of patterning genes in the root epidermis (Xu and Scheres, 2005). Hyper-acetylation of histone

by chemical inhibition of histone deacetylases (HDAC) or in a mutant HDAC (*hda18*) leads to increased numbers of root hairs. Based on these results, a model was proposed where a positional clue inhibits HDAC activity in the files of hair cells (Xu et al., 2005). In an alternative model, GEM (GL2-expression modulator) controls root epidermal fate by regulating H3 acetylation and methylation of lysine 9 in the *GL2* and *CPC* promoters (Caro et al., 2007). In a GEM mutant (*gem-1*), with reduced root hair density, H3K9Me3 and acetylation were increased and H3K9Me2 was decreased at the promoters of GL2 and CPC genes (Caro et al., 2007). These two models are seemingly inconsistent with each other; in the first model, hyperacetylation, a marker for an open chromatin state, increased hair numbers. In contrast, increased H3K9Me3 and acetylation, both marks of euchromatin and an open chromatin state, were associated with a reduction of root hair numbers. A possible explanation to this contradiction is a spatial operation of the two models in the *Arabidopsis* root. This hypothesis is supported by the clear in situ experiments demonstrating that the difference in chromatin state between root hairs and non root hairs is only evident in a small zone in the meristem transition zone of *Arabidopsis* root (Costa and Shaw, 2006).

In accordance with the in situ results, we report here a mechanism whereby PIE1 complex participates in root epidermal-cell fate determination in the meristem transition zone of the Arabidopsis root. The model that emerges is one wherein cell fate is partially determined by differential incorporation of H2A.Z by the PIE1 complex. There are four key pieces of evidence supporting this model. First, mutants of PIE1 complex have reduced incorporation of H2A.Z and increased number of root hairs. Second, an increased H2A.Z incorporation in the chromatin of atrichoblast in comparison to trichoblast cells is evident only in the meristem transition zone and can reset upon change in cell position as previously reported for the changes in chromatin state (Costa and Shaw, 2006). Third, loss of H2A.Z patterning leads to aberrant expression of GL2 and CPC. Fourth, both WER and SCM control the differential incorporation of H2A.Z suggesting a positional regulation of PIE1 complex.

Our findings indicate that one of the mechanisms by which developmental plasticity is achieved in the Arabidopsis root epidermis is simply based on the quick incorporation or depletion of a histone variant from the chromatin in a very small zone or Arabidopsis root. A positional clue from a receptor like kinase is transmitted in a genome-wide differential incorporation of a histone variant that controls gene expression and ultimately cell fate. Interestingly, *Arabidopis* has over 600 receptor like kinases and rice more than 1000 (Dardick et al., 2007; Shiu and Bleecker, 2003) that are involved in diverse biological functions including embryo patterning, pathogen recognition, steroid signalling, stem cell control and

epidermal patterning (Gish and Clark, 2011). Given that in all biological functions mediated by receptor like kinases lead to differential gene expression it is likely that genome wide chromatin changes are part of a mechanism controlling gene expression and ultimately cell fate. Taken together, our results add to the understanding of how a positional clue regulates root hair patterning and lead to a model where genome wide chromatin changes are part of the cell fate decision mechanism.

4.6. Acknowledgments

All results referring to root-hair measurements, constructs and plant transformation were provided by Ali Pendle and Vardis Ntoukakis, and all transversal sections were done by Elizabeth Bell.
I also would like to thanks Vardis Ntoukakis for comments and advice.

4.7. References

Berger, F., Haseloff, J., Schiefelbein, J., and Dolan, L. (1998). Positional information in root epidermis is defined during embryogenesis and acts in domains with strict boundaries. Curr Biol *8*, 421-430.

Bernhardt, C., Lee, M.M., Gonzalez, A., Zhang, F., Lloyd, A., and Schiefelbein, J. (2003). The bHLH genes GLABRA3 (GL3) and ENHANCER OF GLABRA3 (EGL3) specify epidermal cell fate in the Arabidopsis root. Development *130*, 6431-6439.

Birnbaum, K., Shasha, D.E., Wang, J.Y., Jung, J.W., Lambert, G.M., Galbraith, D.W., and Benfey, P.N. (2003). A gene expression map of the Arabidopsis root. Science *302*, 1956-1960.

Brady, S.M., Orlando, D.A., Lee, J.Y., Wang, J.Y., Koch, J., Dinneny, J.R., Mace, D., Ohler, U., and Benfey, P.N. (2007). A high-resolution root spatiotemporal map reveals dominant expression patterns. Science *318*, 801-806.

Caro, E., Castellano, M.M., and Gutierrez, C. (2007). A chromatin link that couples cell division to root epidermis patterning in Arabidopsis. Nature *447*, 213-217.

Chevalier, D., Batoux, M., Fulton, L., Pfister, K., Yadav, R.K., Schellenberg, M., and Schneitz, K. (2005). STRUBBELIG defines a receptor kinase-mediated signaling pathway regulating organ development in Arabidopsis. Proc Natl Acad Sci U S A *102*, 9074-9079.

Choi, K., Kim, J., Hwang, H.J., Kim, S., Park, C., Kim, S.Y., and Lee, I. (2011). The FRIGIDA complex activates transcription of FLC, a strong flowering repressor in Arabidopsis, by recruiting chromatin modification factors. Plant Cell *23*, 289-303.

Choi, K., Kim, S., Kim, S.Y., Kim, M., Hyun, Y., Lee, H., Choe, S., Kim, S.G., Michaels, S., and Lee, I. (2005). SUPPRESSOR OF FRIGIDA3 encodes a nuclear ACTIN-RELATED PROTEIN6 required for floral repression in Arabidopsis. Plant Cell *17*, 2647-2660.

Choi, K., Park, C., Lee, J., Oh, M., Noh, B., and Lee, I. (2007). Arabidopsis homologs of components of the SWR1 complex regulate flowering and plant development. Development *134*, 1931-1941.

Clough, S.J., and Bent, A.F. (1998). Floral dip: a simplified method for Agrobacterium-mediated transformation of Arabidopsis thaliana. Plant J *16*, 735-743.

Costa, S., and Shaw, P. (2006). Chromatin organization and cell fate switch respond to positional information in Arabidopsis. Nature *439*, 493-496.

Dardick, C., Chen, J., Richter, T., Ouyang, S., and Ronald, P. (2007). The rice kinase database. A phylogenomic database for the rice kinome. Plant Physiol *143*, 579-586.

Deal, R.B., and Henikoff, S. (2010). A simple method for gene expression and chromatin profiling of individual cell types within a tissue. Dev Cell *18*, 1030-1040.

Deal, R.B., Kandasamy, M.K., McKinney, E.C., and Meagher, R.B. (2005). The nuclear actin-related protein ARP6 is a pleiotropic developmental regulator required for the maintenance of FLOWERING LOCUS C expression and repression of flowering in Arabidopsis. Plant Cell *17*, 2633-2646.

Di Cristina, M., Sessa, G., Dolan, L., Linstead, P., Baima, S., Ruberti, I., and Morelli, G. (1996). The Arabidopsis Athb-10 (GLABRA2) is an HD-Zip protein required for regulation of root hair development. Plant J *10*, 393-402.

Dolan, L., and Okada, K. (1999). Signalling in cell type specification. Semin Cell Dev Biol *10*, 149-156.

Gish, L.A., and Clark, S.E. (2011). The RLK/Pelle family of kinases. Plant J *66*, 117-127.

Hennig, L., Menges, M., Murray, J.A., and Gruissem, W. (2003). Arabidopsis transcript profiling on Affymetrix GeneChip arrays. Plant Mol Biol *53*, 457-465.

Ingouff, M., Hamamura, Y., Gourgues, M., Higashiyama, T., and Berger, F. (2007). Distinct dynamics of HISTONE3 variants between the two fertilization products in plants. Curr Biol *17*, 1032-1037.

Ingouff, M., Rademacher, S., Holec, S., Soljic, L., Xin, N., Readshaw, A., Foo, S.H., Lahouze, B., Sprunck, S., and Berger, F. (2010). Zygotic resetting of the HISTONE 3 variant repertoire participates in epigenetic reprogramming in Arabidopsis. Curr Biol *20*, 2137-2143.

Koshino-Kimura, Y., Wada, T., Tachibana, T., Tsugeki, R., Ishiguro, S., and Okada, K. (2005). Regulation of CAPRICE transcription by MYB proteins for root epidermis differentiation in Arabidopsis. Plant Cell Physiol *46*, 817-826.

Krogan, N.J., Keogh, M.C., Datta, N., Sawa, C., Ryan, O.W., Ding, H., Haw, R.A., Pootoolal, J., Tong, A., Canadien, V.*, et al.* (2003). A Snf2 family ATPase complex required for recruitment of the histone H2A variant Htz1. Mol Cell *12*, 1565-1576.

Kumar, S.V., and Wigge, P.A. (2010). H2A.Z-containing nucleosomes mediate the thermosensory response in Arabidopsis. Cell *140*, 136-147.

Kwak, S.H., and Schiefelbein, J. (2007). The role of the SCRAMBLED receptor-like kinase in patterning the Arabidopsis root epidermis. Dev Biol *302*, 118-131.

Kwak, S.H., Shen, R., and Schiefelbein, J. (2005). Positional signaling mediated by a receptor-like kinase in Arabidopsis. Science *307*, 1111-1113.

Lazaro, A., Gomez-Zambrano, A., Lopez-Gonzalez, L., Pineiro, M., and Jarillo, J.A. (2008). Mutations in the Arabidopsis SWC6 gene, encoding a component of the SWR1 chromatin remodelling complex, accelerate flowering time and alter leaf and flower development. J Exp Bot *59*, 653-666.

Lee, M.M., and Schiefelbein, J. (1999). WEREWOLF, a MYB-related protein in Arabidopsis, is a position-dependent regulator of epidermal cell patterning. Cell *99*, 473-483.

Lin, Y., and Schiefelbein, J. (2001). Embryonic control of epidermal cell patterning in the root and hypocotyl of Arabidopsis. Development *128*, 3697-3705.

Martin-Trillo, M., Lazaro, A., Poethig, R.S., Gomez-Mena, C., Pineiro, M.A., Martinez-Zapater, J.M., and Jarillo, J.A. (2006). EARLY IN SHORT DAYS 1 (ESD1) encodes ACTIN-RELATED PROTEIN 6 (AtARP6), a putative component of chromatin remodelling complexes that positively regulates FLC accumulation in Arabidopsis. Development *133*, 1241-1252.

Masucci, J.D., Rerie, W.G., Foreman, D.R., Zhang, M., Galway, M.E., Marks, M.D., and Schiefelbein, J.W. (1996). The homeobox gene GLABRA2 is required for position-dependent cell differentiation in the root epidermis of Arabidopsis thaliana. Development *122*, 1253-1260.

Meagher, R.B., Deal, R.B., Kandasamy, M.K., and McKinney, E.C. (2005). Nuclear actin-related proteins as epigenetic regulators of development. Plant Physiol *139*, 1576-1585.

Mizuguchi, G., Shen, X., Landry, J., Wu, W.H., Sen, S., and Wu, C. (2004). ATP-driven exchange of histone H2AZ variant catalyzed by SWR1 chromatin remodeling complex. Science *303*, 343-348.

Ryu, K.H., Kang, Y.H., Park, Y.H., Hwang, I., Schiefelbein, J., and Lee, M.M. (2005). The WEREWOLF MYB protein directly regulates CAPRICE transcription during cell fate specification in the Arabidopsis root epidermis. Development *132*, 4765-4775.

Shiu, S.H., and Bleecker, A.B. (2003). Expansion of the receptor-like kinase/Pelle gene family and receptor-like proteins in Arabidopsis. Plant Physiol *132*, 530-543.

Wada, T., Kurata, T., Tominaga, R., Koshino-Kimura, Y., Tachibana, T., Goto, K., Marks, M.D., Shimura, Y., and Okada, K. (2002). Role of a positive regulator of root hair development, CAPRICE, in Arabidopsis root epidermal cell differentiation. Development *129*, 5409-5419.

Wada, T., Tachibana, T., Shimura, Y., and Okada, K. (1997). Epidermal cell differentiation in Arabidopsis determined by a Myb homolog, CPC. Science *277*, 1113-1116.

Walker, A.R., Davison, P.A., Bolognesi-Winfield, A.C., James, C.M., Srinivasan, N., Blundell, T.L., Esch, J.J., Marks, M.D., and Gray, J.C. (1999). The TRANSPARENT TESTA GLABRA1 locus, which regulates trichome differentiation and anthocyanin biosynthesis in Arabidopsis, encodes a WD40 repeat protein. Plant Cell *11*, 1337-1350.

Wolpert, L. (2003). Cell boundaries: knowing who to mix with and what to shout or whisper. Development *130*, 4497-4500.

Won, S.K., Lee, Y.J., Lee, H.Y., Heo, Y.K., Cho, M., and Cho, H.T. (2009). Cis-element- and transcriptome-based screening of root hair-specific genes and their functional characterization in Arabidopsis. Plant Physiol *150*, 1459-1473.

Xu, C.R., Liu, C., Wang, Y.L., Li, L.C., Chen, W.Q., Xu, Z.H., and Bai, S.N. (2005). Histone acetylation affects expression of cellular patterning genes in the Arabidopsis root epidermis. Proc Natl Acad Sci U S A *102*, 14469-14474.

Xu, J., and Scheres, B. (2005). Dissection of Arabidopsis ADP-RIBOSYLATION FACTOR 1 function in epidermal cell polarity. Plant Cell *17*, 525-536.

Zimmermann, P., Hirsch-Hoffmann, M., Hennig, L., and Gruissem, W. (2004). GENEVESTIGATOR. Arabidopsis microarray database and analysis toolbox. Plant Physiol *136*, 2621-2632.

Chapter 5

Cold-induced physical clustering of *FLC* alleles is an early event in vernalization

The work described in this chapter was carried out in collaboration with the Dean Lab (JIC). I have been directly involved in all fluorescence microscopy work, image processing and data analysis. It has been submitted for publication as:

Cold-induced physical clustering of *FLC* alleles is an early event in vernalization.

Filomena De Lucia+, Stefanie Rosa+, Joshua. S. Mylne+, Nobuko Ohmido, Ali Pendle, Naohiro Kato, Peter Shaw and Caroline Dean

+ These authors contributed equally to this work

Chapter 5:

Cold-induced physical clustering of *FLC* alleles is an early event in vernalization

5.1. Abstract

Vernalization synchronises plant flowering with the favourable conditions of spring. Central to vernalization is the epigenetic silencing of the floral repressor *FLOWERING LOCUS C (FLC)* through a mechanism involving cold-induced non-coding RNAs and a Polycomb silencing mechanism. Nuclear organization has been established as an important parameter in chromatin regulation, but nothing is known about its influence in the vernalization process. Here, we use live imaging of an *FLC-lacO* array transgene to monitor nuclear organization and dynamics of *FLC* during vernalization in *Arabidopsis*. This revealed a cold-induced physical clustering of *FLC* alleles in both meristematic and endoreduplicated cells. The number of cells showing this clustering increases quantitatively with exposure to cold, paralleling the gene silencing. The clustering is epigenetically stable after returning plants to warm and is disrupted by loss of two trans-factors required for vernalization. We propose that physical clustering of *FLC* alleles is an important component of cold-induced *FLC* epigenetic silencing.

5.2. Introduction

Vernalization is a tightly regulated process that allows plants to flower in more favourable conditions in spring, and is a classic example of environmentally-induced epigenetic regulation (Henderson and Dean, 2004a). This is achieved via down-regulation of FLOWERING LOCUS C (FLC), a MADS box protein that represses flowering in response to a prolonged period of cold (Michaels and Amasino, 1999; Sheldon et al., 1999). When grown in floral inductive conditions without extended cold treatment (vernalization) flowering of some accessions are severely delayed. These accessions thus require vernalization to ensure an appropriate response to floral inductive conditions (Henderson and Dean, 2004b). A large proportion of Arabidopsis accessions such as the commonly used Columbia (Col) and

Landsberg *erecta* (L*er*) strains do not require vernalization to flower. The growth habit they adopt reduces the time-span in between subsequent generations and is referred to as a rapid cycling habit (Toomajian et al., 2006). It has been shown that rapidly cycling *Arabidopsis* strains can be converted to adopt a winter annual growth habit by virtue of a dominant, monogenic locus termed *FRIGIDA* (*FRI*) (Napp-Zinn, 1955). The Col and L*er Arabidopsis* wild types in fact carry independently acquired *fri* loss of function mutations that are responsible for their rapid cycling growth habit (Johanson et al., 2000). *FRI* encodes a plant specific protein with two coiled-coil domains but the molecular mechanism of *FRI*-mediated *FLC* activation is not fully understood.

The current understanding of vernalization has been derived from forward genetics combined with chromatin analysis. Polycomb Repressive Complex (PRC2) is required for the memory of cold (Gendall et al., 2001), together with proteins (VRN5, VIN3 and VEL1) containing PHD and FNIII domains (Greb et al., 2007; Sung and Amasino, 2004; Sung et al., 2006b). Analysis of the dynamic associations of these proteins at the target *FLC* locus has suggested a sequence of events during vernalization (De Lucia et al., 2008) (Fig. 5.1). PRC2 is associated over the whole locus at all phases, even before cold when the gene is expressed. Prolonged cold induces expression of VIN3, which heterodimerizes with VRN5 and VEL1 to form a PHD-PRC2 complex, which assembles at a specific site within *FLC* and results in increased H3K27me3 at that site. After plants are returned to the warm the PHD-PRC2 complex (now without VIN3) spreads across the whole gene and leads to very high levels of H3K27me3 blanketing the locus. These very high levels of H3K27me3 are required for the epigenetic stability of *FLC* repression through the rest of development. The cold-induced suppression of *FLC* transcription precedes, and is independent of, the cold-induced accumulation of VIN3, indicating additional cold-induced steps are involved. These appear to involve *FLC* antisense RNAs, capable of cold-induced silencing of the corresponding gene, which increase coincidently with the suppression of *FLC* transcription (Swiezewski et al., 2009). Non-coding sense RNAs are also proposed to be involved through interaction with PRC2 (Heo and Sung, 2010). How these activities are integrated with additional functions required for vernalization, those of VRN1- a non-sequence specific DNA binding protein (Levy et al., 2002) and LHP1- the single Arabidopsis homologue of HP1 (Mylne et al., 2006; Sung et al., 2006a) - remains to be elucidated.

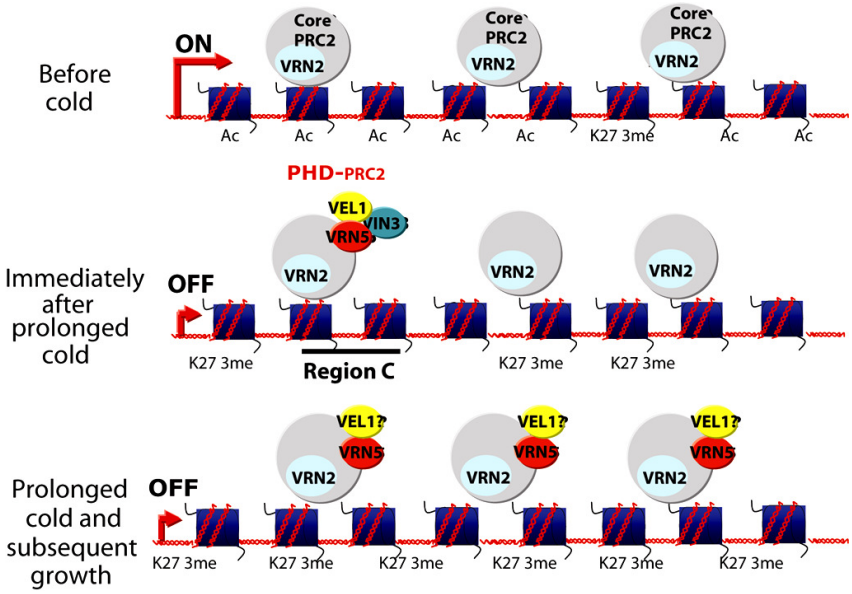

Figure 5.1. Polycomb-mediated *FLC* repression during vernalization.
The *FLC* genomic region (red line) wrapped around nucleosomes (blue) is shown in three different contexts of vernalization. Before the cold period (top) *FLC* is transcribed (ON), histone tails carry predominantly active acetylation marks (Ac) and few repressive (H3K27me3) marks. VRN2 and the core Polycomb repressive complex 2 (PRC2) are already associated. Immediately after the cold (middle), *FLC* transcription is shut down (OFF) and the repressive H3K27me3 marks are increased. The VRN5/VIN3/VEL1 proteins associate to the core PRC2 at a specific *FLC* region to form the PHD-PRC2 complex (region C). After an additional growth period at ambient temperature (bottom) VRN5/VEL1 spread across the whole *FLC* locus and H3K27me3 levels increase significantly. (De Lucia et al., 2008)

An emerging theme in gene regulation is the importance of physical position in the nucleus (Fraser and Bickmore, 2007). Shuttling of genes between specific nuclear domains, clustering of heterochromatic repeated sequences (Towbin et al., 2009) and Polycomb silenced loci (Bantignies et al., 2011; Lanzuolo et al., 2007), and looping associated with enhancer activities (Levine, 2010) are well-characterized examples. This positioning is thought to be highly dynamic (Hübner, 2010) but live cell imaging techniques have enabled monitoring of relocalization of loci to the nuclear periphery during silencing in *S. cerevisiae* (Taddei et al., 2004) and the visualization of loci in Arabidopsis interphase nuclei (Kato and Lam, 2001; Matzke, 2010).

In this chapter we exploited live cell imaging in Arabidopsis to investigate how FLC and its components are organized within the three-dimensional space of the nucleus.

5.3. Materials and methods

5.3.1. Constructs and transgenic lines

Three constructs were used in this study; an *FLC*-reporting construct containing genomic *FLC* with a *lacO* array and kanamycin resistance cassette inserted at either the *Swa*I site downstream of the *FLC* poly (A) site (*FLC-lacO*) or at the *Bst*EII site within the first intron (*FLC-lacO-Bst*), and a control containing only the *lacO* array and kanamycin resistance cassette (*lacO* only). To produce the *FLC*-reporting construct (*FLC-lacO*) a 12 kb *Sac*I fragment of Columbia genomic DNA cloned in pBS (pFLC15) was used and included 3.7 kb upstream of the *FLC* start ATG to 2.7 kb downstream from the end of the *FLC* 3′ UTR. The *lacO* array was obtained from the vector pLAU41, which contains some 120 copies of the *lacO* DNA sequence, each interspersed with random 10-mers and a kanamycin resistance (Km^R) cassette within a pUC18 backbone similar to the published vector pLAU43(Sherratt et al., 2001). This interspersed repeat array reduced problems with repeat-induced silencing (Sherratt et al., 2001). Before cutting out the *lacO* array and kanamycin cassette, pLAU41 was made ampicillin sensitive.The resulting plasmid was ampicillin sensitive and named pLAU41-Amp^S (pJM48).

To create the *FLC-lacO* construct used in this study, pFLC15 was digested with *Swa*I which cuts 510 bp downstream from the end of the *FLC* 3′ UTR. pJM48 was digested with *Nhe*I and *Xba*I to release a 5.3 kb *lacO-*Km^R fragment which was treated with Klenow and ligated into the *Swa*I-cut pFLC15. Successful ligation was screened by double selection on kanamycin and ampicillin. To produce *FLC* construct with the *lacO* array in the first intron (*FLC-lacO-Bst)* a similar approach to *FLC-lacO* was used but instead the 5.3 kb *lacO-*Km^R fragment was inserted at the *Bst*EII site.

To produce the untethered control containing only the *lacO* array and kanamycin resistance cassette (*lacO-only*), pLAU41-Amp^S (pJM48) was digested with *Nhe*I and *Xba*I to release a 5.3 kb *lacO-*Km^R fragment which was treated with Klenow DNA polymerase and ligated with pSLJ755I5 cut with *Pst*I and treated with Klenow DNA polymerase.
Ligations including the *lacO-*Km^R fragment (*lacO*-only and *FLC-lacO*) were selected for with double selection for kanamycin and tetracycline, with the *FLC* construct selected only on tetracycline.

Constructs were moved from *E. coli* into *Agrobacterium tumefaciens* strain LBA4404 by tri-parental mating and used to transform *flc-3 FRI*^{SF2} by floral dip. This genetic

background contains an active *FRIGIDA* allele from the *Arabidopsis* accession San-Feliu-2 which confers a strong vernalization requirement by elevating *FLC* expression; however the *flc-3* mutation means *flc-3* FRI^{SF2} remains early flowering (Michaels, 1999). In this FRI+ background lacking *FLC*, we were able to test the functionality of the *FLC*-containing transgenes by examining transgenics for a substantial delay in flowering.

Genomic DNA from the transgenic reporting lines (*FLC-lacO, FLC-lacO-Bst* and *lacO*-only) was extracted, digested with *Sac*I and *Eco*RI and analysed by Southern blot for single and complete T-DNA insertions (Fig. 5.6). Southern blots were hybridised consecutively with probes for the T-DNA right border, the bialaphos resistance (*bar*) cassette and one for the *lacO* array. The *Bst*EII *lacO*-containing *FLC* constructs did not delay the flowering time of *flc-3* FRI^{SF2} at all and therefore were deemed non-functional.

5.3.2. LacI-eYFP constructs

A detector line was specifically designed for this study. It was inducible by ethanol and encoded a protein fusion containing eYFP, the *lacO*-binding protein LacI and a nuclear localisation signal (NLS). This construct was assembled using three plasmids, one plasmid (pJM67) containing the ORF for enhanced yellow fluorescent protein (eYFP) in pBS which, a second (pJM68) containing a NLS-LacI repressor protein fusion with the NLS from the SV40 large T-antigen and the LacI CDS from pAFS144 and containing the *lacI-I12* mutation that increases the affinity for *lacO* (Straight, 1998), and a third (pDM7) a gift from Eric Lam (unpublished) which was a binary vector containing the alcR expression cassette and an *alcA* promoter cassette.

This binary vector was similarly moved into *Agrobacterium* and used to transform *flc-2* FRI^{SF2}. The *flc-2* mutation is a fast-neutron deletion of parts of the *FLC* gene (Michaels, 1999).

5.3.3. TAIL PCR

To determine the physical location of the *FLC-lacO* T-DNAs within the *Arabidopsis* genome, DNA was extracted from the original *FLC-lacO* lines used for crosses with the YFP-LacI-NLS detector line. This genomic DNA was used for TAIL-PCR performed essentially as described by Liu *et al.* (Liu et al., 1995). Direct sequencing of PCR products indicated the *FLC-lacO* T-DNA #2 was on the top arm of chromosome I (position 61742057,

between At1g17940 and At1g17950). The *FLC-lacO* T-DNA #1 was on the bottom arm of chromosome V (position 21369875, between At5g52680 and At5g52690). In this work, both lines were examined for *FLC-lacO* clustering, but the T-DNA on chromosome V was the one chosen for crosses to *vrn1* and *vrn5* and in most figures.

5.3.4. Transgenic lines and crosses

To obtain a line containing both a reporter construct (*FLC-lacO, FLC-lacO-Bst* and *lacO*-only) and the YFP-LacI detector, crosses were made between a detector line and a line containing a single T-DNA of, *FLC-lacO* (two separate lines), *FLC-lacO-Bst* (one line) or *lacO*-only (one line). Plants grown on plates were sown aseptically in Petri dishes containing Murashige and Skoog (MS) medium (pH 5.8) supplemented with 1% w/v sucrose and 0.8% w/v agar. This media typically contained kanamycin 50 µg/mL to select for the detector construct and phosphinothricin (PPT) 10 µg/mL to select for the various reporter constructs. Non-vernalized plants were stratified for two days at 4°C with an 8-hr photoperiod. Vernalized plants were stratified as above, grown for seven days under fluorescent lights at 23°C with a 16-hr photoperiod and then vernalized for two to six weeks. For flowering time analysis, young seedlings were transferred to trays with 40 cells of 2 cm x 2 cm. Flowering time was measured by counting total leaf number, which was scored as the number of rosette leaves plus cauline leaves. Crosses were made with the *vrn1-2* mutation (Levy et al., 2002) and the *vrn5-1* mutation (Greb et al., 2007).

5.3.5. Microscopy

Arabidopsis seedlings were placed in a biochamber. The biochamber was constructed from a standard cover slip (number 1.5, 50x22 mm) as the top (viewing part) of the chamber. A well (approx. 16 x 24 mm) was made in Secure Seal (double-sided adhesive sheet; Grace Bio-Labs) and attached to the cover slip. The plant was placed in the well with liquid MS media, and a gas-permeable membrane (BioFolie; Viva Science) was attached to the Secure Seal as the bottom of the chamber. The chamber with the gas-permeable membrane facing down was then placed over a 1 cm hole drilled into a plastic support slide to allow free gaseous exchange through the gas-permeable membrane and the edges of the sandwich sealed with tape.

Imaging was performed using a 60X oil lens on a Nikon Eclipse 600 epifluorescence microscope equipped with a Hamamatsu Orca ER cooled CCD digital camera and a Prior Proscan x–z stage. The following wavelengths were used for fluorescence detection: excitation 340-380 nm and emission 425-475 nm for DAPI and excitation 490-510 nm and emission 520-550 nm for YFP.

For all experiments series of optical sections with z-steps of 150 or 200 nm were collected using MetaMorph software (Universal Imaging). The images from z sections were projected using the maximum intensity projection algorithm in ImageJ program (http://rsb.info.nih.gov/ij/).

For the time course analysis we randomly counted the number of foci (one, two or more than two) in ten nuclei in five different plants.

5.4. Results

5.4.1. A functional *FLC-lacO* transgene in root cells

In order to analyse whether nuclear re-organisation played any role in vernalization we used live cell imaging in Arabidopsis. Transgenic *Arabidopsis* lines containing the entire 12 kb *FLC* genomic locus and including an array of 120 copies of the *lacO* DNA sequence were generated (Fig. 5.2a). The *lacO* array, where each *lacO* sequence was separated by a random 10 bp nucleotide sequence, was cloned either downstream of the sense transcript poly (A) site (Fig. 5.2a and Fig. 5.3) or into the *FLC* large first intron (Fig. 5.4k and Fig. 5.3). We also produced a control construct of the *lacO* array alone to monitor any problems of repeat-induced silencing (Jovtchev et al., 2008; Pecinka et al., 2005; Schubert and Shaw, 2011). The *FLC-lacO* and *lacO*-only transgenes were transformed into an *flc* mutant containing an active copy of *FRIGIDA*, which elevates *FLC* expression. Only the *FLC-lacO* construct carrying the *lacO* array downstream of the poly (A) site was fully functional *in planta,* as judged by fully restoring the flowering time of the *flc* mutant and response to vernalization (Fig. 5.5). Two *FLC-lacO* transgenic lines containing single and complete T-DNA insertions were selected to avoid complications of transgene silencing due to complex integration sites (Fig. 5.6). These transgenes were found to be integrated into intergenic regions between At1g17940/At1g17950 and At5g52680/At5g52690. A separate line was made expressing a

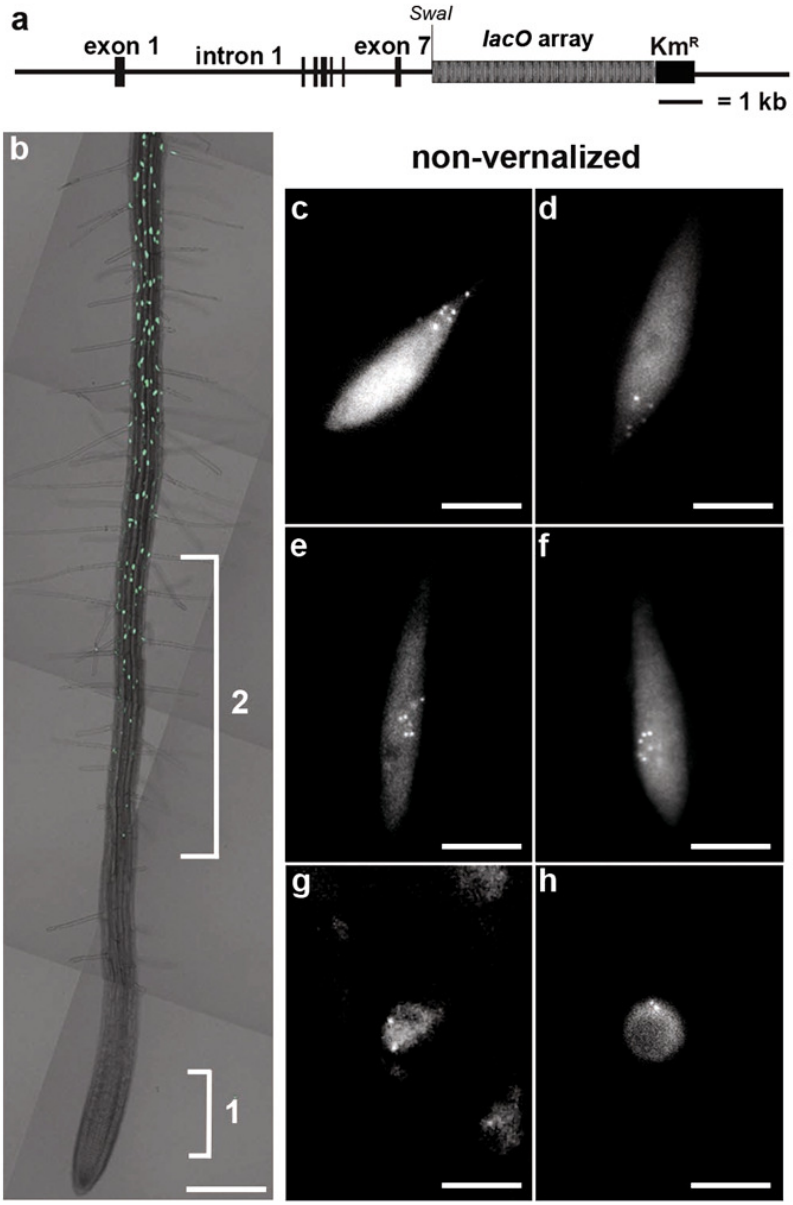

Figure 5.2. *FLC-lacO* transgene in root cells

(a) *FLC-lacO* transgene with *lacO* array inserted at the SwaI restriction site downstream of the polyadenylation site of the genomic *FLC* sequence. **(b)** One week-old *Arabidopsis* Col-0 FRI^{SF2} root harbouring the *FLC-lacO* transgene showing expression of LacI-YFP on nuclei from the differentiation zone. LacI-YFP signal is very low or absent in the meristematic region (region 1) and increases towards the differentiation zone. *FLC* foci are more easily observed in the region labelled as 2. In region 2 epidermal cells are endoreduplicated. **(c-f)** Representative fluorescence images of nuclei from region 2 showing multiple *FLC* foci. **(g-h)** Representative fluorescence images of nuclei from meristematic cells (from region 1). (scale bars: 5 µm)

LacI-YFP-NLS fusion protein in a *FLC*-deficient background. Separation of the array and the reporter protein has previously been found to alleviate silencing problems associated with live cell imaging (Matzke, 2010). This fusion was driven by the ethanol-inducible promoter but we found leaky expression of this fusion made ethanol addition unnecessary. The *FLC-lacO* and *LacI-YFP* lines were crossed and F2 plants selected to carry both transgenes. For technical ease the *lacO/LacI* foci were monitored in root epidermal cells but this tissue is biologically relevant for vernalization. Root cells strongly express *FLC*, cold-induced epigenetic silencing of *FLC* occurs in root tissue, and root cells can regenerate into plants that have 'remembered' the cold exposure (Burn, 1993). In addition, chromosomal regions in epidermal cells undergo a series of endoreduplications (Galbraith, 1991) amplifying the number of *lacO* foci making their identification much easier. The expression level of LacI-YFP was highest in cells above the root meristematic zone (Fig. 5.2b) so we focused most of the analyses on cells in this region.

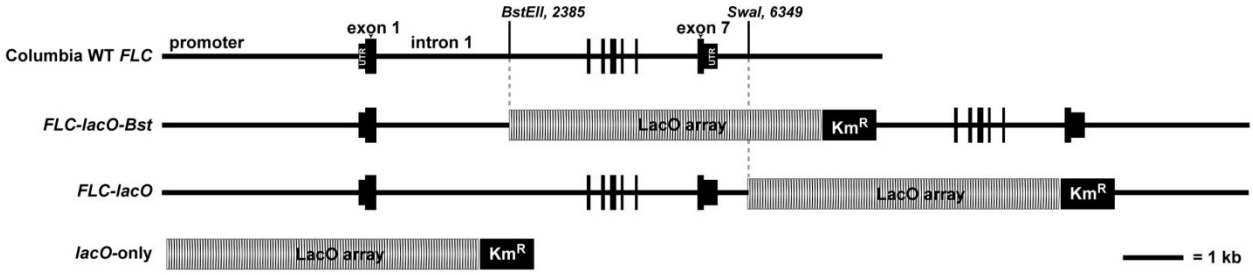

Figure 5.3. Sensor constructs produced for this study and cloned into the *PstI* site of the 27 kb binary vector pSLJ755I5 (pSLJ755I5 not included with these maps). A full 12 kb region of genomic *FLC* (At5g10140) from the accession Columbia was used and the construct named *FLC*. An array of 120 *lacO* sequences interspersed with random 10-mers as well as a trailing bacterial kanamycin resistance cassette were inserted at two different points in *FLC*; 1) within the large, first intron using the unique *BstEII* site to produce the construct named throughout as *FLC-lacO-Bst*, and 2) at the *SwaI* site downstream from the polyadenylation point of *FLC* which produced the most commonly used and biologically functional construct named simply *FLC-lacO*. The insert containing the *lacO* array and bacterial kanamycin resistance cassette was also cloned directly into pSLJ755I5 to examine its behaviour without adjacent *FLC* sequences and this construct was called *lacO*-only. All sensor constructs were transformed into the *flc-3* FRI^{SF2} background which would allow us to determine the functionality of any introduced *FLC* constructs. The detector construct containing ethanol-inducible YFP-LacI was transformed independently into the *flc-2* FRI^{SF2} background. Detector and sensor constructs were brought together by crossing the lines.

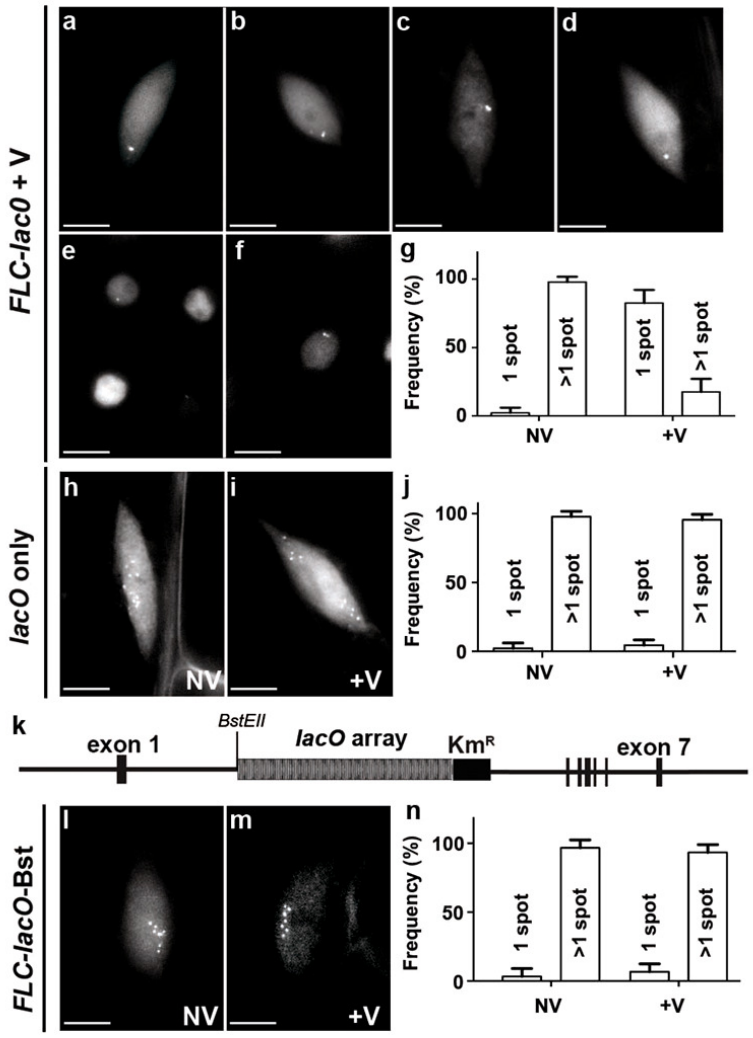

Figure 5.4. Cold-induced clustering of *FLC-lacO* copies.

(a-d) Representative fluorescence images of *Arabidopsis* root cells (from region 2, see Figure 1) in plants vernalized for two weeks (and imaged immediately afterwards), showing clustering of *FLC-lacO* copies into one focus. **(e-f)** Clustering of *FLC-lacO* copies in meristematic cells in plants vernalized for two weeks. **(g)** Quantification of the *FLC-lacO* foci (30 cells counted in three different roots) from cells in region 2. **(h-i)** Representative fluorescence images of nuclei from cells in region 2 expressing a *lacO*-only transgene. Plants were either non-vernalized (NV) or vernalized for 2 weeks (+V). **(j)** Quantification of the lacO foci (30 cells counted in three different roots) from cells in region 2. **(k)** *FLC-lacO* transgene with *lacO* array inserted at the *BstEII* restriction site in *FLC* intron 1 of the genomic *FLC* sequence. **(l)** Representative fluorescence images of *FLC-lacO-Bst* transgene in root cells from region 2 non vernalized and **(m)** vernalized for two weeks. **(n)** Quantification of the *FLC-lacO-Bst* foci from cells in region 2 (30 cells counted in three different roots) non-vernalized and vernalized for two weeks. (scale bars: 5 µm).

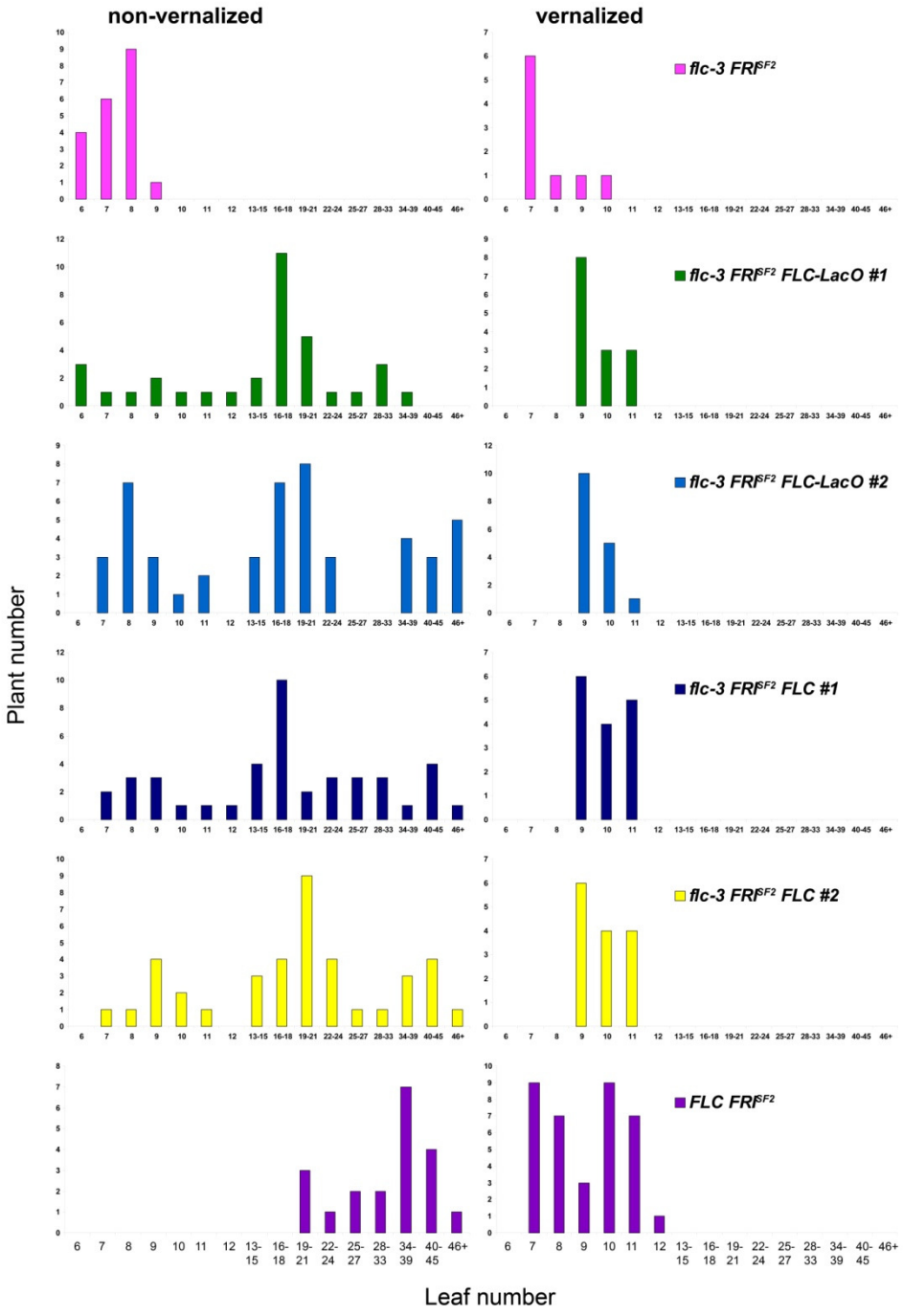

Figure 5.5. Flowering time of segregating T2 populations for two transgenic *FLC-lacO* lines (with lacO array at the *Swa*I site) and transgenic *FLC* lines.

Flowering time controls included *flc-3* FRI^{SF2}, the genetic background containing the transgenes, plus wild type Col FRI^{SF2} containing active FRIGIDA and native *FLC*. Flowering time was measured by counting total leaf number, which was scored as the number of rosette leaves plus cauline leaves for approx 40 plants of each genotype. Plants were either non-vernalized (left panels) or had been vernalized for six weeks (right panels). Segregation of 1:2:1 for early:mid:late flowering is due to semi-dominant nature of *FLC*. The flowering time was similar for both *FLC-lacO* and *FLC* constructs. Both transgenes responded fully to vernalization.

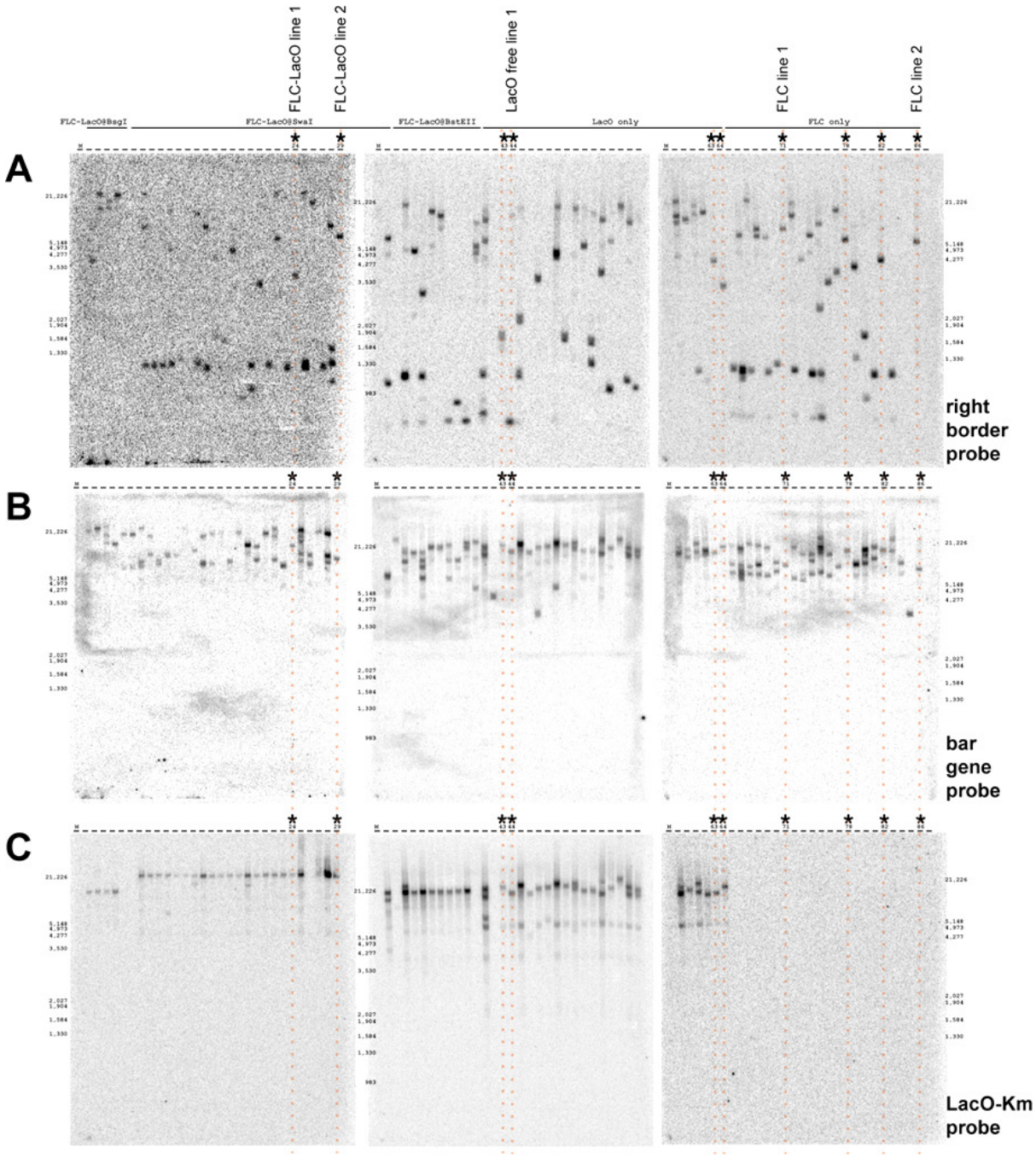

Figure 5.6. Southern analysis of transgenic lines.

Genomic DNA (2 µg) from transgenic lines containing *FLC* and/or *lacO* sequences was digested with *SacI* and *EcoRI* and analysed by Southern blot. Blots were probed consecutively for the T-DNA right border, the bialaphos resistance (*bar*) cassette and the *lacO-Km*^{R} cassette. Selected single T-DNA lines (marked with star) were chosen for crosses to single locus YFP-LacI detector lines. The line most used in this study was *FLC-lacO* line 1 (lane 29).

5.4.2. Clustering of *FLC-lacO* copies is induced by cold

In non-vernalized plants, multiple (six or more) *FLC-lacO* foci were always detected in the root epidermal cells in the zone where endoreduplication occurs (representative images shown in Fig. 5.2c-f), whereas only two foci were ever detected in meristematic 2C cells (representative images shown in Fig. 5.2g-h). These foci did not associate with an obvious location in the nucleus, sometimes being found at one pole in the nucleus of the elongating cells, sometimes in the centre with no obvious preference for peripheral or internal positioning. In contrast, in plants given two weeks of 5^{o}C the number of foci was reduced to one or two in the endoreduplicated nuclei (Fig. 5.4 a-d, g) and one in the meristematic cells (Fig. 5.4e-f). This cold-induced clustering was reproduced in a second independent *FLC-lacO* line with a different integration site in the Arabidopsis genome (Fig. 5.7), but was not observed in an Arabidopsis line carrying a single and complete *lacO*-only transgene (Fig. 5.4 h-j). It was also not observed in the line carrying a *FLC-lacO* transgene harbouring the *lacO* array in the first intron of *FLC* (*FLC-lacO-Bst*), which did not complement the *flc-3* mutation (Fig. 5.3 and Fig. 5.4 k-n). These data suggest that the cold causes a clustering of *FLC-lacO* foci in the nucleus that is dependent on either elements within intron 1 (disrupted in *FLC-lacO-Bst*) or functionality of the *FLC* gene.

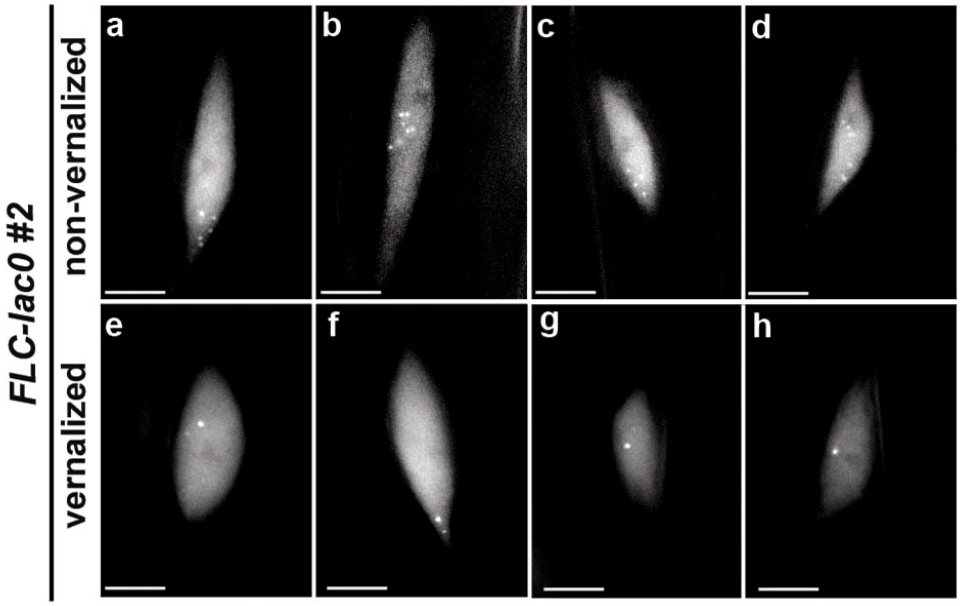

Figure 5.7. Images of root cells showing the behaviour of *FLC-lacO* foci in a second transgenic line where the *FLC-lacO* T-DNA insertion event was found to have occurred on top arm of chromosome I. **(a-d)** Nuclei from NV plants. **(e-h)** Nuclei from plants vernalized for 2 weeks (scale bars: 5 µm).

5.4.3. The clustering of *FLC-lacO* is impaired in *vrn1* and *vrn5* mutants

In order to investigate what determined the clustering we exploited tools developed during genetic dissection of vernalization. *vrn1* and *vrn5* mutations were introduced into one of the complementing *FLC-lacO* lines containing YFP-LacI. Both mutations impair the epigenetic silencing of *FLC* but through different mechanisms; VRN5 is a central component of the PHD-PRC2 and is required for accumulation of H3K27me3 at the nucleation site. The role of VRN1 is still being elucidated but we consider its function to act in parallel with PHD-PRC2 and consistent with this *vrn2 vrn1* or *vrn1 vrn5* double mutants are more severely disrupted in *FLC* silencing than any single mutants (Greb et al., 2007). Analysis of the *FLC-lacO* foci in the root epidermal cells revealed that the cold-induced clustering was abolished by the presence of either mutation (Fig. 5.8).

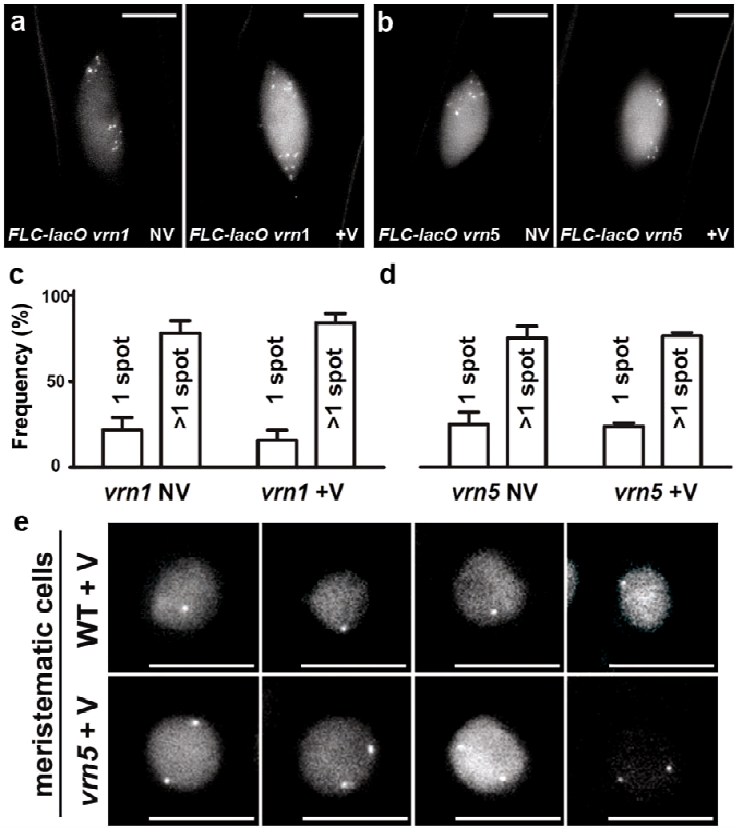

Figure 5.8. *FLC-lacO* clustering is impaired in *vrn1* and *vrn5* mutants.

(a) Images of *FLC-lacO* transgene in *vrn1* region 2 root cells either non vernalized (NV) or vernalized for two weeks (+V) plants. **(b)** Images of *FLC-lacO* transgene in *vrn5* background (NV) or (+V). **(c)** Quantification of *FLC-lacO* foci in 30 cells of region 2 in *vrn1*. **(d)** Quantification of *FLC-lacO* foci in 30 cells of region 2 in *vrn5*. **(e)** Representative fluorescence images of nuclei from meristematic cells harbouring the *FLC-lacO* from +V plants in wild-type (upper panels) and *vrn5* (lower panels). (scale bars: 5 µm).

These results support the idea that nuclear clustering of the *FLC* alleles is an outcome of multiple processes that occur in the cold and that contribute to the overall accumulation of silencing.

5.4.4. The clustering of *FLC-lacO* increases quantitatively with increasing cold exposure

A particular feature of vernalization is its quantitative nature; increasing weeks of cold lead to progressively higher levels of silencing. This issue has been addressed recently through quantitative modeling of H3K27me3 accumulation at *FLC* and developed an experimentally validated model, which suggests that the underlying mechanism involves a cell-autonomous epigenetic switch (Angel, 2011). Cold-induced nucleation of H3K27me3 occurs at one site in *FLC* and is followed by flipping of the entire locus into a silenced state. This is driven by dynamic histone turnover and a positive feedback loop whereby H3K27me3 recruits complexes that methylate other nucleosomes. This flipping occurs after the plants are transferred to the warm and is associated with the spreading of PHD-PRC2 across the whole gene. The quantitative nature of the silencing results from an increasing proportion of cells that have flipped into a fully silenced state (Angel, 2011). We asked how physical clustering might fit into this mechanism by quantitatively analysing the number of cells showing reduced *FLC-lacO* foci number after different lengths of cold. We found that the number of cells showing clustering to two and then just one focus increased with increasing time in the cold (Fig. 5.9a). These plants were analysed immediately at the end of the cold period so the clustering reflects steps that have occurred during the cold and not the cell-autonomous flipping into the epigenetically stable silent state.

We then investigated the correlation of the observed clustering with the epigenetic stability of the vernalization response. Plants were given different lengths of cold and then transferred to the warm for seven days after which the number of *FLC-lacO* foci was counted. The majority of the cells analysed still showed the clustering suggesting that once initiated in the cold the physical clustering is maintained during development in the warm (Fig. 5.9b). Since cells carrying endoreduplicated chromosomes no longer divide, the analysis was repeated on root cells formed after transfer from cold to warm, ie. cells several cm below the point at which the root meristem had reached at the point of transfer. The clustering was still detected in these newly formed cells (Fig. 5.9c) suggesting that the changes in nuclear positioning of *FLC* that occurred in the cold are epigenetically transmitted to daughter cells.

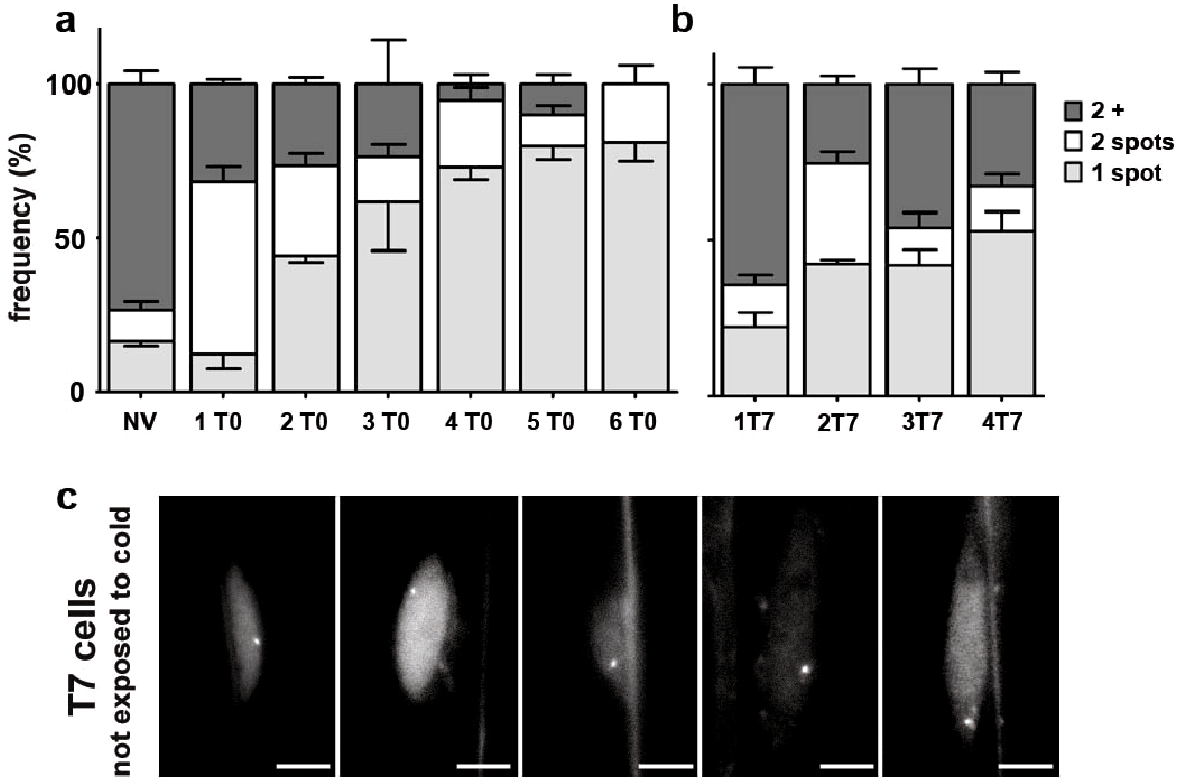

Figure 5.9. *FLC-lacO* clustering increases quantitatively with cold exposure.

(a) Time course of *FLC-lacO* clustering in region 2 root cells in seedlings vernalized for different weeks of cold (0-6 weeks). The number of foci (one, two or more than two) was counted in ten randomly selected nuclei in five different plants. **(b)** Same analysis but after the different lengths of cold the plants were grown for 7 days (T7) at 20^{o}C before imaging. The number of foci (one, two or more than two) was counted in ten randomly selected nuclei in five different plants. **(c)** Representative nuclei from root cells in region 2 in a section of root produced since transfer of the plants from cold to warm. Seedlings were exposed to three weeks cold and grown for one week at ambient temperature (scale bars: 5 μm).

5.5. Discussion

The maintenance of nuclear positioning through successive cell divisions is an active area of research (Bantignies et al., 2003; Brickner et al., 2007) and our data support the view that position of a locus in the nucleus correlates with epigenetic memory. Examples of dynamic repositioning in nuclear organization have previously been associated with regulation of gene expression and differentiation (Finlan et al., 2008) but live imaging has

now allowed us to explore nuclear dynamics involved in response to environmental signals. The slowness of vernalization enables us to analyse the sequence of events and associate particular processes with different steps in the mechanism. By comparing the various changes as a sequence of events we found the time-dependent increase in clustering mirrors the increase in H3K27trimethylation at the nucleation site (Fig. 5.10), consistent with the quantitative accumulation of H3K27me3 also representing a population-based average of a bistable state, either high or low H3K27me3 at the nucleation site (Angel, 2011).

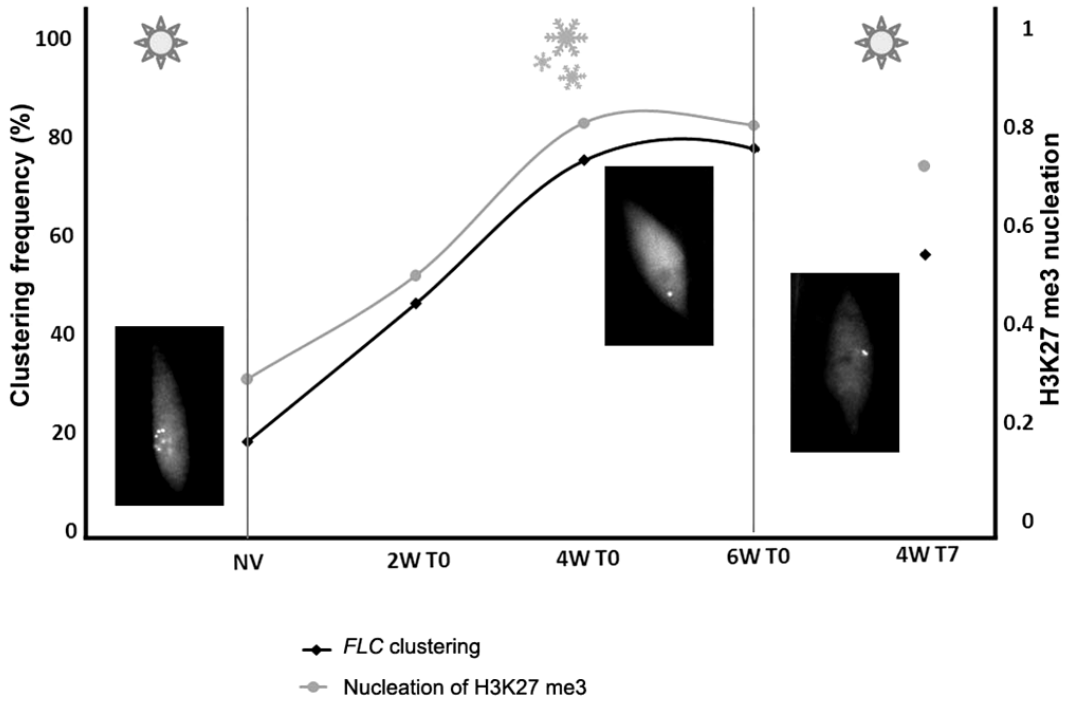

Figure 5.10. Clustering dynamics parallel the cold-induced increases in H3K27me3 at the nucleation site.

With increasing cold exposure, H3K27me3 levels increase at the nucleation site (end of exon 1- start intron 1), the timing of which is coincident with the reduction in *FLC-lacO* foci number. *FLC* is fully silenced after six weeks of cold and this is associated with high H3K27me3 and stable maintenance of the clustering during subsequent growth at warm temperatures. Grey line represents the levels of H3K27 me3 at the nucleation site normalized to H3 and STM. Black line represents the frequency of one dot in the clustering of FLC foci (data from Fig. 5.9).

We speculate that the clustering of *FLC* occurs at the same time as the nucleation of chromatin silencing, which involves the localized recruitment of PHD-PRC2. However, since clustering is also disrupted in *vrn1,* clustering may be an event that occurs as a consequence of this initial silencing and the parallel VRN1-dependent activities. Interestingly, the dynamics of *FLC* repression has several parallels with Sir-dependent silencing in yeast (Buhler and Gasser, 2009). Both systems involve a nucleation and spreading mechanism of silencing by multi-protein silencing complexes and early in the sequence of events there is a change of nuclear organization involved in the transition to the fully silenced state. These parallels may help in future dissection of the silencing mechanisms.

In summary, using live cell imaging on a whole-organism we provide evidence that changes in *FLC* nuclear organization can be induced by environmental conditions and that transmission of nuclear architecture through cell division at the level of a single locus might contribute to inheritance of chromatin states.

5.6. Acknowledgments

The transgenic lines described in this work as well as their characterization (Southern blot, TAIL-PCR and flowering time) were provided by Joshua Mylne – Figs 5.3, 5.5 and 5.6. The crosses with the mutants were done by Filomena De Lucia and Caroline Dean. I also would like to thank Robert Sablowski, Silvia Costa and Clive Lloyd for comments on the manuscript. F.D.L. was supported by a Biotechnology and Biological Sciences Research Council (BBSRC) grant BB/C517633/1 and European Research Council grant 233039 ENVGENE, S.R. was supported by a grant SFRH/BD/23202/2005 from the Portuguese Fundação para a Ciência e a Tecnologia, J.S.M. was supported by European Commission grant QLK5-CT-2001-01412 and is an ARC QEII Fellow (DP0879133), P.S. and C.D. acknowledge Core Support to the JIC from BBSRC.

5.7. References

Angel, A., Song, J, Dean, C & Howard M (2011). A Polycomb-based switch underlying quantitative epigenetic memory. Nature, in press.

Bantignies, F., Roure, V., Comet, I., Leblanc, B., Schuettengruber, B., Bonnet, J., Tixier, V., Mas, A., and Cavalli, G. (2011). Polycomb-Dependent Regulatory Contacts between Distant Hox Loci in Drosophila. Cell *144*, 214-226.

Bantignies, F.d.r., Grimaud, C., Lavrov, S., Gabut, M., and Cavalli, G. (2003). Inheritance of Polycomb-dependent chromosomal interactions in Drosophila. Genes & Development *17*, 2406-2420.

Brickner, D.G., Cajigas, I., Fondufe-Mittendorf, Y., Ahmed, S., Lee, P.-C., Widom, J., and Brickner, J.H. (2007). H2A.Z-Mediated Localization of Genes at the Nuclear Periphery Confers Epigenetic Memory of Previous Transcriptional State. PLoS Biol *5*, e81.

Buhler, M., and Gasser, S.M. (2009). Silent chromatin at the middle and ends: lessons from yeasts. Embo J *28*, 2149-2161.

Burn, J.E., Bagnall, D J, Metzger, J D, Dennis, E S and Peacock, W J (1993). DNA methylation, vernalization, and the initiation of flowering. Proc Natl Acad Sci U S A *90*, 287-291.

De Lucia, F., Crevillen, P., Jones, A.M., Greb, T., and Dean, C. (2008). A PHD-polycomb repressive complex 2 triggers the epigenetic silencing of FLC during vernalization. Proc Natl Acad Sci U S A *105*, 16831-16836.

Finlan, L.E., Sproul, D., Thomson, I., Boyle, S., Kerr, E., Perry, P., Ylstra, B., Chubb, J.R., and Bickmore, W.A. (2008). Recruitment to the Nuclear Periphery Can Alter Expression of Genes in Human Cells. PLoS Genet *4*, e1000039.

Fraser, P., and Bickmore, W. (2007). Nuclear organization of the genome and the potential for gene regulation. Nature *447*, 413-417.

Galbraith, D., Harkins, KR & Knapp,S (1991). Systemic Endopolyploidy in Arabidopsis thaliana Plant Physiol *96*, 985-989.

Gendall, A.R., Levy, Y.Y., Wilson, A., and Dean, C. (2001). The *VERNALIZATION2* Gene Mediates the Epigenetic Regulation of Vernalization in Arabidopsis. Cell *107*, 525-535.

Greb, T., Mylne, J.S., Crevillen, P., Geraldo, N., An, H., Gendall, A.R., and Dean, C. (2007). The PHD Finger Protein VRN5 Functions in the Epigenetic Silencing of Arabidopsis FLC. Current Biology *17*, 73-78.

Henderson, I.R., and Dean, C. (2004a). Control of Arabidopsis flowering: the chill before the bloom. Development *131*, 3829-3838.

Henderson, I.R., and Dean, C. (2004b). Control of *Arabidopsis* flowering: the chill before the bloom. Development *131*, 3829-3838.

Heo, J.B., and Sung, S. (2010). Vernalization-Mediated Epigenetic Silencing by a Long Intronic Noncoding RNA. Science *331*, 76-79.

Hübner, M., Spector, DL (2010). Chromatin Dynamics. Annu Rev Biophys *39*, 471-489.

Johanson, U., West, J., Lister, C., Michaels, S., Amasino, R., and Dean, C. (2000). Molecular analysis of *FRIGIDA*, a major determinant of natural variation in *Arabidopsis* flowering time. Science *290*, 344-347.

Jovtchev, G., Watanabe, K., Pecinka, A., Rosin, F., Mette, M., Lam, E., and Schubert, I. (2008). Size and number of tandem repeat arrays can determine somatic homologous pairing of transgene loci mediated by epigenetic modifications in *Arabidopsis thaliana* nuclei. Chromosoma *117*, 267-276.

Kato, N., and Lam, E. (2001). Detection of chromosomes tagged with green fluorescent protein in live Arabidopsis thaliana plants. Genome Biology *2*, 0045.0041 - 0045.0010.

Lanzuolo, C., Roure, V., Dekker, J., Bantignies, F., and Orlando, V. (2007). Polycomb response elements mediate the formation of chromosome higher-order structures in the bithorax complex. Nat Cell Biol *9*, 1167-1174.

Levine, M. (2010). Transcriptional Enhancers in Animal Development and Evolution. Current Biology *20*, R754-R763.

Levy, Y.Y., Mesnage, S.p., Mylne, J.S., Gendall, A.R., and Dean, C. (2002). Multiple Roles of Arabidopsis VRN1 in Vernalization and Flowering Time Control. Science *297*, 243-246.

Liu, Y.-G., Mitsukawa, N., Oosumi, T., and Whittier, R.F. (1995). Efficient isolation and mapping of *Arabidopsis thaliana* T-DNA insert junctions by thermal asymmetric interlaced PCR. The Plant Journal *8*, 457-463.

Matzke, A., Watanabe K, van der Winden J, Naumann, U and Matzke M (2010). High frequency, cell type-specific visualization of fluorescent-tagged genomic sites in interphase and mitotic cells of living Arabidopsis plants. Plant Methods *6*.

Michaels, S.D., and Amasino, R.M. (1999). The gibberellic acid biosynthesis mutant ga1-3 of Arabidopsis thaliana is responsive to vernalization. Dev Genet *25*, 194-198.

Michaels, S.D., Amasino, R.M. (1999). FLOWERING LOCUS C encodes a novel MADS domain protein that acts as a repressor of flowering. Plant Cell *11*, 949-956.

Mylne, J.S., Barrett, L., Tessadori, F., Mesnage, S., Johnson, L., Bernatavichute, Y.V., Jacobsen, S.E., Fransz, P., and Dean, C. (2006). LHP1, the Arabidopsis homologue of HETEROCHROMATIN PROTEIN1, is required for epigenetic silencing of FLC. PNAS *103*, 5012-5017.

Napp-Zinn, K. (1955). Genetische Grundlagen des Kältebedürfnisses bei Arabidopsis thaliana (L.) Heynh. Naturwissenschaften *42*, 650.

Pecinka, A., Kato, N., Meister, A., Probst, A.V., Schubert, I., and Lam, E. (2005). Tandem repetitive transgenes and fluorescent chromatin tags alter local interphase chromosome arrangement in Arabidopsis thaliana. J Cell Sci *118*, 3751-3758.

Schubert, I., and Shaw, P. (2011). Organization and dynamics of plant interphase chromosomes. Trends in Plant Science *In Press*.

Sheldon, C.C., Burn, J.E., Perez, P.P., Metzger, J., Edwards, J.A., Peacock, W.J., and Dennis, E.S. (1999). The FLF MADS box gene: a repressor of flowering in Arabidopsis regulated by vernalization and methylation. Plant Cell *11*, 445-458.

Sherratt, D.J., Lau, I.F., and Barre, F.-X.a. (2001). Chromosome segregation. Current Opinion in Microbiology *4*, 653-659.

Straight, A., Sedat, J & Murray, A.W. (1998). Time-Lapse Microscopy Reveals Unique Roles for Kinesins during Anaphase in Budding Yeast J Cell Biol *143*, 687-694.

Sung, S., and Amasino, R.M. (2004). Vernalization in Arabidopsis thaliana is mediated by the PHD finger protein VIN3. Nature *427*, 159-164.

Sung, S., He, Y., Eshoo, T.W., Tamada, Y., Johnson, L., Nakahigashi, K., Goto, K., Jacobsen, S.E., and Amasino, R.M. (2006a). Epigenetic maintenance of the vernalized state in *Arabidopsis thaliana* requires LIKE HETEROCHROMATIN PROTEIN 1. Nat Genet *38*, 706-710.

Sung, S., Schmitz, R.J., and Amasino, R.M. (2006b). A PHD finger protein involved in both the vernalization and photoperiod pathways in Arabidopsis. Genes Dev *20*, 3244-3248.

Swiezewski, S., Liu, F., Magusin, A., and Dean, C. (2009). Cold-induced silencing by long antisense transcripts of an Arabidopsis Polycomb target. Nature *462*, 799-802.

Taddei, A., Hediger, F., Neumann, F.R., Bauer, C., and Gasser, S.M. (2004). Separation of silencing from perinuclear anchoring functions in yeast Ku80, Sir4 and Esc1 proteins. Embo J *23*, 1301-1312.

Toomajian, C., Hu, T.T., Aranzana, M.J., Lister, C., Tang, C., Zheng, H., Zhao, K., Calabrese, P., Dean, C., and Nordborg, M. (2006). A nonparametric test reveals selection for rapid flowering in the Arabidopsis genome. PLoS Biol *4*, e137.

Towbin, B.D., Meister, P., and Gasser, S.M. (2009). The nuclear envelope -- a scaffold for silencing? Current Opinion in Genetics & Development *19*, 180-186.

Chapter 6

General Discussion

Chapter 6:

General Discussion

Chromatin is increasingly recognized as not only as a structure simply used for packing the DNA within the nucleus, but also a dynamic material that changes and responds to developmental and environmental cues to determine the correct spatial and temporal expression of genes. There are several ways by which chromatin structure can be remodelled. Post-translational modifications of histone proteins can generate localized distinct chromosomal domains by recruiting diverse chromatin-binding protein complexes or by directly modulating the interactions with the DNA. Also, the composition of nucleosomes can be modified by replacing major histones with variants. And finally, the 3D spatial location of genes in respect to their chromosome territories represents another level of chromatin organization known to affect gene expression. While the dynamic nature of chromatin has been previously described it was often simply considered an intrinsic property without much functional relevance. However, analysis of cellular processes using *in vivo* techniques has begun to reveal the functional importance of chromatin dynamics. In this thesis we described how these three different aspects of chromatin organization affect processes like cell differentiation and development using a variety of *in vivo* microscopy techniques.

Arabidopsis is well suited to be used as a model organism to participate in the elucidation of chromatin dynamics and development. In fact, plants are faced with successive developmental phase changes during their life cycle. These transitions are very well regulated to co-ordinate the correct expression of many genes, and chromatin remodelling plays a key role in this regulation. The main goal of this work was to investigate how chromatin structure is able to shape different aspects of Arabidopsis development.

In the first part of this thesis (Chapter 2 and 3) we looked at a global aspect of chromatin dynamics. We investigated in a general way, in a non-gene-specific manner, how histone mobility affects cell differentiation. We used FRAP as a tool to examine the molecular behaviour of histone proteins during development. Although the technique only measures average properties of a large population of molecules (Anderson et al., 1992) it has been successfully applied to DNA repair studies (Essers et al., 2006), as well as to assess the

mobility of several histones in various systems (Kimura and Cook, 2001; Lever et al., 2000; Misteli et al., 2000).

In chapter 2, using the well defined developmental gradient in Arabidopsis roots we observed that the overall histone mobility decreases with the progression of cell differentiation. We show that these changes are primarily caused by overall changes in histone acetylation, and, conversely, that manipulation of histone acetylation causes corresponding changes in development. We further identified that the plant hormone auxin modulates these changes, suggesting that the auxin gradient, known to regulate root patterning, acts at least in part through histone acetylation and consequent chromatin mobility changes.

In chapter 3, we looked at histone mobility in root stem cells. By using two-photon photoactivation we showed that in stem cells from the root – quiescent centre (QC) and initial cells - the mobility of the core histone H2B is reduced when compared with the surrounding cells of the meristem. Additionally, we showed that histone acetylation controls QC cell maintenance and that hyperacetylation by TSA not only induces QC division but also the loss of expression of QC markers.

These observations lead to a number of exciting conclusions. First, because high rates of recovery were observed in undifferentiated cells of the meristem versus relatively low recoveries on fully differentiated cells, this might represent a global mechanism for gene regulation. Because the packaging of the DNA into nucleosomes acts as a barrier to transcription, the modulation of these interactions through mechanisms such as histone modifications might represent a model by which histone mobility regulates in a co-ordinated fashion the expression of many genes. This idea of a global gene regulation has been discussed over the past years (Cosgrove et al., 2004; Henikoff, 2008), and here we not only support this thought but further put it into a developmental context. Secondly, our results represent a novel link between chromatin dynamics and hormone signalling in plants. The effects of auxins in histone acetylation and histone mobility represent a molecular explanation of how this plant hormone shapes development through chromatin remodelling and consequently by the maintenance of a division potential. The ability of cells to divide, thus, seems correlated with high histone mobilities and histone acetylation. In fact, although histone acetylation at the gene level has been well correlated with transcriptional activity, in field bean the overall acetylation of large chromatin domains was shown to be correlated with DNA replication rather than with transcription (Jasencakova et al., 2000). Finally, the somewhat contradictory results obtained for root stem cells (QCs and initial cells) showed

that in respect to their overall histone dynamics, these cells behave more similarly to differentiated cells. In fact the concept of stem cells in plants is still a matter of debate. We propose that even though plant stem cells have a very immobile chromatin, they must keep the potential to divide and differentiate into more dynamic states.

Another level of complexity in chromatin regulation is brought by the possibility of replacing the major histones by histone variants. In chapter 4, we studied the role of a histone variant, H2A.Z, on cell fate switches on the Arabidopsis root epidermis. We showed that a higher incorporation of H2A.Z in atrichoblasts cells is crucial for the development of a non-hair cell. In plants where this process is impaired, formation of ectopic hair cells is observed. Here again the dynamic change in level of H2A.Z throughout the genome seems to represent a mechanism by which the expression of many genes (including *GL2*) is regulated co-ordinately. The mechanism by which H2A.Z is targeted to specific genes still remains unproven. In yeast a genome-wide survey of H2A.Z occupancy suggested a role for transcription factors in recruiting SWR1 to specific promoters (Zhang et al., 2005). We speculate that WER acts by recruiting PIE1 for deposition of H2A.Z on *GL2*. Although we know that WER binds to *GL2* (Lee and Schiefelbein, 1999) and that it is necessary for the H2A.Z-GFP patterning observed on the meristem transition zone, we still do not have a direct evidence for WER/PIE1 interaction.

A further attractive hypothesis about how chromatin regulates transcription is that a gene locus can move into more favourable positions within the nucleus for regulatory purposes. Some classical examples are the brown locus in Drosophila that was shown to be specifically silenced during larval development by a specific contact with centromeric heterochromatin (Dernburg et al., 1996), or the repositioning of genes during lymphocyte development mediated by the DNA-binding protein Ikaros (Fisher and Merkenschlager, 2002).

Techniques using several copies of a *lac* or *tet* operator sequence allow visualization of this sequence within nuclei of living cells (Belmont 2001; Gasser 2002). In chapter 5, we used the lac operator system to monitor nuclear organization and dynamics of the floral repressor gene FLC, during vernalization. We observed that alleles of FLC locus physically associate and reposition in the nucleus as an early step in the silencing process. This cold-induced clustering is quantitative and coincident with the timing of the nucleation of chromatin silencing, marked through accumulation of H3K27me3. Furthermore we have evidence that this physical association of alleles is epigenetically stable, i.e. positional

information is stable through cell divisions. Finally, the biological significance of clustering was revealed by its dependence on trans factors (VRN1 and VRN5) previously shown to be required for the Polycomb silencing mechanism.

In conclusion this work provides an important insight into how different levels of chromatin organization shape development. Our results included the role of histone mobility in plant cell differentiation (chapter 2 and 3), the role of histone variants in cell-fate specification (chapter 4) and the role of nuclear positioning in the regulation of a Polycomb target locus in response to an environmental cue. Together, the results presented here represent an important step on our understanding of chromatin organization and its role in plant development. We emphasize the importance of microscopy methods for this type of study given its cell type specificity and the possibility to apply it *in vivo*. In the future new strategies, such as super-resolution microscopes will allow not only cell specificity but also adjacent genes to be identified as individual objects providing therefore a major improvement in analysing chromatin organization.

6.1. References

Anderson, C.M., Georgiou, G.N., Morrison, I.E., Stevenson, G.V., and Cherry, R.J. (1992). Tracking of cell surface receptors by fluorescence digital imaging microscopy using a charge-coupled device camera. Low-density lipoprotein and influenza virus receptor mobility at 4 degrees C. J Cell Sci *101 (Pt 2)*, 415-425.

Cosgrove, M.S., Boeke, J.D., and Wolberger, C. (2004). Regulated nucleosome mobility and the histone code. Nat Struct Mol Biol *11*, 1037-1043.

Dernburg, A.F., Broman, K.W., Fung, J.C., Marshall, W.F., Philips, J., Agard, D.A., and Sedat, J.W. (1996). Perturbation of nuclear architecture by long-distance chromosome interactions. Cell *85*, 745-759.

Essers, J., Houtsmuller, A.B., and Kanaar, R. (2006). Analysis of DNA recombination and repair proteins in living cells by photobleaching microscopy. Methods Enzymol *408*, 463-485.

Fisher, A.G., and Merkenschlager, M. (2002). Gene silencing, cell fate and nuclear organisation. Curr Opin Genet Dev *12*, 193-197.

Henikoff, S. (2008). Nucleosome destabilization in the epigenetic regulation of gene expression. Nat Rev Genet *9*, 15-26.

Jasencakova, Z., Meister, A., Walter, J., Turner, B.M., and Schubert, I. (2000). Histone H4 acetylation of euchromatin and heterochromatin is cell cycle dependent and correlated with replication rather than with transcription. Plant Cell *12*, 2087-2100.

Kimura, H., and Cook, P.R. (2001). Kinetics of core histones in living human cells: little exchange of H3 and H4 and some rapid exchange of H2B. J Cell Biol *153*, 1341-1353.

Lee, M.M., and Schiefelbein, J. (1999). WEREWOLF, a MYB-related protein in Arabidopsis, is a position-dependent regulator of epidermal cell patterning. Cell *99*, 473-483.

Lever, M.A., Th'ng, J.P., Sun, X., and Hendzel, M.J. (2000). Rapid exchange of histone H1.1 on chromatin in living human cells. Nature *408*, 873-876.

Misteli, T., Gunjan, A., Hock, R., Bustin, M., and Brown, D.T. (2000). Dynamic binding of histone H1 to chromatin in living cells. Nature *408*, 877-881.

Zhang, H., Roberts, D.N., and Cairns, B.R. (2005). Genome-wide dynamics of Htz1, a histone H2A variant that poises repressed/basal promoters for activation through histone loss. Cell *123*, 219-231.

A bolsa de doutoramento com a referência SFRH/BD/23202/2005 foi atribuída pela Fundação para a Ciência e Tecnologia (FCT), no âmbito do Quadro Comunitário de Apoio, comparticipado pelo Fundo Social Europeu (FSE).

FCT Fundação para a Ciência e a Tecnologia
MINISTÉRIO DA CIÊNCIA, TECNOLOGIA E ENSINO SUPERIOR Portugal

ITQB-UNL | Av. da República, 2780-157 Oeiras, Portugal
Tel (+351) 214 469 100 | Fax (+351) 214 411 277

www.itqb.unl.pt